

See discussions, stats, and author profiles for this publication at: <https://www.researchgate.net/publication/283090466>

Strategies and Molecular Design Criteria for 3D Printable Hydrogels

ARTICLE *in* CHEMICAL REVIEWS · OCTOBER 2015

Impact Factor: 46.57 · DOI: 10.1021/acs.chemrev.5b00303

READS

66

5 AUTHORS, INCLUDING:



Jürgen Groll

University of Wuerzburg

124 PUBLICATIONS 2,370 CITATIONS

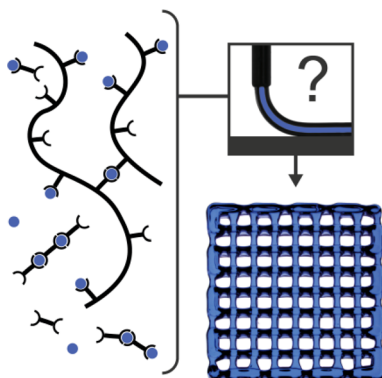
[SEE PROFILE](#)

Strategies and Molecular Design Criteria for 3D Printable Hydrogels

Tomasz Jungst,^{†,§} Willi Smolan,^{†,§} Kristin Schacht,[‡] Thomas Scheibel,[‡] and Jürgen Groll^{*,†}

[†]Department for Functional Materials in Medicine and Dentistry, University of Würzburg, Pleicherwall 2, 97070 Würzburg, Germany

[‡]Chair of Biomaterials, Faculty of Engineering Science, University of Bayreuth, Universitätsstrasse 30, 95447 Bayreuth, Germany



CONTENTS

1. Introduction
2. Fabrication Systems
 - 2.1. Laser-Induced Forward Transfer
 - 2.2. Inkjet Printing
 - 2.3. Robotic Dispensing
 - 2.4. Comparison of the Fabrication Methods
3. Rheological Considerations
 - 3.1. Rheology of Non-Newtonian Liquids
 - 3.2. Important Aspects of the Printing Process
 - 3.3. Underlying Molecular Concepts: Colloidal Solutions
 - 3.4. Underlying Molecular Concepts: Polymer Solutions
 - 3.5. Characterization of Rheological Properties
4. Chemical Cross-Linking
 - 4.1. Post- and Prefabrication Cross-Linking
 - 4.2. Application of Dynamic Covalent Bonds for Printing
5. Molecular Physical Gels
 - 5.1. Supramolecular Approaches
 - 5.1.1. Ionic Interactions and Coordination Bonds
 - 5.1.2. Hydrogen Bonds
 - 5.1.3. Host–Guest and Aromatic Donor–Acceptor Interactions
 - 5.1.4. Low Molecular Weight Gelator
 - 5.2. Macromolecular Gels
 - 5.2.1. Naturally Occurring Biopolymers Used for Hydrogel Formation
 - 5.2.2. Synthetic Peptides and Proteins
 - 5.2.3. Host–Guest Interaction
 - 5.2.4. Ionic Interactions and Coordination Chemistry
 - 5.2.5. Hydrogen Bonds
 - 5.3. Colloidal Systems

5.3.1. Silica Nanoparticles and Laponite-Based Hydrogels	W
5.3.2. Carbon-Nanotube- and Graphene-Sheet-Rich Compounds	X
5.3.3. Metal-Based Gels	Z
6. Biotechnological Approaches toward Bioinks	Z
6.1. Designable Biopolymers: Recombinantly Produced Proteins	AA
6.1.1. Methods for Recombinant Protein Production	AA
6.1.2. Silk-like Proteins	AB
6.1.3. Recombinant Collagen/Collagen-like Proteins	AB
6.1.4. Elastin-like Polypeptides	AC
6.1.5. Resilin-like Polypeptides	AC
6.1.6. Hybrid Proteins	AC
6.2. Designable Biopolymers: Polynucleotides	AD
7. Conclusions and Outlook	AD
D. Author Information	AE
F. Corresponding Author	AE
G. Author Contributions	AE
G. Notes	AE
H. Biographies	AE
H. Acknowledgments	AF
I. References	AF

1. INTRODUCTION

Additive manufacturing (AM), also referred to as rapid prototyping, solid free-form fabrication, or simply three-dimensional (3D) printing, comprises a number of technologies that allow the direct generation of objects in a layer-by-layer fashion through computer-aided design (CAD) and/or computer-aided manufacturing (CAM).¹ With these processing technologies, objects can be generated without the need for molds, enabling a high degree of freedom in design and allowing the direct production of structures that cannot be fabricated using classical subtractive manufacturing techniques. AM technologies have been primarily used in the engineering and fabrication community² for decades but have matured into high-precision (e.g., via electron beam melting) or low-cost (e.g., fused deposition modeling, FDM) printers. AM is increasingly relied upon for certain industrial production processes, for example, in the case of laser sintering for titanium hip implants, and is regarded as the next industrial or manufacturing revolution.³

Special Issue: Frontiers in Macromolecular and Supramolecular Science

Received: May 18, 2015

The high degree of automation and reproducibility in AM, together with the precise control over where different components can be placed in a 3D model, renders AM particularly interesting for tissue engineering (TE), which aims for the full restoration of damaged or degenerated tissues and organs. Traditionally, the three main components of TE (cells, prefabricated scaffolds, and growth factors) are combined to form a construct that can be either directly implanted or incubated *in vitro* for maturation prior to implantation.⁴ AM techniques have predominantly been applied for the fabrication of scaffolds for such TE approaches.^{5–8} Seeding of cells onto such prefabricated scaffolds usually results in a nonordered and random distribution of cells which does not reflect the complex hierarchical organization of functional tissue.

However, recapitulating the hierarchical complexity of native tissues in cell-loaded constructs is a highly attractive strategy for the creation of functional tissue equivalents. Therefore, cells, biomaterials, and bioactive compounds have to be processed simultaneously, and AM technologies are regarded as a method to achieve this.⁹ This relatively young approach is termed biofabrication and can be defined as the creation of biological structures for TE, pharmacokinetic, or basic cell biology studies (including disease models) by a computer-aided transfer process for patterning and assembling living and nonliving materials with a prescribed 3D organization.¹⁰ This research field holds the promise to overcome some of the most urgent challenges of TE, such as the direct generation of large constructs including vessel-like structures for initial nutrient and oxygen supply of the embedded cells.

Biofabrication research has rapidly developed over the past decade and has very recently been addressed by several excellent review papers.^{11–14} It places high demands on the AM process and the materials used for it, including so-called “bioinks”, cell loadable and printable formulations that solidify after printing for shape fidelity of the desired structure. The entire manufacturing must produce defined structures using cell-compatible conditions such as buffered aqueous solution and a narrow temperature range and with limited mechanical shear forces. Also, the materials and chemistry used for printing have to be cytocompatible. This significantly limits the variety of applicable AM technologies and suitable materials, with hydrogels as predetermined candidates for bioinks. Hydrogels are three-dimensionally cross-linked hydrophilic polymer networks that swell without dissolution up to 99% (w/w) water of their dry weights.¹⁵ These materials are particularly attractive for biomedical applications as they recapitulate several features of the natural environment of cells, the so-called extracellular matrix (ECM),¹⁶ and allow for efficient and homogeneous cell seeding in a highly hydrated mechanically supportive 3D environment. Depending on the type of cross-linking, hydrogels can be divided into two classes: (i) chemically cross-linked hydrogels (also termed chemical hydrogels) and (ii) physically cross-linked hydrogels (also termed physical hydrogels). Chemical hydrogels are formed by covalent networks and cannot dissolve in water without breakage of covalent bonds. Physical hydrogels are, however, formed by dynamic and reversible cross-linking of synthetic or natural building blocks based on noncovalent interactions such as hydrophobic and electrostatic interaction or hydrogen bridges. Hence, physical hydrogels exhibit promising properties for bioink development since they can rapidly retain their shape after printing. Some recent reviews give a comprehensive overview on the design and application of

hydrogels for biomedical applications,^{17–19} TE,²⁰ and regenerative medicine.²¹

There has been intensive research with regard to injectable hydrogel formulations based on the fact that the gelation behavior of hydrogels can be adjusted so that a hydrogel precursor solution can be prepared and injected into a mold or cavity and subsequently gelate and form a hydrogel after injection.^{22–24} This can, for example, be achieved through shear thinning properties leading to a viscosity decrease with increasing shear stress accompanied by the injection through a cannula.²⁵ However, for 3D printing of cell-containing hydrogels, the prerequisites are even more stringent than for injectable hydrogels. For printing, the cell-loaded bioink formulation has to be stable in the reservoir for the time of the printing procedure (typically at least several minutes, depending on the size and complexity of the structure to be printed) with rheological properties imposed by the fabrication process and with a homogeneous three-dimensional distribution of the cells. To achieve reasonable resolutions, the nozzle diameters are also significantly lower in printing than for simple injection, and after printing, the (re)gelation needs to be rapid enough to ensure shape stability of the printed construct. Ideally, the resulting structure is self-supporting, and no postprocessing treatment is needed for mechanical stabilization. The lack of geometrical constraints and the need for rapid gelation to ensure shape fidelity is the most significant and at the same time the most challenging difference of injectable versus printable hydrogels.

As biofabrication eventually aims at delivering human tissue models for biomedical research and eventually as a therapeutic treatment option, it is important to keep in mind that a general suitability for clinical translation should be taken into account for the development of a new bioink. Generally, the materials have to be sterile when entering the fabrication process, either through sterile production or through conformity with a sterilization method. Moreover, the materials should ideally be endotoxin free but definitely cannot exceed the limits set by regulation, which may be a more critical point for biopolymers than for synthetic systems. These few but important general considerations should therefore always be taken into account for bioink development.

Bioprinting and biofabrication originated from the technology- and application-oriented (bio)engineering community and did not evolve from chemistry or materials science. Hence, the field has for long worked with established hydrogel systems available in quantities that are necessary for the processes. The vast majority of bioprinting and biofabrication studies thus use alginate- and gelatin-based bioink formulations. Although this has allowed achieving some remarkable successes, it has recently become evident that the lack of a bigger variety of printable hydrogel systems is one major drawback that hampers progress of the complete field.^{26–28}

Hence, the scope of this review paper is neither to simply recapitulate and summarize established printing methods and printable hydrogels nor to summarize the achievements obtained with the present biofabrication approaches toward the construction of complex cellular arrangements or tissue-like structures and their evaluation *in vitro* and *in vivo*. For this information, we refer the reader to several excellent and most recent review papers.^{11–14,26–28} The main objective of this paper is to complement this information with a material-focused but integral summary of the most important rheological aspects relevant for printing together with an overview on the most important printing techniques. Core part of the paper is an interdisciplinary overview of possibilities to create tailored

(macro)molecular building blocks for printable hydrogels. This overview comprises existing strategies in related research fields such as supramolecular chemistry for self-assembly strategies or biotechnological approaches for bioinspired building blocks. Our aim is to deliver a comprehensive set of information to be used as a toolbox for polymer chemists and material scientists with a basic set of fundamental design criteria for the rational development of novel strategies toward bioinks.

In this review, we first introduce the most common 3D printing techniques for hydrogel printing, followed by the rheological demands on printable hydrogel systems with respect to the different techniques and the additional limitation of cytocompatibility during printing. We then briefly summarize the role of chemical cross-linking, so far mainly used for pre-cross-linking of the hydrogel building blocks before printing or postfixing of printed structures, but also introduce dynamic chemical bonds as a new and promising option for printing. We then summarize the physical cross-linking possibilities potentially exploitable for hydrogel printing, divided into supramolecular systems, functionalized polymers, and other strategies such as particulates. Finally, we outline the potential of biotechnological processes for the production of tailored biomolecules for bioink development and review the most promising biotechnologically produced systems.

2. FABRICATION SYSTEMS

Open source projects such as RepRap and Fab@home made AM affordable for private users and led to increased popularity of 3D printing. The developed desktop printers are based on FDM and enable fabrication of 3D constructs from thermoplastic materials in a layer-by-layer fashion with resolutions of about 200–400 μm . A constantly growing number of users can experience the benefits of AM and appreciate the new freedom of designing printable objects. Other processes such as selective laser sintering (SLS) allow production of very complex structures with high resolution of 50–300 μm but are still mainly limited to industry use.²⁹ Both methods—FDM and SLS—can be used to process polymers. They generate heat to melt the material and create structures by controlled solidification of the thermoplasts. Due to the thermal conditions during printing, they do not allow for hydrogel processing, but there are a variety of technologies that enable structuring hydrogels into 3D constructs.

Two very interesting processes capable of fabricating complex 3D objects from hydrogels are two-photon polymerization (2PP) and stereolithography (SLA). They use light to induce spatially limited polymerization and can be used to create well-defined structures. For both processes the construct is mainly generated by light-induced radical polymerization within a monomer reservoir or light-induced cross-linking of a photopolymer. In 2PP a femtosecond laser is focused onto a spot within this reservoir, releasing radicals from a photoinitiator on its path. These radicals start a polymerization/cross-linking reaction leading to solidification of material along the laser track. Usually a drop of material, enclosed between two microscopy glass coverslips with spacers in the millimeter range defining the construct thickness, is used as the reservoir. Relating the reservoir size to coverslips and taking into account that prints usually are much smaller than the overall size of the slips gives an indication of the producible sample size. Although the object size is limited, 2PP offers the possibility to produce constructs with spatial resolutions as small as 100 nm and is thus especially interesting for analyzing cell–construct interactions.³⁰ SLA enables the size limitations of 2PP prints to be easily overcome, generating

constructs with dimensions in the centimeter range. Although compared to that of 2PP the resolution is decreased, it still is as high as 80–125 μm .³¹ In SLA the objects are produced in a layer-by-layer fashion. The most frequently applied setup is the bottom-up system where a laser scans and solidifies the top layer of a reservoir. After one layer is created, a movable platform lowers the construct further into the resin, covering it with the next material layer. Print speeds can be increased using digital light projectors, instead of scanning lasers, illuminating and solidifying the whole layer at the same time. Another setup of SLA is top-down systems where the construct is stepwise pulled out of the resin after irradiation of one plane.³² A new version of top-down SLA using digital light projectors that has recently attracted attention is continuous liquid interface production (CLIP).³³ In contrast to other SLA systems, CLIP utilizes an oxygen-permeable window delivering oxygen to the glass–resin interface. The oxygen inhibits the polymerization reaction, creating a persistent liquid interface, allowing—in combination with precise process timing—print speeds to be further increased. CLIP enables the production of structures at hundreds of millimeters per hour and thus is much faster than traditional SLA techniques. Further research needs to be carried out to confirm if the high print speeds can be realized for biomedical applications. The main disadvantage of the light-induced processes introduced in this section is the limited number of suitable resins. Especially when printing structures from cell-containing hydrogels, a special focus needs to be put on the cytotoxicity of the photoinitiator.³²

As this short introduction shows, there is a large selection of fabrication systems available. The choice of the method mainly depends on the material that shall be processed and on the structure (size, architecture, resolution) that needs to be created. As we will discuss, each method has limitations, and none of the approaches can be considered better than another one. For some applications, also the combination of different processes might be beneficial. Fabrication systems are also still developed further, and new technologies do arise. However, as this review focuses on exploring material strategies that have been and/or can be exploited for bioprinting and biofabrication, we focus here on the three most important and best established technologies for printing of hydrogels under cell-friendly conditions: laser-induced forward transfer, inkjet printing, and robotic dispensing. These techniques will be described in detail and compared to each other in the following sections.

2.1. Laser-Induced Forward Transfer

The reviews of Chrisey et al.,³⁴ Ringisen et al.,³⁵ and Schiele et al.³⁶ give excellent summaries of laser-induced forward transfer (LIFT) techniques used for cell printing and also show examples of structures being produced with these methods. For biomedical applications, mostly modified LIFT techniques are applied. Generally, all these systems have the same setup in common and are comprised of three main components. The first is a pulsed laser, the second is a donor slide (ribbon) from which the material is propelled, and the third is a receiving substrate. The laser is focused onto a laser-absorbing layer, evaporating the material and thus generating a high gas pressure propelling material toward the substrate. By controlled movement of the donor and/or substrate, it is possible to build up 2D and 3D structures from material droplets.^{37–42} For processing biological materials, two different versions of modified LIFT are utilized: matrix-assisted pulsed laser evaporation direct writing (MAPLE-DW) and absorbing film-assisted laser-induced forward transfer

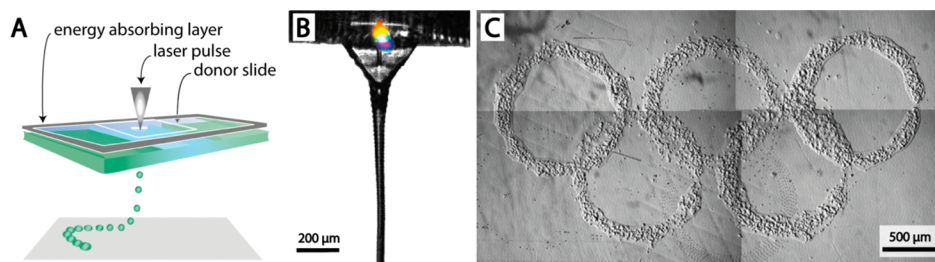


Figure 1. Laser-induced forward transfer (LIFT). (A) Schematic drawing of the process. Reprinted in part with permission from ref 27. Copyright 2013 John Wiley and Sons. (B) Close-up view of the jet generated by the incident laser pulse. Adapted with permission from ref 44. Copyright 2011 Springer. (C) Cell pattern printed with LIFT. Reprinted in part with permission from ref 39. Copyright 2010 Elsevier.

(AFA-LIFT). The main difference between those two techniques can be found in the donor slide setup. In the most frequently used MAPLE-DW setups, the donor slide comprises two different layers—a laser transparent support layer and a laser absorption layer. If the printing material itself is not absorbing light efficiently, it needs to be mixed with a matrix that will adsorb light and transfer the energy. In the case of cell printing, this matrix usually is a hydrogel, cell culture medium with addition of glycerol, or an extracellular matrix.³⁵ In contrast to that in AFA-LIFT and its related versions such as biological laser printing (BioLP), the donor contains three different layers—a laser transparent support layer, a laser absorption layer, and a layer with the deposition material (Figure 1A). The laser adsorption layer in general is a thin (about 100 nm) metal coating that absorbs the laser light, leading to evaporation of the coating. This evaporation leads to a high-pressure bubble expanding toward the surface and finally to material deposition. Although not obligatory,⁴³ the receiving substrate in modified LIFT processes for biomedical applications is mainly coated with a thin (20–40 μm) hydrogel layer that prevents the deposited material from drying and in the case of printing cells cushions the impact.³⁵ In the following section, we compare AFA-LIFT and MAPLE-DW in regard to printing hydrogels for biomedical applications.³⁶

As discussed, the main difference between MAPLE-DW and AFA-LIFT is the ribbon. In MAPLE-DW the light-absorbing matrix is mixed with the biomedical material. The heating within this layer and the irradiation with light might cause problems when printing sensitive materials, but as many researchers could confirm, it did not seem to have a negative effect on the cell viability.^{45–47} AFA-LIFT and BioLP use an additional light-absorption layer mainly from Au, Ti, or TiO₂.^{40,48,49} This layer protects the underlying biological layer from radiation-induced damage, but upon its evaporation the printed material will be contaminated. It could be shown that by using an energy conversion layer the reproducibility and resolution are enhanced (Figure 1C shows a 2D pattern printed with LIFT). Furthermore, this additional layer increases the selection of possible printing materials.³⁵

After having commented on the differences between the setups, we now briefly point out special demands on the material accompanied by the LIFT process. Using a laser as the driving force, the resolution of the LIFT techniques is mainly influenced by the laser energy and laser pulse duration, but also the material properties and the thickness of the deposition material layer will influence the propelled material volume. The laser pulse will evaporate material at the donor slide, leading to a vapor bubble. This bubble needs to expand toward the surface, finally leading to material ejection. As discussed by several groups,^{50–54} there is a distinct laser fluence leading to material jetting (jetting regime; see Figure 1B). If the fluence is too small, the bubble will collapse

(subthreshold regime), and if the laser pulse energy is too high, the bubble will generate undirected submicrometer droplets (plume regime). For a given laser fluence, the material properties will influence the bubble expansion. The thickness of the biological layer on the donor slide will influence the energy of the jettisoned material. The thicker the layer, the lower the amount of kinetic energy that will be transferred to the jet. In addition, the viscoelastic properties of the material will influence the propagation of the gas pressure. Finally, also the surface tension will determine material ejection.

2.2. Inkjet Printing

The process of inkjet printing is well-known from desktop applications. Many private users have printed 2D graphical printouts and maybe even refilled cartilages unwittingly, gaining experiences potentially useful for biofabrication. The first printers used modified setups and especially have cleaned and reused cartilages originally produced for desktop applications.⁵⁵ This straightforward approach in combination with the accessibility of printers led to a profound understanding of the inkjet printing process for biomedical applications. In the following section, we give a basic overview of the different setups. For a more detailed discussion of inkjet printing, we refer the reader to a variety of excellent reviews dealing with the inkjet technology and material properties for inkjet printing.^{56–63}

Inkjet printing can generally be operated in two modes. In continuous inkjet (CIJ) processes, the ongoing generation of drops creates a jet. Usually these drops are individually charged and deflected by a second pair of electrodes for printing. Droplets that are not needed for printing are collected in a gutter and can be reused. CIJ is primarily used as a fast process for marking and coding of products. The second inkjet printing mode is drop-on-demand (DOD) printing. Here drops are only generated when needed for printing. DOD is the setup well-known from consumer inkjet printers used for 2D graphical printouts. The working principle is based on an actuator generating triggered pulses, leading to the ejection of a defined material volume from a reservoir. Ideally, on its way to the substrate, the ejected material will transform into a single drop being collected on a predefined position on the substrate. As shown in Figure 2A, there are mainly two possible driving forces for pulse generation applied for DOD printing. In thermal inkjet printers, a heater is used to evaporate its surrounding ink, generating a vapor bubble that leads to ejection of material. Simply put, the droplet generation is triggered by an electrical pulse leading to a temperature increase in the heater accompanied by ink evaporation and material ejection. Material is also expelled from the reservoir using piezoelectric actuators. Here the applied voltage will generate a distortion of a piezoelectric crystal, leading to triggered ejection of material. In the next two sections, we discuss the benefits and

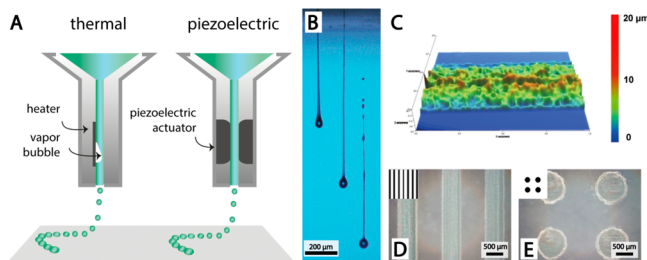


Figure 2. Inkjet printing. (A) Schematic drawing of the process. Reprinted in part with permission from ref 27. Copyright 2013 John Wiley and Sons. (B) Example for propelled material after ejection at different time points using a drop-on-demand printer. Adapted with permission from ref 61. Copyright 2008 IOP Publishing. (C) Surface profile of a linear pattern printed with inkjet-printed poly(lactic acid-co-glycolic acid) (PLGA). (D, E) Different patterns of PLGA printed with a piezoelectric inkjet. Panels C–E adapted with permission from ref 64. Copyright 2010 Elsevier.

disadvantages of the different inkjet printing methods described above with a focus on hydrogel printing for biomedical applications.

The main disadvantage of CIJ for laboratory-scale and biomedical applications is the high material throughput accompanied by the continuous stream of drops. Compared to other printing methods used for these applications, more material is needed, and concerns regarding sterility and potential material property changes due to processing might arise when the material is reused. In contrast, the DOD process uses material very efficiently and can also handle small batch sizes, making it highly interesting for small-scale and nonindustrial applications. In addition, the spatial resolution of DOD inkjet printers is higher than for CIJ systems.⁶⁰

In thermal inkjet printers, the temperature of the heated resistor can reach about 300 °C.⁵⁷ Nevertheless, Xu et al.⁶⁵ and other groups—as reviewed by Boland⁵⁶—were able to print viable cells using thermal DOD printers. It is believed that the short duration of heating pulses in the range of several microseconds only leads to a slight temperature increase (a few degrees) of the bulk material, not negatively influencing the cell viability.⁶⁵ Setti et al.⁶⁶ could also print enzymes with negligible loss of activity using a thermal inkjet. As pointed out by Saunders et al.,⁶² further research on the influence of thermal damage while printing biomolecules needs to be undertaken to establish thermal inkjet printing in the field of biomedicine. Due to this concern, most researchers working with inkjet printers for biomedical application use piezoelectric DOD inkjet systems to avoid ink property changes by heat exposure. Another important benefit of piezoelectric actuators in contrast to thermal actuators

is that they allow for an easy change of the piezoelectric crystal distortion and thus in the pulsing. This again enables controlling the ejected material volume and velocity of the created drop, making the process more flexible to parameter adjustment depending on the material characteristics.⁶⁰

We now analyze inkjet printing from a material scientist's perspective and thus focus on the material properties that are decisive for this method. Inkjet printing as a noncontact printing method with typical working distances of 1–3 mm⁶² can be divided into three crucial steps: (1) ink ejection, (2) drop formation during flight, (3) impact and interaction of drops after collection on the substrate. The ink ejection and possible expelling mechanisms have already been discussed. It has to be taken into account that typical nozzle sizes are in the range of 20–30 μm.⁵⁷ This limits the viscosity of ink used for biomedical applications to values that are typically below 20 mPa s⁻¹. In addition to the viscosity, the ejection may be influenced by the wetting behavior and thus for a given nozzle by the surface tension of the ink, as wetting of the nozzle may lead to spray formation rather than jet formation.⁵⁸ Surface tension is also critical for the second step and is typically in the range of 20–70 mJ m⁻² for graphical prints.⁶² In inkjet printing, each pressure pulse should ideally generate an individual droplet, but the dispensed material is initially composed of a leading drop accompanied by a tail that can break up into satellite drops (see Figure 2B) during flight,⁶¹ decreasing the resolution. Drop formation in inkjet processes is complex and cannot be discussed in detail in context of this work. Interested readers are referred to the work of Fromm,⁶⁷ Reis et al.,⁶⁸ and Jang et al.⁶⁹ Briefly, these works used a dimensionless number defined as the ratio between the Reynolds number and the square root of the Webber number. They used this to determine printable materials for DOD inkjet printing. Further research investigating drop formation with a focus on bioprinting was done by Xu et al.⁷⁰ The third crucial step during inkjet printing is the impact and interaction of drops after collection on the substrate. Depending on the droplet velocity (typically in the range of 5–10 m s⁻¹⁶¹) and material properties, the drop will splash or keep its shape after impact (examples for different patterns fabricated with inkjet printing are shown in Figure 2 C–E).⁶⁰ Typically, inks spread on surfaces and increase their size, limiting the resolution of the method to approximately 75 μm for bioprinting applications.⁷¹ As shown by Sirringhaus et al.⁷² for inkjet-printed polymer transistors, substrate surface energy patterning can further increase the resolution. Also changing the surface charge can increase the printing resolution as shown by Cobas et al.⁷³ These surface modifications can be applied on 2D constructs when printing dots or lines. When printing lines or structures, drop overlap is needed and interaction between the droplets



Figure 3. Robotic dispensing. (A) Schematic drawing of robotic dispensing showing the different mechanisms of ejection. Reprinted in part with permission from ref 27. Copyright 2013 John Wiley and Sons. (B) Magnified view showing material dispensing from the needle and collection onto a substrate. (C) Stereomicroscopic image of a printed Pluronic F127 construct.

Table 1. Comparison of Fabrication Systems

feature	modified LIFT	inkjet	robotic dispensing	refs
material viscosity range	1–300 mPa·s	3.5–12 mPa·s	$30 - 6 \times 10^7$ mPa·s	14 , 38 , 64 , 76 , 82
mechanical/structural integrity	low	low	high	77
resolution	10–100 μm	~75 μm	100 μm to mm range	31 , 71 , 83 , 84
working principle	noncontact	noncontact	contact	
nozzle size	nozzle free	20–150 μm	20 μm to mm range	84 – 86
load volume	>500 nL	mL range	mL range	31
cheap/easily interchangeable reservoirs	yes	no (if using commercial printer cartridges)	yes	
fabrication time	long	long to medium	short	
preparation time	medium to high	low to medium	low to medium	14
commercially available	no	yes	yes	77
costs for printer	high	low	medium	14
advantages	accuracy	affordable, versatile	printing of large constructs in cm range	31 , 77
disadvantages	ribbon fabrication, not suitable for constructs in mm range	nozzle clogging	accuracy	31 , 77

must be considered. The surface energy is crucial for those interactions, and they need to be stable enough to keep their geometry previous to solidification.⁶² To generate uniform lines, the spacing between the drops has to be adapted.^{74,75} In cases where inkjet printing is used for 3D printing, surface modification methods cannot be applied because droplets need to be collected on top of each other. Here interactions between the droplets are even more important than for generating 2D structures with droplet overlap,⁷⁴ making creation of 3D structures highly dependent on droplet solidification.

2.3. Robotic Dispensing

Especially during the past few years, a large number of great reviews dealing with technologies applied in biofabrication have been published.^{11,12,14,26,27,76–78} All of these reviews also discuss the process of robotic dispensing, displaying how promising this comparatively new technique is for the field of biofabrication. This is mainly due to the fact that robotic dispensing allows production of 3D objects with sizes and dimensions relevant for biomedical applications in short processing times. In the following section, we will give an introduction to the different setups (**Figure 3A**) used for biomedical applications termed robotic dispensing.

Robotic dispensing is mainly used for printing 3D constructs from continuous filaments. Material is loaded into a reservoir and dispensed through a nozzle. By automated movement of the nozzle relative to the build plate, constructs can be generated in a layer-by-layer fashion. The driving mechanism of dispensing can generally be either pneumatic or mechanical. In the most frequent pneumatically driven setup, the valve triggering material ejection sits between the inlet of the pressurized air and the material. Mechanically driven dispensing is mainly screw- or piston-based. Piston-based systems eject material triggered by controlling the linear displacement of a plunger. The displacement of the piston can directly be related to the dispensed volume. In screw-driven systems, rotation of the screw transports the material to the nozzle and is thus responsible for dispensing. The material feed can be controlled not only by the screw rotation speed but also by the screw design.²⁷ All robotic dispensing systems have in common that material is dispensed through a fine nozzle determining the resolution of the process.⁷⁶ As known from industrial dispensing applications, the design of the nozzle has a big effect on the dispensing homogeneity. Because most printer setups for biomedical application use

disposable and interchangeable needles, it is important to choose the right needle with respect to the given ink properties. In their latest review, Dababneh et al.⁷⁷ pointed out that further improving the nozzle design might be necessary in the field of bioprinting. Combining the fundamentals of the work of Yan et al.,⁷⁹ who mathematically modeled the forces cells experience during printing, with nozzle-design-dependent shear stress analysis during dispensing might help to improve cell survival. In the next section, we compare the different robotic dispensing modes explained above and again focus on processing of hydrogels for biomedical applications.

Utilizing a concept known from thermopolymer extrusion, screw-driven systems are the method of choice when it comes to processing high-viscosity materials because they are able to generate high pressures for material dispensing. Tailoring the screw design helps to adjust the process in regard to the feed rate and dispensing homogeneity. Having the most complicated setup in addition to being able to generate the highest shear stresses makes screw-driven systems the least applied approach in biofabrication. From an engineering point of view, pneumatically driven systems have the easiest setup. Nevertheless, applying high pressure typically makes them more suitable for processing higher viscosity materials than piston-driven systems.⁷⁶ Being able to deal with a broad range of pressures and thus with a broad range of material viscosities makes pneumatic dispensing the most versatile robotic dispensing mode. Using pressurized gas to apply a dispensing force at the same time implies its biggest disadvantage. The gas used for dispensing is compressible, which will result in a delay between the material flow start/stop signal and actual dispensing start/stop. This problem can be addressed either by applying a time delay before reaching the printing position and a vacuum to stop dispensing or by using a valve sitting just in front of the orifice. Piston-driven systems have the most direct control over dispensing. As described above, the linear piston displacement directly leads to material ejection. Because most printers use disposable syringes made from plastics, the maximum dispensing pressure is limited by the stability of the piston and the quality of the sealing between the piston and barrel. Taking into account that at the laboratory scale dealing with small batch sizes might be necessary, piston and pneumatic systems using disposable barrels that can be emptied nearly entirely will be preferential to screw-driven systems where material will remain in the system.

Just as the other fabrication techniques, robotic dispensing also puts specific demands on material properties. In contrast to inkjet printing where single droplets are required in robotic dispensing, collection of a continuous strand is crucial (Figure 3). The material properties need to be designed in a way that avoids strut breakup.⁷⁸ Schuurman et al.⁸⁰ could influence drop formation of low-viscous gelatin methacrylamide solutions by introducing high molecular weight hyaluronic acid. Using 20% (w/v) gelatin methacrylamide solutions resulted in drop formation at the needle tip. Adding 2.4% (w/v) hyaluronic acid changed the viscoelastic properties of the ink, and strands could be generated, highly improving the printing fidelity. As mentioned by Lewis,⁸¹ printing functional 3D structures using robotic dispensing places high demands on the inks. Ideally, the inks should even self-support when spanning features need to be printed. When it comes to building a 3D construct layer-by-layer, the interaction of the substrate and the first layer is crucial and the wetting behavior needs to be adjusted. This can be done by choosing the right material combination or the right ink composition⁸⁰ or by surface modification as mentioned in section 2.2.

2.4. Comparison of the Fabrication Methods

Now that the different fabrication systems for biomedical applications have been described, we compare those techniques with regard to hydrogel processing. Table 1 shows a comparison of the main differences and features of the printing methods. For more detailed information, the reader is referred to a variety of reviews.^{14,27,31,77} These reviews will also offer a good overview of the applications and give an excellent insight into the state-of-the art research and latest developments in the field of biofabrication. Some further excellent reviews focus on material systems for biofabrication and connect bioink to the fabrication techniques and applications.^{27,28,31}

In the following paragraph, the fabrication processes will be investigated and compared from three different aspects: (i) material and structural, (ii) processing, and (iii) economical. From a material and structural point of view, robotic dispensing is the most versatile process. It enables generation of constructs from a wide range of material viscosities displayed in Table 1. Robotic dispensing mainly uses interchangeable needles and thus allows the nozzle diameter to be easily adjusted to the dispensed material's viscosity. In contrast to the other processes, it deposits a material filament instead of a single droplet and thus increases the structural integrity. For many applications, the most important processing aspect is the resolution. Modified LIFT processes offer the highest resolution followed by inkjet printing. The process with the lowest resolution is robotic dispensing. Inkjet printing and LIFT as noncontact techniques allow deposition of material with jetting distances of about 1–3 mm. The benefit of noncontact deposition is that it allows printing onto surfaces that do not need to be smooth. Ovsianikov et al., for example, used BioLP to print cells into a 3D scaffold fabricated with two-photon polymerization.⁸⁷ From a material research point of view, the amount of material needed for the process and material throughput are important—especially when materials are synthesized on the laboratory scale. The methods where the least material is needed are LIFT-based processes. Here, usually very small material amounts in the range of several hundred nanoliters are processed. The disadvantage that accompanies this small material demand is of course that this process only allows the building up of small-scale constructs.³¹ Even though high-throughput versions of modified LIFT

techniques have been developed for tissue engineering applications,³⁸ they still have the lowest material throughput of all discussed techniques. Robotic dispensing allows fabrication of constructs on the millimeter scale in a reasonable time, but depending on the nozzle diameter can easily generate throughputs in the range of milliliters per minute. From an economical point of view, we first compare the processes with regard to fabrication and preparation time. Of course, fabrication time goes along with resolution. If high resolution is not needed and big constructs such as clinically relevant implants are to be fabricated, robotic dispensing is the method of choice. In robotic dispensing and inkjet printing, the preparation times are low, and preparation mainly consists of filling a reservoir that can be as big as several milliliters. In modified LIFT techniques, a thin film of material needs to be applied to the ribbon, and when the material is used (one ribbon usually contains several hundred nanoliter volumes of material), a new ribbon needs to be prepared, increasing the preparation time. From a different point of view, using ribbons can also be beneficial. On one hand, the preparation is time-consuming, but on the other hand, the material cost for the ribbon—it mainly consists of a glass coverslip—is very low. Just as the needles, in robotic dispensing, the reservoirs are disposables and can be easily purchased from industrial or medical supply companies. Although the trend is changing—more and more specialized systems are available—most researchers use modified desktop inkjet printers for biomedical applications. Using off-the-shelf printers is accompanied by high costs for new printheads compared to those of the other techniques. Even if cartridges are reused, the preparation is time-consuming. Of course, the benefit of using modified printers also needs to be taken into account. They are cheap and available and can easily be fixed. In robotic dispensing, scientists also started to use modified low-cost open source printers. Nevertheless, there are commercially available systems that are adapted to the special needs of material dispensing for biomedical applications, and most researchers prefer this more expensive alternative. Contrary to the other methods for modified LIFT techniques, there are no commercially available printing systems available⁷⁷ to date. The high resolution of the process further necessitates using expensive high-precision actuators.

3. RHEOLOGICAL CONSIDERATIONS

After having discussed the different fabrication systems and the demands put on the inks by these techniques in the last section, we now take a closer look at rheological aspects important for designing printable hydrogels for nozzle-based dispensing. This section can only introduce the topic generally, since the variety of different hydrogel inks and their molecular properties (molecular architecture, molecular interaction, ink formulation, ion strength, colloidal components, reactive processes, etc.) have a strong influence on the respective individual behaviors. However, the information given in this section is intended as a basis and starting point for bioink design and development.

From a rheological point of view, printing using nozzle-based systems can be considered as material flow through a contraction followed by tube flow. After the material is ejected and deposited onto the collector, it needs to undergo a fast phase transition obligatory to preserve the shape and thus enabling fabrication of 3D structures. As highlighted in the Introduction, the rate of this process is crucial for printing and is one of the biggest differences in demands between injectable and printable hydrogel systems. After discussing some fundamentals of liquid dynamics in the

next sections, we will subsequently increase the complexity of the regarded models, approaching toward printable inks highlighted with examples of applied ink systems. For further review on liquid dynamics and polymer rheology, we refer the reader to a, by far not complete, list of excellent literature dealing with this topic.^{88–93}

3.1. Rheology of Non-Newtonian Liquids

Liquids can generally be divided into two categories: Newtonian and non-Newtonian. For Newtonian fluids, the viscosity is independent of the shear rate, whereas, for non-Newtonian liquids, the viscosity tensor exhibits a shear-rate-dependent behavior (Figure 4). This dependence can be used to separate

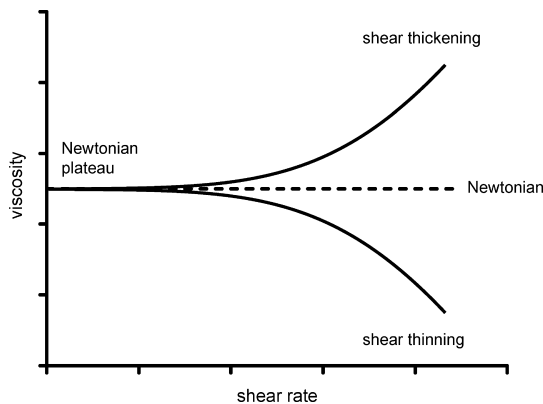


Figure 4. Viscosity against shear rate for Newtonian and different non-Newtonian fluids.

non-Newtonian liquids mainly into the following types: shear thinning, shear thickening, thixotropic, and rheopectic. A complete list with example systems developing the different properties can be found elsewhere.⁹⁰ As shown in Figure 4, shear thinning materials show a decrease of viscosity with increasing shear rates. Despite very low molecular weight materials, most polymer solutions show this behavior. Polymeric liquids further usually depict a linear plateau at low shear rates called zero shear viscosity (also low shear viscosity or first Newtonian plateau). This linear plateau is, in the literature, often set on a level with yield stress, but there is a difference between those two phenomena that can, for example, be observed at low shear. By definition, yield stress materials will not flow—also taking into account the very long time scales—until a critical stress, the so-called yield stress, is exceeded. In contrast to that, the majority of the systems discussed in this review will flow—even at observable shorter time scales—under shears beneath the shear stress plateau. This led to an ongoing⁹⁴ debate about the yield stress concept.^{95–97} For practical applications this discussion seems to be somewhat excessive and most researchers stick to the concept.⁹⁸ Nevertheless, it is important to be aware of the difference as this may, under certain circumstances, have an impact on printing. Although not displayed in Figure 4 non-Newtonian polymeric liquids usually evolve a second plateau called high-shear viscosity or second Newtonian plateau.⁹¹ Since in most cases, this plateau is only slightly higher than the solvent viscosity, the second Newtonian plateau is not relevant for printing processes.

Another interesting phenomenon observed for non-Newtonian fluids is thixotropy. Especially when analyzing only limited shear rate ranges, viscosity against shear rate plots of thixotropic materials are often similar to those of shear thinning materials,

but there is a very distinct difference: thixotropy is time-dependent, whereas shear thinning is not. This becomes obvious when the viscosity is plotted against time for a constant shear rate. For shear thinning fluids, the viscosity will be constant, but for thixotropic materials, it will decrease with time. A detailed discussion of thixotropy and also the hysteresis that can be examined by measuring material properties during increasing and decreasing shear rates is not within the scope of this paper and is described elsewhere.^{99,100} In terms of printing, the time-dependent viscosity thixotropic materials depict is important and must be considered as it might lead to inhomogeneous dispensing.

Shear thickening (see Figure 4) is the opposite of shear thinning and is characterized by an increase of viscosity with increasing shear rates. Also, just as shear thinning has shear thickening as its counterpart, rheopectic materials evolve characteristics opposite thixotropy. It is obvious that these both behaviors are not favorable for printing applications.

3.2. Important Aspects of the Printing Process

For printability of non-Newtonian fluids, it is important to take into account flow phenomena known from other technical applications such as injection molding as summarized briefly by Larson et al.¹⁰¹ and Irgens¹⁰² and detailed in the papers of Barnes⁹¹ and Shenoy.⁹⁰ In accordance with the rheological discussion above, especially the phenomenon of extrudate swell—also known as the Barus effect—is of interest. The practical observation accompanied by this phenomenon is the increase of the jet diameter after material exits the orifice of the tube it was flowing through. This observation is mainly limited to elastic materials such as polymer solutions⁹¹ and can in simple terms be explained as follows: Flowing through the tube, the material is compressed by the given confinement, and the polymer chains are stretched. After the material is ejected, it will expand due to the elasticity of the chains and their partial relaxation, so that the diameter of the jet will increase. Extrudate swell especially needs to be taken into account for high-resolution printing using robotic dispensing. Usually, by adjusting the process parameters—mainly the deposition speed—it is possible to compensate this effect at least to some extent.

As mentioned above, a very important property for printable hydrogels and thus a crucial parameter to take into account during ink development is the recovery rate of transition to the solid state after printing. To achieve shape fidelity, the material must undergo a rapid structural change and keep its shape after dispensing. The faster the material gels after ejection the higher the resolution of the resulting structure. In the case of recovering materials, the interactions between the molecules will strongly influence the transition and the time it takes after flow stops. Although the aspect of solidification is important for injectable materials too—for that reason we will take this class of materials into account in the following sections—the conditions are much more stringent for printable systems, as the nozzle diameters used for printing are smaller and the time acceptable for gelation is shorter.

Summarizing this discussion, from a rheological point of view, an ideal ink for hydrogel printing combines the following characteristics:

- Physical gel formation before printing with a shear thinning but not thixotropic behavior down to a viscosity that allows printing with the selected technology.

- Rapid regelation after printing for shape fidelity at high resolution.
- No or little pronounced extrudate swell.

If cells are part of the formulation, the viscosity before printing must allow mixing and homogeneous 3D distribution of cells throughout the printing process without affecting the viability. Cell sedimentation that might lead to nozzle clogging and/or uncontrolled inhomogeneous cell distribution through the printed construct must be avoided. Also, shear forces cannot exceed limits tolerable for cell survival.^{79,103} Hence, cell aggregation during the time frame of printing is usually not beneficial as it affects the shear-rate sensitivity.

In practice, a combination of these parameters is hard to achieve. Especially the regelation rate after printing remains a challenge. Hence, printed hydrogel structures usually have to be stabilized if real 3D structures are to be obtained. One strategy is to double print with a Thermoplast, resulting in a 3D interdigitating structure of hydrogel and Thermoplast, thus mechanically reinforcing the construct.^{104,105} Most commonly, the printed hydrogels are stabilized by postfabrication treatment, increasing the cross-linking density of the network, for example, by incubation in a solution that contains physical or chemical cross-linker molecules, or by UV illumination if hydrogel components are equipped with photopolymerizable groups. These strategies are in principle undesired necessities for suboptimal inks and will briefly be summarized and discussed in section 4.

3.3. Underlying Molecular Concepts: Colloidal Solutions

In the following sections, we introduce some basic particular and molecular concepts that comply with the terminology and the ideas gained from discussing non-Newtonian fluids. One of the simplest models able to depict non-Newtonian fluid behavior is a so-called hard-sphere system. This can be considered as a monodisperse suspension of spherical particles in a Newtonian fluid not experiencing interparticle and particle–liquid interactions. Although there are only a few real model systems showing all necessary properties,^{106,107} there is some general knowledge one can gain from that model, such as the fact that non-Newtonian characteristics will only be developed when concentrations are high enough.

When interparticle interactions are additionally taken into account, these interactions are manifold and will strongly influence the rheological properties of the particulate systems, inducing suspensions to be able to depict all known non-Newtonian behavior.¹⁰⁷ The general character of interparticle interactions can be distinguished using the concept of interaction potential energy,¹⁰⁶ which helps to describe the resulting forces and relevant length scales. Roughly, these interactions can be separated into electrostatic, steric, electrosteric, and structural. Mentioning the relevant length scales of these interactions underlines why the properties of suspensions will be concentration-dependent. At low solid loadings, the particles will not alter the linearity of the Newtonian fluid because the distances between particles are much bigger than the length scales of the interactions. Increasing the loading, interactions will more likely appear. If interparticle interactions dominate over Brownian motions, so-called rest structures can form.⁹¹ In the case of repulsive interactions, this will result in pseudolattice structures, whereas, in the case of attractive interactions, the particles will aggregate. When shear is applied to those systems and is slowly increased, these structures will first withstand the generated forces and then will be rearranged due to the reversible

character of the interactions. Depending on the interaction properties, this can lead to a macroscopic shear response comparable to a first Newtonian plateau or even induce yield stress. A further increase in shearing results in permanent disintegration of the aggregates and nonrestored arbitrary particle distribution after shearing. The shear-induced velocity gradient leads to an orientation of the particles that enables them to move over each other more freely. This in turn leads to shear thinning or in the case of attractive interactions also to thixotropy.¹⁰⁸ Generally, such systems will depict a second Newtonian plateau if all particles show the orientation and, by disruption of those layer orientations, show shear thickening with further increasing shear rates. If shearing stops, the particles will return to a rest structure.⁹¹ Of course, these descriptions are very pictorial, and there are theoretical models that represent the properties of the suspension more adequately.^{91,109–111} Furthermore, scientific descriptions of colloidal suspensions are also discussed in specialized literature.^{106,108} In the next section, we give an example of how colloidal systems can be exploited for ink development.

As described, particle interactions are crucial for the properties of suspensions and thus need to be considered when designing colloidal inks as shown by the Lewis laboratory. Jennifer Lewis and co-workers transferred knowledge from ceramics science to develop concentrated colloidal gel-based inks for direct-writing applications.¹¹² Over the past few years, they have generated inspiring work,^{113–115} continuously improving their inks by analyzing and controlling interparticle forces. Here, we use one of their earlier systems¹¹⁶ as it comprises a model system containing monodisperse silica microspheres that displays their meticulous scientific work on developing printable colloidal inks. Coating the colloids with poly(ethylene imine), they exploited the concept of electrosteric¹⁰⁶ interparticle forces to tailor the viscoelastic properties of the system. Electrostatic interactions between negatively charged silica particles and positively charged poly(ethylene imine) induced strong ionic interactions between the two species. In addition, changing the pH of the solution, they were able to vary the ζ potential of the coated particles and found the point of zero charge to be at a pH of about 10. At this pH, the absence of electrostatic repulsion between the colloids led to a system strongly flocculated by van der Waals forces and thus to a fluid-to-gel transition. Finally, they added cellulose as a thickening agent to increase the ink viscosity and reduce the flocculation kinetics, even enabling fabrication of unsupported spanning structures that are considered to be the most difficult structures to print using robotic dispensing systems.

In describing ceramic colloid systems to a nonexpert, it might seem strange that there are only a few real systems displaying the properties of the hard-sphere model. However, due to surface charges, even uncoated rigid ceramic particles will depict an interaction potential energy longing for a classification as soft-sphere systems.¹⁰⁶ Taking into account that spheres can also be deformable will be the next step approaching toward the description of polymeric systems. As outlined before, low concentrations of hard spheres in a solution will not change the Newtonian character of the liquid they are suspended in. Nevertheless, they will increase the viscosity by deviating the fluid flow lines.⁹¹ By shear-induced shape adaptation, deformable particles will lead to less deviation and thus to a less pronounced viscosity increase considering shear.¹⁰⁷ For higher concentrations, this will further result in more pronounced shear thinning. This effect contributes to the extraordinary properties of blood.¹¹⁷ Under shear, red blood cells will deform,¹¹⁸ enabling

blood to flow even through the tiniest capillaries in the human body. For synthetic systems, the particle elasticity also has a major impact on the rheological properties as reviewed by Vlassopoulos et al.¹¹⁹ They pointed out that colloid elasticity has an impact not only on flow-induced material response but also on the zero shear viscosity of colloidal suspensions and that the decrease of zero shear viscosity with increasing particle deformability is generally more pronounced at higher volume fractions. The models they considered for their review contained polymer coils and star polymers evolving the lowest elasticity of the discussed systems. Singh et al.¹²⁰ performed computer simulations of ultrasoft colloids under linear shear flow, showing that star polymers deform due to shearing. Furthermore, Huang et al.^{121,122} used simulations calculating that linear polymers will depict shear-induced decoiling and stretching accompanied by orientation along the flow direction. Huber et al.¹²³ could visualize the tumbling dynamics of semiflexible polymers under shear conditions by imaging fluorescently labeled actin molecules.

3.4. Underlying Molecular Concepts: Polymer Solutions

Polymer solutions are commonly used as model systems for soft colloids which lead to the field of polymer solutions. Just as for the hard-sphere model, the concentration will be crucial for the rheological response of such systems. At very low volume fractions, the distance between the chains will be larger than their size. These systems are called dilute. As already discussed for hard and deformable spheres, at very low concentrations, the solvent properties will not be altered significantly. Increasing the concentration results in coil overlap and leads to semidilute solutions. Although the solvent will occupy most of the volume, the coils will overlap and have a considerable impact on the rheological properties. Being able to overlap clearly distinguishes polymeric systems from the suspensions discussed before. Raising the solid loading further will lead to concentrated solutions dominated by coil interactions.⁸⁹ Printable hydrogels will usually depict concentrations in either the semidilute or concentrated regime, and thus, for the following discussions, only these systems will be considered. Even early models describing semidilute systems, not taking into account interactions other than topological, had to deal with coil overlap and with the concept of entanglements.¹²⁴ Although used in one context, it is important to mention that overlap and entanglement should not be put on one level. Semidilute and concentrated solutions are defined by coil overlap but do not need to be entangled.¹⁰⁷ For the chains to entangle, they will need to be long and flexible enough. Experimental results could show that there is a critical molecular weight for the formation of entanglements that depends on the flexibility of the polymer backbone.^{91,107} Entanglement can, however, only occur in semidilute or concentrated solutions. If chains are separated from each other, they will not be able to interact. To some extent, these findings are connected to each other. The longer the chains, the bigger their interaction potential and the higher the number of entanglements at the same concentration. Connecting the entanglement density to rheological properties, the concept of entanglements drastically changed the scientific understanding of polymers. Accompanied by the model of reptation, researchers were able to relate macroscopic polymer properties to the microscopic behavior of single molecules. Due to that, the concept of entanglements is an excellent example of how theoretical models can enrich and evolve general understanding. As we will not focus on models here, we refer the interested

reader to excellent reviews dealing with this topic^{101,125} and continue our argumentation describing general factors influencing the properties of semidilute and concentrated polymer solutions.

Aside from entanglements and the movement of polymer chains within semidilute/concentrated solutions, intermolecular interactions have to be taken into account. In general, an increase of concentration will increase the amount of interactions, and thus, polymer concentrations in solutions will have an influence on the rheological properties. As shown in Figure 5, a general

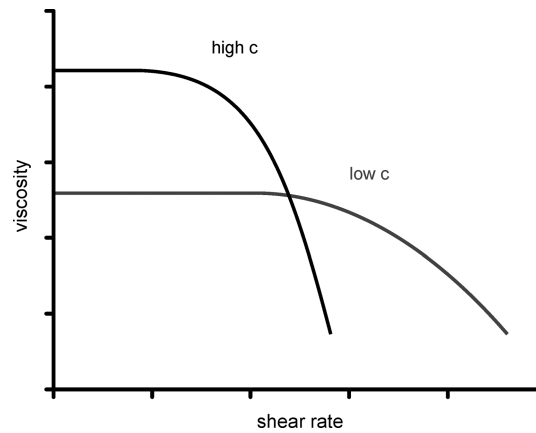


Figure 5. Viscosity against shear rate for high and low polymer concentrations (c) of a homopolymer solution in a good solvent.

observation dealing with polymer solutions is that with increasing concentration the zero shear viscosity is raised and the onset of shear thinning is shifted toward lower values.¹¹⁰ With increasing load volume, the viscoelastic properties will be more pronounced and lead to a bigger difference between first and second Newtonian plateau values.⁹¹ Another aspect is the influence of the molecular weight distribution on the rheological properties of polymeric liquids. Generally, it can be observed¹⁰⁷ that increased polydispersity influences the transition from Newtonian to non-Newtonian behavior. Solutions with a broader molecular weight distribution will evolve non-Newtonian properties at lower shear rates, but shear thinning will not be as pronounced, and the decrease of viscosity against shear rate will be broadened.

Recently, researchers have exploited this concept for designing printable materials. Although using materials with a broader molecular weight distribution was not the only aspect influencing the rheological behavior of the inks, they could tune the flow properties of their systems either by mixing batches of different molecular weight distributions of identical materials¹¹⁵ or by combining two types of materials with different distributions.¹²⁶ These examples show that modern inks usually are—from a rheological point of view—complex systems. The complexity is mainly introduced by interactions between the molecules and by molecule–liquid interactions. Due to the huge number of interactions, a closer rheological discussion is outside the scope of this review. We rather intended to present and discuss simplified basic views of rheological concepts aiming for a more generalized understanding of the possible system variations allowing control of the rheological properties.

3.5. Characterization of Rheological Properties

Although it is not the main focus of this paper, we briefly introduce some general aspects of rheological hydrogel analysis

before moving on to the next sections. Rheological characterization is often underestimated in terms of hydrogel design for biomedical applications.^{27,127} The spectrum of rheological characterization methods for hydrogels is nearly as manifold as the gels themselves, which sometimes makes comparability difficult, which contributes to delaying general systematic progress, especially for ink development. An excellent book describing rheological concepts and explaining the different characterization methods was provided by Malkin et al.¹²⁸ For a short overview focusing on hydrogel rheology, the interested reader is also referred to less detailed reviews.^{127,129}

As described, non-Newtonian fluids have shear-rate-dependent properties. Furthermore, their characteristics will be dependent on the kinetics and the magnitude of deformation. This needs to be considered when choosing the test parameters. They should be adapted to the processing and application conditions as closely as possible. In terms of biofabrication, we can roughly divide the measurement conditions into those that are adjusted for the fabrication step or, postfabrication, for the demands of the application. Due to the cellular component usually present in TE applications, postfabrication characterization is mainly limited to analysis of the linear viscoelastic properties of the printed hydrogels in the zero shear viscosity region under static or dynamic conditions. In contrast, fabrication conditions in the case of nozzle-based systems mainly long for characterizations of the shear thinning region and the recovery of the hydrogel after printing. Rheological measurements with alternating shear rates are a helpful tool to analyze the important recovery rate of printable materials. Eventually, the correct set of characterization method and conditions has to be selected for each ink system taking into account the envisioned application. Independent of the fabrication method and application, we nonetheless highlight the importance of rheology and underline that taking into account rheological considerations from the beginning is crucial for a rational and successful development of a printable hydrogel formulation.

This section has underlined how crucial the rheological properties of an ink are for successful printability. Before presenting the different strategies to induce intermolecular interaction and to design molecular components for printable hydrogels which will be discussed in sections 5 and 6, the following section will focus on the limitation of using chemical cross-linking for 3D printing and its potential and common use for postfabrication stabilization of constructs.

4. CHEMICAL CROSS-LINKING

As already introduced in section 1, hydrogels can be classified according to the mechanism of their formation in chemical and physical hydrogels. Physical hydrogels rely on noncovalent interactions between their building blocks for network formation. This makes the gels dynamic and endows them with self-healing properties;¹³⁰ however, this is often accompanied by low mechanical strength and stability, which is undesired in 3D printing for the final printed construct. Chemical hydrogels in contrast are formed through chemical reactions and the formation of covalent bonds that constitute the network. Hence, these networks are less dynamic but stable until forces are big enough to irreversibly break the covalent bonds. Such properties are ideal for generation of mechanically stable constructs. However, for the application of covalent cross-linking during 3D printing of hydrogels, an ongoing chemical reaction imposes a number of demands. A general challenge is noncontinuous printing with stop–go phases, since the chemical

reaction should not continue in the stop phase. Throughout the printing procedure, no or only very limited cross-linking should occur for the formulation remaining printable and also not significantly changing its behavior over time during printing, which would lead to structural inhomogeneity in the printed object. During or immediately after printing, the cross-linking should occur rapidly to ensure shape fidelity. These two demands are best met by two-component systems that rapidly react upon mixing. Such approaches have already been followed more than 10 years ago in work by Mülhaupt et al., who used isophorone diisocyanate for the cross-linking of poly(ethylene glycol) (PEG) and glycerin during 3D plotting, an approach which they termed “reactive plotting”.¹³¹ However, they did not plot a hydrogel but did create a water-swellable 3D hydrogel construct, and the chemistry used is not cytocompatible and would definitely not allow printing in the presence of cells.

Nonetheless, various *in situ* gelations via chemical cross-linking methods such as polymerization, classical organic reactions (e.g., Michael addition, click reactions), redox reactions, and enzyme-driven reactions were used for the generation of injectable hydrogels,^{132–134} and numerous cytocompatible cross-linking reactions for hydrogels are known and have been used for encapsulation of cells within hydrogels.¹³⁵ Moreover, a number of hydrogels have been developed that chemically cross-link via peptide sequences which are substrates for matrix-remodeling enzymes (so-called matrix metalloproteases, or MMPs),¹³⁶ so that chemical cross-linking can be combined with tailored specific biodegradability. However, a most critical challenge for printing cells containing covalently cross-linked two-component hydrogels remains the mixing step, as cells are sensitive toward shear rates, but on the other side, homogeneous mixing of the formulation has to be ensured in a short time.

4.1. Post- and Prefabrication Cross-Linking

In accordance to the discussion above, the main application of chemical cross-linking for hydrogel printing is postfabrication stabilization of the printed constructs. Therefore, the hydrogel precursors are endowed with chemically reactive groups, mostly photopolymerizable groups such as acrylates, and the printed construct is illuminated by UV light immediately after plotting. Examples for this approach are numerous, and the most common precursors used are poly(ethylene glycol) methacrylate,¹³⁷ poly(ethylene glycol) diacrylate,¹³⁸ polydiacetylene/poly(ethylene glycol) acrylate,¹³⁹ poly(2-hydroxyethyl methacrylate)/2-hydroxyethyl methacrylate,¹¹⁵ succinimidyl valerate (SVA)–poly(ethylene glycol)/gelatin/gelatin methacrylate/fibrinogen/poly(ethylene glycol) amine/atelocollagen,¹⁴⁰ hyaluronic acid/hydroxyethyl methacrylate-derivatized dextran,¹⁴¹ gelatin methacrylate,^{142,143} poly(ethylene glycol) diacrylate/alginate,¹⁴⁴ and GRGDS (Gly-Arg-Gly-Asp-Ser) acrylate/matrix metalloproteinase-sensitive peptide acrylate/poly(ethylene glycol) methacrylate/gelatin methacrylate.¹⁴⁵

Hyaluronic acid methacrylate/gelatin methacrylate¹⁴⁶ was chemically cross-linked before and after printing to tune the formulation properties for the printing process and stabilize the printed structure afterward. Combination of photoinitiated and thermal cross-linking after printing was also used to adjust the properties of gelatin methacrylamide/hyaluronic acid,⁸⁰ Lutrol,¹⁴⁷ and poly(*N*-(2-hydroxypropyl)methacrylamide lactate)–poly(ethylene glycol).¹⁴⁸ Finally, in some studies chemical cross-linking was solely performed prior to printing, for example, applying photopolymerization for poly(ethylene glycol) dia-

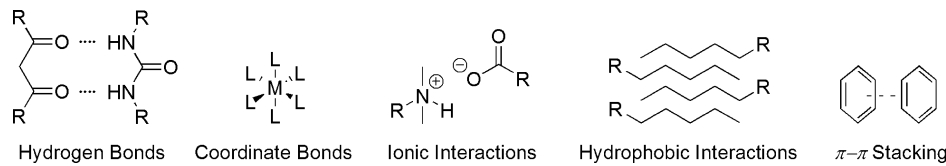


Figure 6. Basic physical molecular interactions exploitable for physical gel formation.

crylate,¹⁴⁹ gelatin methacrylate,¹⁵⁰ or Michael-type addition between thiolated hyaluronic acid/thiolated gelatin/four-armed poly(ethylene glycol) acrylate.¹⁵¹

Also combinations of different intermolecular interactions (ionic interaction and thermoswitchable hydrophobic interaction plus photochemical cross-linking) have been exploited for optimizing the formulation properties for poly(*N*-isopropylacrylamide)/*N,N'*-methylenebis(acrylamide)/poly(ethylene glycol) dimethacrylate before printing.¹⁵² The same strategy to combine different interaction types was also exploited with chemical reaction as the fixation step of the structure after printing. Examples comprise gelatin,¹⁵³ a gelatin/hyaluronic acid mixture,¹⁵⁴ a formulation containing gelatin, alginate, and fibrinogen,^{155,156} a mixture of gelatin and chitosan,¹⁵⁷ a fibrinogen/collagen formulation,¹⁵⁸ a collagen/agarose/chitosan system,¹⁵⁹ and a gelatin methacrylamide/gellan/alginate formulation.¹⁶⁰ Finally, systems containing alginate acrylamide/*N,N'*-methylenebis(acrylamide)/ethylene glycol and Ca²⁺ ions¹⁶¹ as well as alginate/poly(ethylene glycol) diacrylate/laponite and Ca²⁺ ions¹⁶² were ionically tuned for printability before and structurally stabilized through irradiation after the printing process.

4.2. Application of Dynamic Covalent Bonds for Printing

Some chemical bonds exhibit dynamic character after they have been formed, meaning that they are stable under some conditions but labile under others, or that they are in a constant equilibrium between two states. Examples of dynamic chemical bonds from nature are the switching of disulfides or thioester exchanges in biosynthetic processes. For a detailed and comprehensive presentation and discussion of such reversible and dynamic chemical bonds, we refer to excellent reviews on that topic.^{163,164} Chemical cross-linking toward networks that are covalently built up by such dynamic bonds is possible prior to the printing procedure and would allow, under the conditions necessary for the respective bond, reversibility of the cross-linked network during and after the printing, similar to the healing phenomenon in physically cross-linked systems. One example that has recently been exploited for hydrogel printing is the dynamic chemistry of imines.¹⁶⁵ Imine chemistry has been used for preparation of injectable hydrogels for several years, for example, through mixing of oxidized hyaluronic acid with chitosan. Gelation in this system was attributed to the reaction between aldehydes in the oxidized hyaluronic acid and amines of the chitosan.¹⁶⁶ A dynamic chemically cross-linked hydrogel system for bioplotting was prepared along this cross-linking rationale by cross-linking partially oxidized alginate with gelatin.¹⁶⁷ Imine formation resulted in gelation before plotting, but the gel could be printed using a robotic dispensing setup. The viscosity of the system facilitated good printability and sufficient stability of the printed structure so that the chemical cross-linking could further stabilize the construct. As a beneficial byproduct, gelatin improved the cytocompatibility of the system, and cells could be plotted with this system. In another example of a dynamic chemical bond, Meng et al.¹⁶⁸ used boronic ester

formation for supramolecular hydrogels based on boronic acid-modified alginate and poly(vinyl alcohol) under basic conditions. Step strain measurements show shear thinning behavior, e.g., at low strain $G' \approx 10^3$ Pa/ $G'' \approx 500$ Pa, and at high strain $G' \approx 400$ Pa/ $G'' \approx 600$ Pa with recovery properties. This combination of reversible chemical cross-linking with shear thinning and self-healing properties is very promising for printing applications. Furthermore, disulfide cross-linked hydrogels have been prepared from thiolated star-shaped PEG molecules and linear polyglycidols. Disulfide formation and thus gelation could be achieved and controlled under mild and cytocompatible conditions either by using alloxan as the catalyst¹⁶⁹ or by exploiting horseradish peroxidase without the need to add hydrogen peroxide.¹⁷⁰ The dynamic equilibrium between thiols and disulfides presents another attractive example of dynamic covalent bonds with potential application for printable hydrogel systems.

5. MOLECULAR PHYSICAL GELS

We now focus on physically cross-linked hydrogels. As highlighted in section 3, such gels inherently possess beneficial properties for the printing procedure due to the dynamic and reversible nature of their cross-links. Some of the established printable systems, most prominently alginate, belong to this group, and these will be included in this review for completion. However, our main focus here is to summarize fundamental principles for molecular assembly that have been developed in polymer chemistry and especially supramolecular chemistry, a very diverse field introduced by Jean-Marie Lehn,¹⁷¹ and outline their possible exploitation for the development of 3D printable hydrogels. These strategies all rely on a small number of basic and well-known interaction mechanisms such as hydrogen bonds, complex formation or coordination bonds, $\pi-\pi$ stacking, and hydrophobic and ionic interactions (Figure 6). These mechanisms found widespread application in different fields of research and, before entering a detailed discussion about promising examples for 3D printing, we give an overview on recent review papers and briefly summarize their contents.

Supramolecular polymer networks are a new class of materials which basically can be categorized into two kinds of macromolecular systems and are compared with respect to their formation, structure, and dynamics in a review by Sprakel and Seiffert:¹⁷² The first one is the “noncovalently bound monomer-based polymer” consisting of small units which interact physically and form a polymer network. The second is the “covalently bound monomer-based polymer” with “noncovalent chain interconnection” whose polymer backbone is covalently fixed, and the polymer possesses side chain functionalities for inter- and intramolecular interactions. A variety of functionalities for supramolecular systems with broad properties and numerous applications have been reviewed extensively by several research groups. Schalley and Qi¹⁷³ reported on macrocycles for functional supramolecular gels, including, e.g., crown ethers, cyclodextrins, and spiroborate cyclophanes, and highlighted different stabilization and gel–sol transition methods via

environmental stimuli. Rim-bound/appended macrocycles and host–guest complexes form stable gels and can be transferred into solutions via temperature/pH change or addition of competitive hosts or guests, e.g., applicable for the host–guest formation of crown ethers and secondary positively charged amines. Furthermore, they can be used for pressure-responsive materials which can recover back to their initial form. Qiao and co-workers¹⁷⁴ gave a deeper insight into cyclodextrin-based supramolecular assemblies and hydrogels. The variety of host–guest interactions with cyclodextrins is an interesting flexible cross-linking method for building blocks, e.g., polyrotaxanes, molecular tubes, and capsules. The different cavity sizes of the cyclodextrins (CDs), α -CD, β -CD, and γ -CD, allow binding of appropriate guest moieties such as poly(ethylene glycol), poly(caprolactone), and phenyl and adamantly groups. The host–guest formation was used for reversible sol–gel transition triggered by light and redox reaction. The morphology of host–guest-based supramolecular structures can be tuned via their overall amphiphilic character and was reviewed by Huang and co-workers.¹⁷⁵ Nanosheets, nanotubes, vesicles, and micelles can be formed in this way for different applications. Hereby, the molecular geometry and amount of hydrophilic and hydrophobic functionalities play an important role in the shape formation. Furthermore, organic compounds possessing π -systems form supramolecular gels via π – π interactions in solutions, so-called low molecular weight gelators. Ajayaghosh and co-workers¹⁷⁶ reported on π -gelators with functional groups which can also form different shapes via stacking, such as nanofibers, columns, and helices. Percec and co-workers¹⁷⁷ presented several complex systems based on dendron-mediated self-assembly. Depending on the molecular geometry, the solvent, and the amount of generations and functionalities, the formed supramolecular structures, such as nanocapsules and columns, can be controlled and are stabilized through π – π interactions and hydrogen bonds. With this wide pool of chemical functionalities and interactions, it is possible to tailor materials with new properties. Zhang and co-workers¹⁷⁸ reported on supramolecular polymers and highlighted the four most common interactions in this field with respect to historical development, preparation, characterization, and function. These are metal coordination bonds, multiple hydrogen bonds, and host–guest and donor–acceptor interactions. The dynamic nature of functional supramolecular polymers opens a wide field of applications in medicine and electronics for this new class of materials.¹⁷⁹ The design and use of these functionalities for supramolecular polymer gels was reported by Matushita and co-workers,¹⁸⁰ who explain some physical properties depending on the functionalities within the gel. Huang and co-workers¹⁸¹ gave further insight into the stimulus responsiveness of these materials induced, e.g., via light, temperature, and concentration. Self-healing supramolecular gels (Figure 7) were recently focused on and were reviewed with

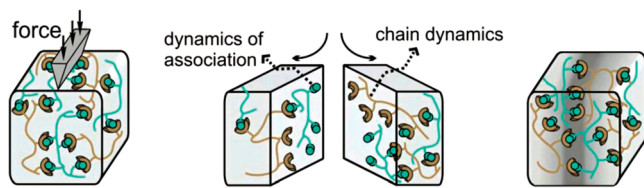


Figure 7. Concept of self-healing materials relying on the reversibility of physical interactions. Reprinted with permission from ref 183. Copyright 2013 John Wiley and Sons.

respect to the influence of basic molecular interactions within the material on its properties. For example, Hayes and co-workers¹⁸² and Binder and co-workers¹⁸³ reported on healable supramolecular polymers based on a variety of hydrogen bonds, donor–acceptor interactions, ionic interactions, and metal coordination, which allow the materials to recover after being damaged. Self-healing is also possible via constitutional dynamic chemistry and was reported by Chen and co-workers.¹⁸⁴ They gave an overview of physical and also chemical self-healing with a variety of healing conditions and efficiencies.

A variety of injectable hydrogels were reviewed by Li et al., who gave an overview of natural and synthetic polymers with a focus on gelation, biodegradation, and biomedical applications. Guvendiren et al.²⁵ summarized shear thinning hydrogels also for biomedical applications, such as peptides and synthetic polymers, and explained the criteria for these properties which are necessary for injection. Also, the necessity of reversible linkages in adaptable hydrogel networks for cell encapsulation was reviewed by Wang and Heilshorn.¹⁸⁶

This brief overview underlines the richness of literature and the multiple applications that rely on (supra)molecular interaction mechanisms. All these basic physical molecular interactions will be reviewed in the following section with respect to their chemical design and possible use for printable hydrogels. Therefore, we categorized them into four systems which will be explained in the following order: supramolecular polymer, supramolecular (low molecular weight gelators), macromolecular, and colloidal (solid particles, also in combination with the aforementioned systems) as depicted in Figure 8.

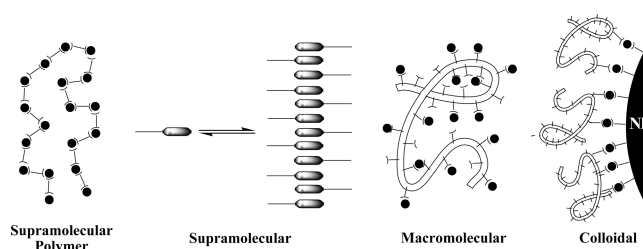


Figure 8. Supramolecular, macromolecular, and colloidal strategies for hydrogel formation.

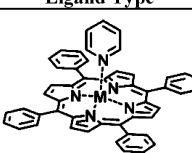
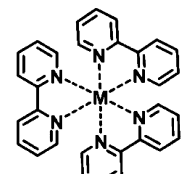
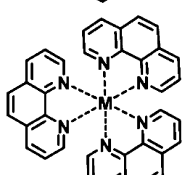
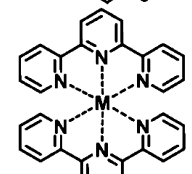
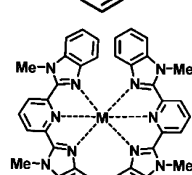
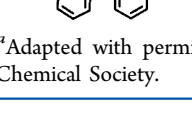
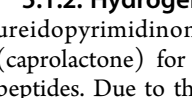
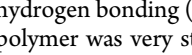
5.1. Supramolecular Approaches

5.1.1. Ionic Interactions and Coordination Bonds.

Dupin and co-workers developed a hydrogel containing chain-end-dithiolated PEG ($\text{PEG}(\text{SH})_2$) possessing 0.8 eq of Au^+ as a zigzag cross-linker.¹⁸⁷ A double-chamber syringe system with solutions of the components was used for the hydrogel formation during the injection. As the thiol's nucleophilic character depended on the pH value, the hydrogel's properties varied with this as well. For example, at pH 11, the thiol groups possessed a strong nucleophilic character and therefore led to a thiolate/ Au –S exchange which made the hydrogel dynamically flow up to a frequency of 0.9 Hz, after which the storage modulus G' became higher than the loss modulus G'' . In contrast, at pH 3.1, the nucleophilic character of the thiols was weaker, causing less thiolate/ Au –S exchange, and therefore, the hydrogel was more stable. Grande and co-workers used glutathione as a binding component to Au^+ with its thiol functionality.¹⁸⁸ Hereby, the pH value was varied to switch between the gel and sol states, which could be an interesting application for the pH-controlled gelation process. Mecerreyres and co-workers synthesized a

variety of polymer gels based on ionic interactions. They used (di/tri)carboxylic acids (e.g., citric acid) and (di/tri)alkylamines (e.g., *N,N',N'',N'''*-tetramethyl-1,3-propanediamine) which formed supramolecular polymers after a proton transfer.¹⁸⁹ Their storage modulus G' and loss modulus G'' were temperature-dependent, and G'' became higher than G' after the gel–sol transition temperature, which varied from 20 to 60 °C on the basis of the used monomers. Rowan and co-workers¹⁹⁰ used 2,6-bis(1'-methylbenzimidazolyl)-4-oxyypyridine for complexation of Zn^{2+} and La^{3+} , which formed shear thinning gels in acetonitrile. They could also be transformed to solutions via addition of acid or by heating. Generally, coordination bonds possess high binding constants and could be used with various metals and ligands for gel stabilization (Table 2).

Table 2. Examples of Metal-Coordination-Based Supramolecular Polymers^a

Ligand Type	Metal	K_a	Solvent/Counterion
	Zn^{2+}	$4.1 \times 10^3 \text{ M}^{-1}$	$CHCl_3/-$
	Co^{2+}	$1.0 \times 10^6 \text{ M}^{-1}$	Pyridine/OAc ⁻
	Zn^{2+}	$\sim 10^{13} \text{ M}^{-1}$	Aqueous KNO_3
	Zn^{2+}	$1 \times 10^{17} \text{ M}^{-1}$	Aqueous KNO_3
	Zn^{2+}	$2 \times 10^{14} \text{ M}^{-2}$	$CH_3CN/ClO_4^- /TBAPF$
	Fe^{2+}	$\sim 10^{21} \text{ M}^{-2}$	Water
	Zn^{2+}	$\sim > 10^6 \text{ M}^{-2}$	$CHCl_3/CH_3CN/ClO_4^-$
	Fe^{2+}	$\sim 10^{14} \text{ M}^{-2}$	

^aAdapted with permission from ref 178. Copyright 2015 American Chemical Society.

5.1.2. Hydrogen Bonds. Meijer and co-workers developed ureidopyrimidinone (UPy)/urea-end-functionalized poly(caprolactone) for binding with UPy/urea-end-functionalized peptides. Due to the strong association constant via quadruple hydrogen bonding ($K_a = 10^7 \text{ M}^{-1}$ in $CHCl_3$), the supramolecular polymer was very stable but also very flexible at the same time. The polymer was processed in a melt just below 80 °C, where the polymer possessed a low viscosity, and was used to produce fibers via electrospinning, films via solvent casting, and scaffolds via fused deposition modeling.¹⁹¹ Further supramolecular gels based

on interactions via hydrogen bonds were obtained by the same group.¹⁹² The dodecane-based monomer possessed UPy and urea functionalities on both chain ends and formed a supramolecular polymer in chloroform via stirring. Mechanically induced gelation is thermoreversible and could be transferred back into the monomer solution via an increase of the temperature. It showed shear thinning properties, whereas the loss modulus G'' became higher than the storage modulus G' in repeatable cycles. A pH-switchable and self-healing supramolecular hydrogel for injection was also investigated by Dankers and co-workers.¹⁹³ End-functionalized PEG possessed at both chain ends urea and UPy functionalities for hydrogel formation via multiple hydrogen bonds which could be controlled by the pH value. UPy groups could be deprotonated at pH 8.5 lowering the strength of the hydrogen bonds, and this led to a solution. The material also showed shear thinning properties in a neutral state and a basic state, where in both cases the loss modulus G'' became higher than the storage modulus G' . Repeatable dynamic strain amplitude tests of hydrogels containing 10 wt % UPy–polymer also showed self-healing behavior over four cycles. Binder and co-workers¹⁹⁴ synthesized end-functionalized poly(isobutylene) with barbituric acid groups and the Hamilton wedge with six hydrogen bonds which formed a gel with self-healing properties. Table 3 shows hydrogen donor–acceptor systems possessing different geometries, binding constants, and amounts of hydrogen bonds which could be used for gel stabilization.

5.1.3. Host–Guest and Aromatic Donor–Acceptor Interactions. Crown ethers interact with compounds containing protonated secondary amines via hydrogen bonds¹⁹⁵ by forming host–guest complexes and were used by several research groups as building blocks for supramolecular polymeric gels. For example, Huang and co-workers synthesized two complementary homoditopic compounds, one containing a crown ether and the other a protonated alkylammonium group.^{196,197} The formation of a supramolecular polymer via host–guest interaction was investigated at different concentrations in acetonitrile and chloroform. $[PdCl_2(PhCN)_2]$ was added as a cross-linker whose Pd^{2+} formed a complex with the triazole groups. The formed gel showed interesting properties: It could be transferred back to a solution by an external stimulus such as pH, temperature, or cations. Additionally, it showed shear thinning and self-healing properties. A gel containing 100 mM equimolar monomers with 60% cross-linker possessed a $G' \approx 10^4 \text{ Pa}$ and $G'' \approx 10^3 \text{ Pa}$ at low strain rates and reached its gel–sol transition at ~100% strain. Strain sweep measurements from 0.1% to 200% showed how the network could be destroyed and recovered back to the initial cross-linked gel. Zheng and co-workers synthesized a series of amphiphilic heteroditopic building blocks with the same functional groups for host–guest interaction as described before and additionally varied the crown ether group, alkylammonium group, or spacer.¹⁹⁸ The gelation process was investigated in water, acetonitrile, and DMSO, and the minimum gelation concentration varied from 0.6 to 4.3 wt % with different functional groups. It might be interesting to transfer a viscous solution into a gel via changing the concentration during printing. Similar supramolecular polymeric gels were investigated by Yin and co-workers, who incorporated additional terpyridine groups for complex formation with Zn^{2+} .¹⁹⁹ The material showed self-healing properties and reversible gel–sol transition via heating/cooling and addition of base/acid, ligands/ Pd^{2+} , and Zn^{2+} .

Table 3. Examples of Donor and Acceptor Hydrogen Bonds^a

Type	Example
Triple	 1 $K_a = 10^2 \text{ M}^{-1}$
	 2 $K_a = 10^4 - 10^5 \text{ M}^{-1}$
Quadruple	 3 $K_a \geq 10^5 \text{ M}^{-1}$
	 4 $K_a = 10^7 \text{ M}^{-1}$ Upy-Upy in CHCl_3
Sextuple	 5 $K_a = 10^7 \text{ M}^{-1}$ DeAP-DeAP in CDCl_3
	 6 $K_a = 10^6 \text{ M}^{-1}$ in CDCl_3
	 7 $K_a = 10^9 \text{ M}^{-1}$ in CHCl_3

^aAdapted with permission from ref 178. Copyright 2015 American Chemical Society.

Pillararene-based supramolecular polymer gels are novel materials stabilized via host–guest interactions. Wei and co-workers used copillar[5]arennes which possessed four 1,4-dimethoxybenzene units and either one 1-methoxy-4-dodecylbenzene (COP5–12) or one 1-methoxy-4-cetylbenzene (COP5–16) unit, forming supramolecular polymers via self-assembly in acetonitrile.²⁰⁰ Thereby, the hydrophobic alkyl chain interacted with the aromatic benzenes via $\text{CH}\cdots\pi$ interactions, and the formed gels showed reversible gel–sol transition via a temperature change (68 °C for COP5–16 and 52 °C for COP5–12). Additionally, the gels possessed self-healing properties; e.g., a gel (20 wt % COP5–16 in acetonitrile) returned back to its initial form after being torn apart for 1 mm within 45 min. To get a hydrophilic supramolecular pillararene-based gel, Yao and co-workers introduced four 1,4-bis((2-ethoxy)-trimethylammonium)benzene units and one 1-methoxy-4-cetylbenzene unit.²⁰¹ The self-assembly in water was also driven by $\text{CH}\cdots\pi$ interaction of the alkyl chain with the benzene units. The rodlike fiber network also showed a gel–sol transition via temperature. Zheng and co-workers developed amphiphilic calix[4]arenes by acylation of the amino groups of the calix[4]arene with dicarboxylic anhydrides which formed supramolecular hydrogels.²⁰² As the gel was not completely stable in water, at least 5% (v/v) ethanol was needed to be added to the solution. They investigated the gel stability from 5% to 25% (v/v) ethanol and showed that with a higher amount of

ethanol the suspension–gel temperature and gel stability increased. These amphiphilic compounds are interesting for forming hydrogels but could be improved as ethanol is harmful for cells and the sol–gel temperature might be tuned by addition of other compounds. Table 4 shows host molecules with associated guest molecules.

Table 4. Examples of Host–Guest Interactions^a

Host Molecules	Molecular Structures	Typical Guest Molecules
β-Cyclodextrin		Adamantane, coumarin
Cucurbit[8]uril		Methyl vologen, charged naphthalene, anthracene and alkene
Calixarene		Charged alkane, viologen
Crown Ether		Viologen, charged amine
Pillarene		Charged imidazole and DABCO

^aAdapted with permission from ref 178. Copyright 2015 American Chemical Society.

Rowan and co-workers²⁰³ designed copolymers possessing π -electron-deficient naphthalenediimide units and π -electron-rich pyrenyl-end-capped polyamides which form self-healing supramolecular materials via $\pi\cdots\pi$ stacking. After damage, the aromatic groups were stretched and could interact again by heating to 87 °C with a recovery of 100% of the material. This concept of $\pi\cdots\pi$ stacking was mostly used for self-healing materials with different polymers and is summarized in Figure 9. Hayes and co-workers filed a patent²⁰⁴ which described similar end-functionalized polymers with $\pi\cdots\pi$ stacking for inkjets.

5.1.4. Low Molecular Weight Gelator. Ravoo and co-workers developed tripeptides Fmoc-L-Cys(Acm)-L-His-L-Cys-OH (1) and Fmoc-L-Cys-L-His-L-Cys-OH (2) which formed supramolecular gels in water with shear thinning properties.²⁰⁵ The Fmoc groups allow the $\pi\cdots\pi$ stacking for stabilization of the gel with a minimum gelation concentration of 1.5 wt % which possessed a storage modulus $G' \approx 10^3 \text{ Pa}$ at low strain decreasing

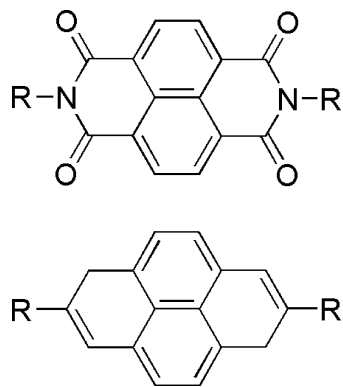


Figure 9. Examples of the two majorly used aromatic groups for donor–acceptor interactions.

to ~ 1 Pa at 100% strain-amplitude sweep for peptide **1**. The viscosity decreased as well for peptide **1** by 6 orders of magnitude with increasing shear rate. Ulijn and co-workers explored the biocatalytic induction of supramolecular gel formation using Fmoc- and methyl ester-terminated dipeptides.²⁰⁶ With these end groups, a solution was present, and just after addition of the hydrolytic enzyme from *Bacillus licheniformis*, which hydrolyzes the methyl ester, a gel was formed via self-assembly of the peptide. The subsequent hydrolysis was investigated with different concentrations of enzyme, and the gelation was confirmed via determination of the melting temperature. The greater the number of enzyme units added, the greater the amount of gel formed, and therefore, the melting temperature increased. The same group developed further interesting hydrogels based on Fmoc-functionalized short peptides.²⁰⁷ The gel–sol/sol–gel transitions might be an interesting tool for printing and stabilizing hydrogels which can be tuned in different ways. Gelation of cyclic dipeptide derivates was induced by Feng and co-workers.²⁰⁸ They used cyclo(L-Phe-L-Lys) and cyclo(L-Tyr-L-Lys) possessing N-acetylated D-(+)-gluconic acid for gel formation, which showed different sol–gel transition temperatures depending on the gelator concentration and perturbation.

Further low molecular weight gelators containing aromatic groups for stabilization of gels via π – π stacking and possessing thermoreversible properties were synthesized by the research group of Schmidt.^{209–211} For example, they used 4-(octanoylamino)benzoic acid and 4-alkoxyanilines, which formed a gel upon addition of sodium hydroxide. Varying the ratio of the base led to different amounts of formed gels and therefore to different gel–sol transition temperatures. Zhang and co-workers²¹² developed a naphthalene-based gelator which formed organogels with different gel–sol transition temperatures dependent on its amount. For example, a gel containing 0.5 wt % gelator possessed a gel–sol transition temperature of ~ 42 °C, and a gel containing 2.0 wt % gelator possessed a gel–sol transition temperature of ~ 58 °C. The group of Stupp²¹³ also used π – π stacking for hydrogel formation with quinquethiophene–oligo peptide sequences at low concentrations. The thiophene groups were modified with amphiphilic peptide residues which improved the water solubility and in addition led to self-assembling via β -sheet formation. The gelation time was dependent on the concentration, e.g., 5 days for 1 wt % and 3–5 h for 3 wt %. While this appears to be too long for cell printing, the gelation time may significantly be optimized for bioink development, for example, by using a multivalent approach with functional polymers. Moreover, gelation times of several hours up to days are not per definition detrimental to biofabrication if the resulting network is dynamic as most recently demonstrated for 3D printing of cell-loaded recombinant spider silk protein hydrogels stabilized via β -sheet formation (see section 6.1.2).

5.2. Macromolecular Gels

5.2.1. Naturally Occurring Biopolymers Used for Hydrogel Formation. Biopolymers have frequently been used in biofabrication, especially since they exhibit excellent bioactivity.^{24,214,215} A broad range of biopolymers has been investigated to assemble injectable/printable hydrogels for biomedical applications. This section summarizes the recent progress on biodegradable and injectable hydrogels fabricated from naturally occurring biopolymers such as polysaccharides

Table 5. Natural Biopolymers Used To Form Injectable or Printable Hydrogels for Biomedical Applications

biopolymer	3D printing technique	applications	refs
Polysaccharides			
alginate	laser-induced forward transfer, inkjet, robotic dispensing, extrusion	tissue repair (myocardial), nerve regeneration, delivery system (drugs, proteins, cells, genes), wound healing	39, 40, 56, 83, 161, 162, 167, 185, 219, 221–223, 225–241
chitosan	extrusion	tissue repair (cartilage, nerve), drug delivery, cancer therapy	185, 242, 243
agar/agarose	robotic dispensing	tissue repair (cartilage), nerve regeneration	138, 159, 214, 222, 236, 244–248
cellulose	robotic dispensing	tissue repair (cartilage), wound healing	222, 233, 249, 250
hyaluronic acid	robotic dispensing, extrusion	tissue repair (cartilage, brain, vascular constructs)	80, 141, 146, 151, 154, 166, 185, 242, 251, 252
chondroitin sulfate		tissue repair (cartilage), drug delivery, wound healing	185, 217, 242
gellan gum	inkjet	tissue repair (cartilage), drug delivery	253–256
Proteins			
collagen	inkjet, robotic dispensing	tissue repair (skin, liver, blood vessels, small intestine), delivery systems (drugs, proteins, cells)	20, 84, 238, 257–261
gelatin	robotic dispensing	tissue repair (cartilage), delivery systems (growth factors, cells), wound healing	150, 185, 239–241, 243, 259, 262, 263
fibrin/fibrinogen	inkjet	tissue repair (nerves, blood vessels, skin, tendons, ligaments, liver, eyes), drug delivery systems (drugs, proteins, genes), wound healing	185, 239, 264–269
silk	robotic dispensing	tissue repair (bone, cartilage), drug delivery	270–274
Mixture			
matrigel	robotic dispensing	tissue repair (liver)	275

(alginate, agarose) and proteins (collagen, gelatin, fibrin, silk). A further overview of hydrogels based on biopolymers applicable for 3D printing is given by Kirchmayer et al.²¹⁶

5.2.1.1. Polysaccharides. Polysaccharides consist of sugars linked via *O*-glycosidic bonds. Most of the polysaccharides are able to form hydrogels, on the basis of bonding (e.g., agarose) or intermolecular electrostatic interactions (e.g., alginate). A broad range of injectable and biodegradable hydrogels made of naturally occurring (or slightly modified) polysaccharides, such as chitosan, hyaluronic acid, alginate, and agarose, have been developed and tested for biomedical applications. For more detailed information, refer to Li et al.,¹⁸⁵ Thiele et al.,²¹⁷ and Table 5. Here, we focus on polysaccharides (alginate and agarose) already used in biofabrication.

Alginate is one of the most frequently used (bio)polymers for biofabrication due to its favorable biocompatibility and the capability to support cell survival and differentiation in culture. Alginate is a linear anionic polysaccharide containing homopolymeric blocks of 1,4-linked β -D-mannuronate and α -L-guluronate. Alginate hydrogels can form through different mechanisms. At pH values below 3, alginate self-assembles into acidic gels by the formation of intermolecular hydrogen bonds.²¹⁸ Furthermore, hydrogels can be formed by cooperative binding of divalent cations such as Ca^{2+} ions. Jia et al. have shown that alginate can be used as a bioink for bioprinting. The alginate-based bioinks were shown to be capable of modulating human adipose-derived stem cell functions without affecting their printability and structural integrity after cell culture.²¹⁹ In terms of alginate-based bioinks, unfortunately, the hydrogel's mechanical properties are quickly lost during *in vitro* culture (approximately 40% within 9 days). Further limitations are cellular responses differing dependent on the source of human and animal cells and the lack of bioactive binding sites.^{219–221} Furthermore, alginate was prepared of different concentrations and was cross-linked via addition of Ca^{2+} ions.^{39,40,56,83,105,222–232} Polymer concentrations and printing conditions were varied, leading to differences in the printing quality. For example, Guillotin et al.³⁹ used up to 1% (w/v) alginate solutions for printing and obtained well-defined constructs and high cell viability. Yan et al.²³² used alginate concentrations from 2% to 8% (w/v), but the higher it was, the more defined structures were obtained. Nanofibrillated cellulose/alginate²³³ was also fabricated with subsequent cross-linking via Ca^{2+} ions in solution.

Agarose, one of the main components of agar, consists of (1 \rightarrow 3)- β -D-galactopyranose-(1 \rightarrow 4)-3,6-anhydro- α -L-galactopyranose as the basic unit and ionized sulfate groups.²⁷⁶ Agarose gels through the formation of intermolecular hydrogen bonds upon cooling, resulting in the aggregation of double helices by the entanglement of anhydro bridges.²⁷⁷ The viscoelastic properties of agarose hydrogels depend on the molecular weight and solution concentration. The tunable elastic moduli of physical gels are between <1 kPa and a few thousand kilopascals, well in the stiffness range of natural tissues except bone.²⁷⁸ Furthermore, agar was recently used with poly(acrylamide) and poly(stearyl methacrylate) to form double-network hydrogels with self-healing properties which exhibit potential for printing as well.²⁷⁹ In 2009, Maher and co-workers produced 3D scaffolds made of thermoreversible agarose hydrogels by pneumatic robotic dispensing with a stainless steel cartridge which could be heated to 100 °C.¹³⁸ The agarose material was printed into a 3% (w/v) gelatin medium bath. The medium bath did not act as a cross-linking agent but merely as a construction support site.

Dispensing of agarose without the incorporation into the gelatin medium bath resulted in the distortion of individual layers and in most cases caused the scaffolds to collapse.¹³⁸ Furthermore, human mesenchymal stem cells were encapsulated within agarose hydrogels and subsequently printed into 3D structures supported in high-density fluorocarbon. This high-density hydrophobic liquid mechanically supported the cell–hydrogel constructs during the printing process. Three-dimensional structures with various shapes and sizes were manufactured, and the resulting cell-laden hydrogel constructs remained stable for more than 6 months. Live/dead and 4',6-diamidino-2-phenylindole (DAPI) staining showed viable cells 24 h after the printing process, as well as after 21 days in culture.¹⁵⁹ Thermal gelation was used for a variety of hydrogels after printing, such as agar,^{244,246} agarose,^{222,247,248} and methylcellulose.²²²

A large number of bacterial extracellular polysaccharides (EPSs) have been recently reported to be useful for biomedical applications. Compared to polysaccharides extracted from plants or algae, bacterial EPSs have improved physical properties.²⁸⁰ Examples of reported bacterial EPSs for biomedical applications include xanthan gum, gellan gum, dextran, bacterial alginate, and bacterial cellulose. Although most bacterial EPSs are composed of repeating sugar units with varying sizes and degrees of ramification, some have an irregular structure, such as bacterial alginate. The properties of the EPSs are determined by their chemical composition, molecular structure, average molecular weight, and distribution.²⁸¹ Good examples for the correlation between chemical properties and functionality are gellan and xanthan gum. While xanthan gum forms double helices without creating a gel structure, gellan gum forms a macroscopic gel.²⁸² At high temperatures (~30 °C), the linear molecules of gellan are in a disordered coiled state which turns into double helices upon cooling. At high concentrations (>2%, w/v), the double helices changed to thicker rodlike aggregates and formed the gel.²⁸³ The final gel properties were dependent on the content of the acyl groups. In a highly acylated form, two acyl substituents such as D-acetate and D-glycerate were present. The acylated form produced thermoreversible, elastic, and flexible gels, whereas the deacetylated type formed hard, nonelastic, and brittle gels.²⁴⁹ Recently, endotoxin-free low-acyl gellan gum has been used as a bioink for the reproducible printing of several cell types.²⁵³ A commercial microvalve deposition system and many-nozzle piezoelectric inkjet printheads have been used for printing. The gellan gum kept cells stable in suspension, preventing the settling and aggregation of cells and showing stringent fluid properties during printing.²⁵³ Additionally, deacetylated gellan gum was thiolated to prepare injectable gellan hydrogels which can be physically and chemically cross-linked *in situ*. The thiolation does not alter the hydrogel formation properties of gellan gum, but leads to a lower phase transition temperature under physiological conditions and to stable chemical cross-linking.²⁵⁴

5.2.1.2. Polypeptides/Proteins. Collagen is the most abundant protein in mammalian bodies, accounting for 20–30% of the total protein, and therefore, it is of interest to be used in biofabrication.^{217,242,284} The main functions of collagen in tissues are to provide mechanical support and to control cell adhesion, cell migration, and tissue repair.²⁸⁵ All fibrous collagens have a triple-helical structure with three parallel polypeptides, α -chains, coiling around each other and forming a right-handed triple-helical chain. Collagen is easy to process and modify, and its abundance, nonantigenicity, biodegradability, and biocompatibility render collagen a promising candidate for biofabrication.²⁸⁶ Moon et al. developed a modified inkjet printer

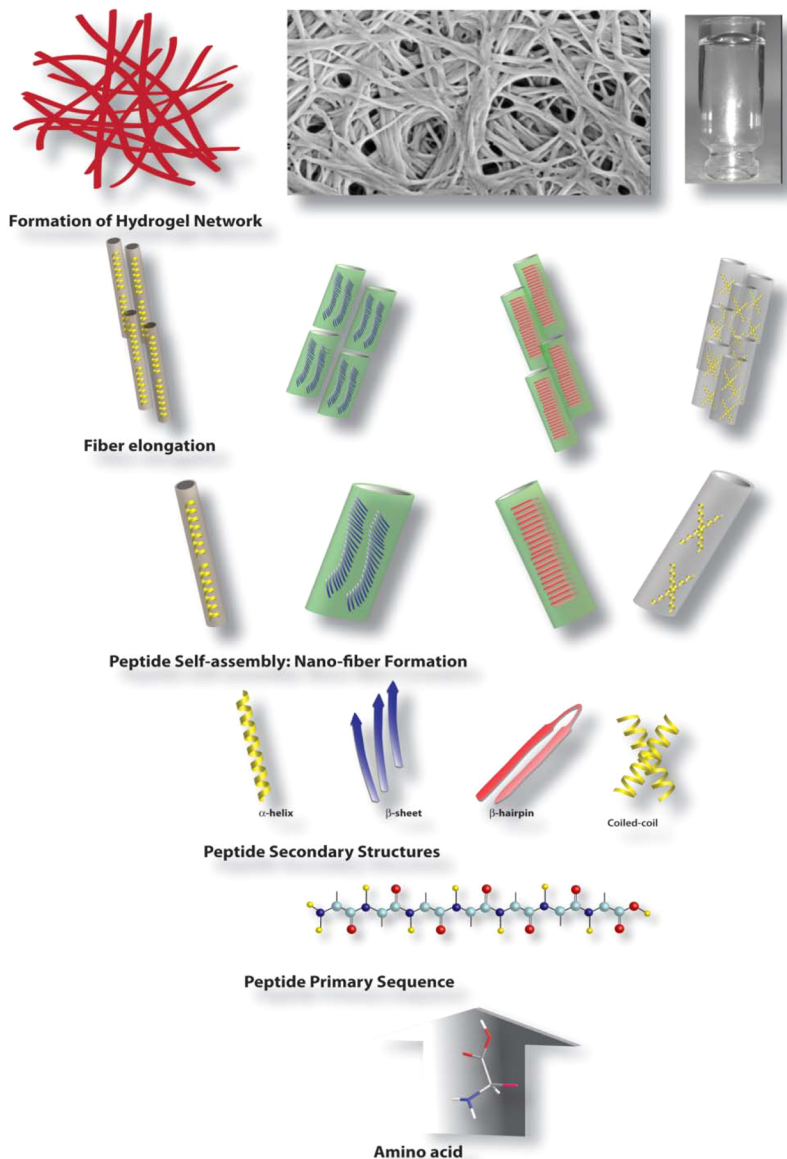


Figure 10. Stepwise formation from amino acids to hydrogel networks. Reprinted with permission from ref 311. Copyright 2013 Royal Society of Chemistry.

using mechanical valves for processing high-viscosity hydrogel precursors, such as collagen solutions, and prepared cell-laden collagen hydrogels using bladder smooth muscle cells.²⁵⁷ However, collagen bioinks suffer from batch-to-batch variations, loss of shape and consistency due to shrinkage, and poor mechanical properties (elastic moduli around 1 kPa).^{84,287} Additionally, it remains especially difficult to sterilize it without alterations of its structure.²⁵⁸ Collagen type 1 was printed as well with subsequent cross-linking with sodium bicarbonate,^{259,288} and a mixture of alginate/collagen type 1 was also reported for printing.²³⁸

Gelatin is partially denatured collagen.²⁸⁹ Compared to collagen, gelatin is less immunogenic, and can be used as a bioink due to its biodegradability, biocompatibility, natural cell-adhesive Arg-Gly-Asp (RGD) motifs, and water solubility.^{20,80,150,262,290,291} However, the gel formation is solely based on physical intermolecular interactions of the gelatin molecules, and the resulting gels are not stable under physiological temperature, but can be cross-linked.²⁹² A mixture of alginate/

gelatin/fibrinogen²³⁹ was fabricated with subsequent cross-linking via Ca^{2+} ions in solution. Thermal gelation was also used for gelatin,²⁵⁹ acetocollagen,²⁶⁰ collagen type 1,²⁶¹ collagen/gelatin,²⁵⁹ matrigel,²⁷⁵ and gelatin/chitosan.²⁴³ Gelatin/alginate was also reported with a double-cross-linking method via temperature and ions.^{240,241} A novel work by Kirchmajer and Panhuis²⁹³ describes a very strong hydrogel based on gelatin/gellan gum cross-linked via genipin and Ca^{2+} ions whose properties can be tuned via the composition.

Fibrin is another example of a specialized extracellular matrix protein with potential applications in biofabrication. Fibrin is formed by thrombin-initiated aggregation of fibrinogen into a network of fibrils.^{294,295} The mechanical properties are governed by the initial concentration of fibrinogen and/or thrombin.²⁹⁶ Fibrin is biocompatible, cell adhesive, and biodegradable, and fibrin hydrogels undergo enzymatic degradation (through activated plasmin) within 2 weeks in cases where no fibrinolytic inhibitors, such as aprotinin, are added.^{297,298} Recently, fibrin was used as a printable hydrogel for inkjet printing to build 3D neural

constructs. 3D neural sheets were generated by alternate printing of fibrin gels and NT2 neuronal precursor cells.²⁶⁴ Since fibrinogen and thrombin can both be easily purified from blood, they offer the opportunity of using an autologous source for making the scaffold.²⁶⁵ However, there are also disadvantages for using fibrin hydrogels as bioink: some fibrin hydrogels possess poor mechanical properties and undergo fast disintegration.^{267,268} The best fibrin hydrogels with mechanical integrity were transparent and stable for 3 weeks.²⁹⁹

Silks are natural protein fibers produced by Arthropoda such as spiders of the class Arachnida as well as insects of the order Lepidoptera. Native silk proteins are highly repetitive and are composed of crystalline domains periodically interrupted by helical or amorphous regions.^{300,301} Due to the absence of toxicity, slow degradation, absence of immunogenicity, and extraordinary mechanical properties, silk is particularly of interest for biomedical applications and biofabrication.^{271,302–305} The fabrication of patterned substrates from silk fibroin via inkjet printing was established²⁷³ by successfully patterning silk arrays by layer-by-layer deposition of dots composed of ionomeric silk proteins chemically modified with poly(L-lysine) and poly(L-glutamic acid) side chains. These “locked-in” silk nests remained anchored to the substrate during incubation in cell growth medium to provide a biotemplated platform for printing-in, immobilization, encapsulation, and growth of *Escherichia coli* cells. Overall, this fabrication process shows potential for the universal and large-scale fabrication of biocompatible dot array templates within a practical processing time scale. The microscopic arrays could be used as prospective biosensors.²⁷³ However, it could also be detected that a plain silk fibroin solution leads to frequent clogging of the needle due to shear-induced β -sheet crystallization.²⁷⁰ Recently, Das et al. provided a strategy for fabrication of 3D tissue constructs using a novel silk-gelatin-based bioink encompassing living progenitor cells and in situ cross-linking through a cytocompatible gelation mechanism.²⁷¹

The use of naturally derived proteins as bioinks is limited mainly due to their varying composition and purity, and they can elicit inconsistent or unwanted biological responses. Since mammalian tissues are the main source of proteins such as collagen, gelatin, and fibrin, further concerns exist regarding disease transmission and immunogenic responses.^{306,307}

5.2.2. Synthetic Peptides and Proteins. A novel method of cross-linking using hydrogen bonds was reported recently where polypeptoids were functionalized with grafted single DNA strands, forming a shear thinning hydrogel after addition of the complementary DNA strand which was used for 3D printing³⁰⁸ and injection.³⁰⁹ Hauser et al.³¹⁰ developed bioinks consisting of trimer, tetramer, and hexamer peptides which self-assembled into nanofibers. The gelation time could be tuned via the solvent (deionized water versus phosphate-buffered saline, PBS), concentration, and amino acid sequences. Various peptide/protein-based hydrogels are also available via solid-phase synthesis. Dasgupta et al.³¹¹ summarized the variety of peptide hydrogels and gave an overview of the relationship between molecular functionalization, conformation, and properties of the hydrogel. Condensation of amino acids first forms a primary peptide sequence which then forms secondary structures such as α -helix, β -sheet, β -hairpin, and coiled-coils. These peptides self-assemble into nanofibers and form a hydrogel network by elongation (Figure 10).

Apostolovic et al.³¹² gave further insight into coiled coils in a review concerning their history and possible applications.

Material properties and rheological measurements of different peptide- and protein-based hydrogels were summarized by Sathaye et al.,³¹³ and these hydrogels might be interesting inks for printing as they show shear thinning and rehealing properties based on their dynamic physical interactions. For example, Chen et al.³¹⁴ investigated a β -hairpin peptide hydrogel which was stabilized via hydrogen bonds within the amino acid units and showed shear thinning properties at the same time. They used different peptides with the sequences $\text{VKVKVKVKV}^{\text{D}}\text{PPTKVKVKV-NH}_2$, $\text{IKIKVKVKV}^{\text{D}}\text{PPTKVVKIKI-NH}_2$, $\text{VKVKIKV}^{\text{D}}\text{PPTKIKVKVK-NH}_2$, and $\text{IKIKIKIKV}^{\text{D}}\text{PPTKIKIKIKI-NH}_2$, where they varied the amount of L-valine and L-isoleucines in the peptide sequences. L-Isoleucine is more hydrophobic than L-valine and possesses a higher affinity to form β -sheets via hydrogen bonds. The hydrogel formation was triggered in a 4-(2-hydroxyethyl)-1-piperazineethanesulfonic acid (HEPES) solution containing 4 wt % peptide by adding Dulbecco's modified Eagle's medium (DMEM). Via dynamic frequency sweeps, it could be shown that with a higher amount of L-isoleucine the hydrogel formation was faster and the storage modulus G' and loss modulus G'' increased. Dynamic time sweep measurements of the peptide showed recovery to the initial G' value after removal of the strain. Schneider and co-workers^{315–317} investigated the rheological properties and the kinetics of $\text{VKVKVKVKV}^{\text{D}}\text{PPTKVVKVKV-NH}_2/\text{VKVKVKVKV}^{\text{D}}\text{PPTKVEVKVKV-NH}_2$ hydrogels in more detail. These are biocompatible and injectable and can be used for the encapsulation of cells. For further stabilization, the peptide sequence $\text{VKVKVKVKV}^{\text{D}}\text{P}^{\text{L}}\text{PTKVVKVKV}$ was modified by the same group³¹⁸ to $\text{VKVXVKVKV}^{\text{D}}\text{P}^{\text{L}}\text{PTKVVKXVKV}$ with X = lysyl sorbamide, which possessed double bonds for photochemical cross-linking. Bakota et al.³¹⁹ synthesized a peptide sequence called $\text{E}_2(\text{SL})_6\text{E}_2\text{GRGDS}$ which formed a hydrogel upon addition of Mg^{2+} . Its storage modulus G' was ~ 480 Pa at low strain, which afterward decreased with higher strain like the loss modulus G'' at $\sim 80\%$ strain. Step strain measurements were also performed and showed the material's shear thinning and recovery properties. It recovered over 75% within 15 s after strain was removed and up to 100% of its initial storage modulus within 10 min. A further temperature- and additionally ion-dependent shear thinning hydrogel was developed by Huang et al.,³²⁰ who used the peptide sequence FLIVIGSIIGPGGDGGD cross-linked in Ca^{2+} solution or under acidic conditions. For example, a hydrogel containing H^+ possessed $G' \approx 4 \times 10^3$ Pa at 5 °C, $G' \approx 3 \times 10^3$ Pa at 50 °C, and a hydrogel with Ca^{2+} possessed $G' \approx 150$ Pa at 5 °C and $G' \approx 400$ Pa at 50 °C. This might be an interesting hydrogel whose properties could be tuned via ionic interactions and temperature. The same research group³²¹ investigated the hydrogel formation of this peptide sequence with Ca^{2+} in different DMSO/water ratios and showed that the gel's stability increases with higher Ca^{2+} concentration and water content.

Werner and co-workers developed a series of noncovalently cross-linked hydrogels based on biomimetic peptide-heparin or receptor-ligand interactions exhibiting properties potentially exploitable for 3D printing. For example, they used four-arm star PEG which was functionalized with positively charged oligopeptides derived from L-lysine/L-arginine. When these polymers were mixed with heparin, the peptides interacted with the negatively charged sulfate groups from heparin and thus formed a hydrogel.^{322,323} Very low concentrations were sufficient for hydrogel formation (5 mM heparin, 2.5 or 5 mM star PEG-peptide conjugate), and the hydrogel's stability could be tuned

through variation of the peptide sequences. Another physically cross-linked hydrogel based on a more specific protein–receptor interaction was prepared by the same group through functionalization of PEG with biotin and interaction with tetrameric avidin.³²⁴ Biotin–avidin recognition resulted in hydrogel formation, and the receptor–ligand-stabilized hydrogel was investigated with respect to stiffness, swelling, and erosion in water and different PBS buffer concentrations.

Besides peptides/proteins, also synthetic biocompatible polymers such as poly(*N*-isopropylacrylamide)-*block*-poly(ethylene glycol)³²⁵ and Lutrol F127^{76,84,222} were printed and thermally stabilized. Physical cross-linking led to reversible interactions which ensured a constant viscosity during printing with a good biological compatibility.^{27,132} There are still capacities in this field, especially in the macromolecular design. The materials were hardly varied, showing a limitation which might be extended by using novel building blocks and functionalizations described in more detail in the following sections.

5.2.3. Host–Guest Interaction. Many research groups developed functional polymers cross-linked via host–guest interaction showing shear thinning properties which could be interesting for printing. Chen and co-workers³²⁶ synthesized poly(ethyl acrylate)-containing protonated dibenzylammonium moieties cross-linked with dibenzo-24-crown-8 bis(crown ether). The resulting gel was pH- and temperature-responsive and the gel–sol transition could be controlled via heating/cooling or by addition of base/acid. Additionally, it possessed self-healing properties, and strain amplitude sweep measurements showed that upon a strain of ~30% the loss modulus G'' became higher than G' . Furthermore, step strain measurements confirmed the material's full recovery after removal of the strain. Huang and co-workers³²⁷ used the same functionalities to produce gels but in the opposite way: They synthesized poly(methyl methacrylate) with pendant dibenzo[24]crown-8 ether groups and cross-linked them by addition of a secondary protonated bisammonium compound. This gel showed as well self-healing properties, pH responsiveness, and recovery after strain. Continuous step strain measurements displayed the repeatable changes of G' and G'' ; e.g., at a strain of 10⁴%, $G' \approx 0.1$ Pa and $G'' \approx 5$ Pa, whereas, after the strain was decreased to 1%, $G' \approx 100$ Pa and $G'' \approx 10$ Pa.

The research group of Burdick developed a series of injectable hyaluronic acid-based hydrogels. They modified hyaluronic acid separately with adamantane and β -cyclodextrin at the side groups³²⁸ in different ratios and investigated the influence of the degree of functionalization and ratio in water on the hydrogel formation, stability, and rheological properties. The storage modulus G' , loss modulus G'' , viscosity, and stability increased with higher amounts of functionalized hyaluronic acid in the hydrogel and with higher ratios of adamantane to β -cyclodextrin functionalities. For example, a hydrogel containing hyaluronic acid functionalized with 20% adamantane and 20% β -cyclodextrin each at 7.5 wt % in total possessed a yield stress at ~60% where the viscosity started increasing drastically and G'' became higher than G' . Continuous step strain measurements of the same hydrogel showed full recovery after several cycles. In a further work, the same research group additionally introduced thiol and Michael acceptor groups for a secondary cross-linking via Michael addition to the same host–guest-functionalized hyaluronic acid.³²⁹ In this work they investigated the effect of post-cross-linking on the stability of the hydrogel with different Michael acceptors, different pH values, and different amounts of

functionalized hyaluronic acid. Finally, Burdick and co-workers used these materials for 3D printing.²⁵² A hydrogel based on a mixture of hyaluronic acid with 25% adamantane and 25% β -cyclodextrin functionalities was printed into a more stable support gel consisting of hyaluronic acid with 40% of the same functionalities. Further stabilization of the constructs was achieved by additional functionalization with methacrylate groups which were used for UV-induced cross-linking.

Ravoo and co-workers used adamantane-functionalized hydroxyethyl cellulose for hydrogel formation via host–guest interactions with amphiphilic β -cyclodextrin possessing *n*-dodecyl chains on the primary side and oligo(ethylene glycol) groups on the secondary side of the macrocycle.³³⁰ These amphiphilic intermolecular cross-linked β -cyclodextrin vesicles are injectable and were investigated with respect to the storage modulus, loss modulus, viscosity, recovery, and different concentrations and host/guest ratios. The storage modulus and yield stress increased with higher amounts of host–guest functionalities in the hydrogel and could also be retransformed into solution by addition of free adamantane or β -cyclodextrin.

There are also other possible guest molecules for cyclodextrin, such as the linear PEG, which has been widely explored in this field. Ito and co-workers showed that the cyclodextrins threaded over PEG (rotaxanes) formed viscoelastic gels whereby two cyclodextrin units were connected with different groups, forming figure-eight cross-linkers.^{331–333} These are interesting functionalities as they are pressure-responsive, and the cyclodextrin units slide over the PEG chain when pressure is applied. The gel therefore avoids the external stimulus to a greater extent compared to chemically fixed cross-linking units, which makes this concept attractive for functionalization of polymers for designing tunable shear thinning properties. For example, the following research groups have developed injectable hydrogels based on the host–guest interaction of PEG with particular α -cyclodextrins: Chen and co-workers³³⁴ developed a reduction-sensitive supramolecular hydrogel based on [poly(ethylene glycol) monomethyl ether]-*graft*-[disulfide-linked poly(amidoamine)] with α -cyclodextrin with shear thinning properties. They investigated the influence of the added amount of dithiothreitol (DTT), which reduced disulfide bonds, on the storage modulus, loss modulus, and viscosity. For example, a gel without DTT possessed a viscosity at a low shear rate of ~135 Pa·s, and a gel with DTT/disulfide bonds at a 5/1 ratio possessed a viscosity of ~90 Pa·s, which both decreased upon a shear rate of 10 s⁻¹ to the second Newtonian plateau, which is near 0 Pa·s. Zhang and Ma³³⁵ prepared a polymeric prodrug (PEGylated indomethacin) which formed a supramolecular hydrogel by addition of α -cyclodextrin. They varied the amount of the host–guest compounds and investigated the influence on the storage modulus, loss modulus, and viscosity, which all decreased with lower host/guest ratios. A further series of host–guest-based supramolecular hydrogels was synthesized by Li et al.,³³⁶ who compared the properties of the triblock copolymer poly[(*R,S*)-3-hydroxybutyrate]–poly(ethylene glycol)–poly[(*R,S*)-3-hydroxybutyrate] (5×10^3 g mol⁻¹) with those of the high molecular weight PEG (27×10^3 g mol⁻¹) and oligo(ethylene glycol) methyl ether (MPEG) (4.7×10^3 mol⁻¹) by threading with α -cyclodextrin. The poly[(*R,S*)-3-hydroxybutyrate] units of the triblock copolymer led to an additional stabilization of the hydrogel due to hydrophobic interactions, and the hydrogel possessed shear thinning properties with a higher yield stress than the other hydrogels containing PEG and MPEG.

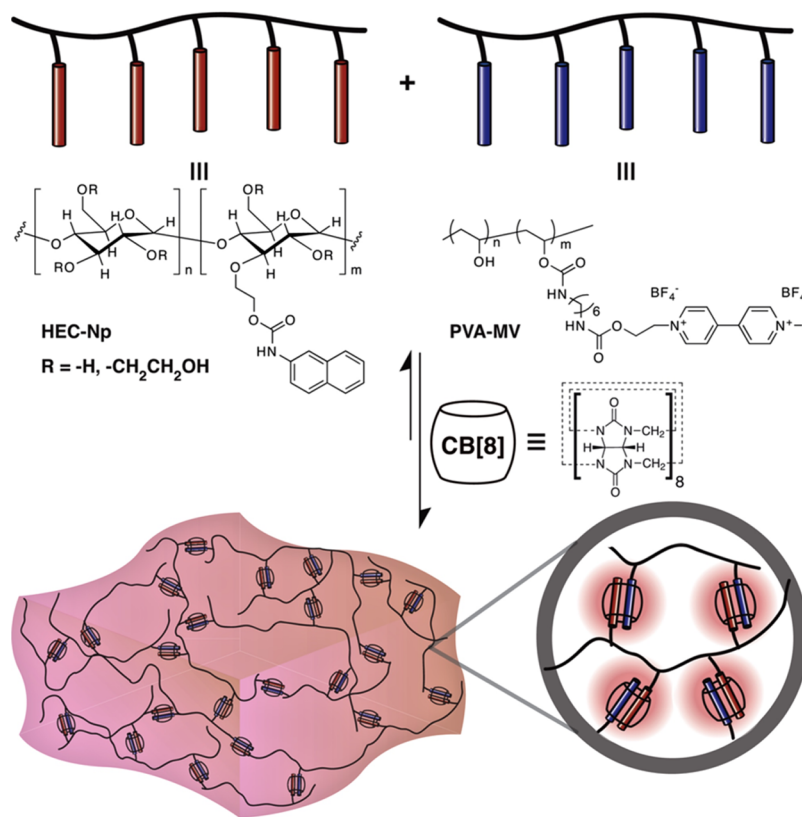


Figure 11. Supramolecular hydrogel with viologen/hydroxyethyl-functionalized cellulose and naphthalene-functionalized poly(vinyl alcohol) forming host–guest complexes with cucurbit[8]uril. Reprinted with permission from ref 343. Copyright 2012 American Chemical Society.

Tian et al.³³⁷ developed an injectable and biodegradable poly(organophosphazene) with pendant MPEG and glycine ethyl ester side groups for supramolecular hydrogel formation with α -cyclodextrin. They varied the chain lengths/amount of MPEG, amount of α -cyclodextrin, and polymer concentration and investigated the influence on the gel formation and the rheological properties. Dynamic step strain measurements showed the hydrogels' shear thinning and recovery properties. For example, a gel containing $5 \times 10^3 \text{ g mol}^{-1}$ MPEG at the side functionalities possessed a storage modulus $G' \approx 10^5 \text{ Pa}$ and a loss modulus $G'' \approx 1.4 \times 10^3 \text{ Pa}$ at 1% strain and $G' \approx 6 \text{ Pa}$ and $G'' \approx 40 \text{ Pa}$ at 100% strain. Wu et al.³³⁸ prepared an injectable electroactive supramolecular hydrogel. They used a copolymer based on ethylene glycol, sebacic acid, and xylitol with a carboxyl-capped aniline tetramer as a pendant side functionality whereby this and the ethylene glycol units formed host–guest complexes with γ -cyclodextrin dimers and led to hydrogel formation. It is interesting that the host–guest formation was conducted at the polymer backbone and at the side chain as well, which extends the possibility of functionalization and could be used for further tuning of the hydrogel's properties. As the aniline tetramer moiety is redox-active, this or other conducting groups might be used for further *in situ* modification of the hydrogel. Additionally, the reversible sol–gel transition can also be controlled via addition of 1-adamantanamine hydrochloride or γ -cyclodextrin dimer into the solution.

There are more compounds for host–guest interactions which were used for hydrogel formation showing controlled sol–gel transition. For example, Nakama et al.³³⁹ modified hyaluronic acid with different amounts of PEG chains along the side groups and added α -cyclodextrin for supramolecular hydrogel for-

mation. They investigated the effect of the degree of substitution and pH value on the gel melting temperature, which decreased with higher pH value/lower degree of substitution. Tomatsu et al.³⁴⁰ developed a redox-responsive hydrogel based on dodecyl-modified poly(acrylic acid), β -cyclodextrin, and ferrocenecarboxylic acid. A hydrogel was formed only with the polymer itself due to the hydrophobic interactions of the long alkyl chains. Addition of β -cyclodextrin led to preferential formation of stronger intramolecular complexes with the alkyl chains, resulting in solutions that exhibited a lower viscosity with rising β -cyclodextrin content. Upon addition of ferrocenecarboxylic acid, its higher association constant with β -cyclodextrin released the alkyl chains from the complexes and thus induced re-establishment of intermolecular interaction and hydrogel formation. The subsequent oxidation of ferrocenecarboxylic acid retransformed the hydrogel into a solution as the oxidized species were too big for the host molecules, which could form complexes with the alkyl chains again.

Loh³⁴¹ described in his review the variety of supramolecular host–guest-based polymeric materials containing cyclodextrins, cucurbit[n]urils, and calix[n]arenes (see section 5.1) and cucurbit[n]urils have received more attention in this field and might be interesting for designing polymers for physical cross-linking which could be used for printing. Cucurbit[n]urils can interact with many different hosts such as diaminohexane/spermine-containing³⁴² and viologen/naphthalene-containing³⁴³ polymers and form hydrogels. The latter work by Appel et al. described poly(vinyl alcohol)-containing viologen moieties and hydroxyethyl cellulose with naphthalene groups which formed host–guest complexes with cucurbit[8]uril (Figure 11). The hydrogels possessed very high water contents up to 99.7 wt

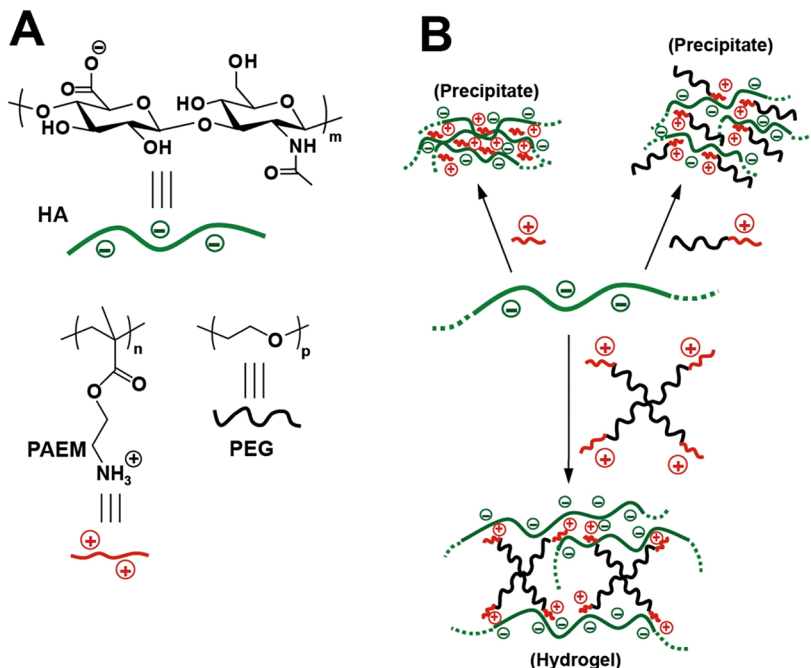


Figure 12. Hyaluronic acid- and PEG-based hydrogels. Adapted with permission from ref 344. Copyright 2015 John Wiley and Sons.

% and showed shear thinning properties and recovery after removal of the strain.

5.2.4. Ionic Interactions and Coordination Chemistry.

Cross et al.³⁴⁴ prepared injectable hybrid hydrogels based on negatively charged hyaluronic acid mixed with positively charged four-arm star poly(ethylene glycol)-block-poly(2-aminoethyl methacrylate) (Figure 12). Investigations were made concerning the influence of the star arm lengths, charge ratio, and osmolarity (pure water and phosphate buffer) on the gel formation; e.g., the most stable hydrogel was formed with $(\text{PEG}_{113}\text{-}b\text{-PAEM}_{12})_4$ and hyaluronic acid with a charge ratio of 1/1 in water. The star-shaped polymer acts as a cross-linker and has a positive influence on the hydrogel formation compared with the linear analogue, which led only to precipitations. Another PEG-based hydrogel stabilized via ionic interaction of charged side groups of the polymer was developed by Hunt et al.³⁴⁵ In this work, PEG was used as a macroinitiator for ring-opening polymerization of allyl glycidyl ether, which was subsequently functionalized with sulfonate, carboxylate, or guanidinium groups via thiol–ene click chemistry. The hydrogel's stability could be tuned via the acidity and basicity of the groups, e.g., a 1/1 ratio of carboxylate/ammonium gave a solution, whereas 1/1 carboxylate/guanidinium yields a stable hydrogel at 10 wt %.

A further shear thinning gel based on positive and negative charge interaction was developed by Wang et al.³⁴⁶ They synthesized poly(D,L-lactic acid-*co*-glycolic acid) nanoparticles coated either with poly(vinylamine) or with poly(ethylene-*co*-maleic acid) which formed a shear thinning network due to electrostatic interactions. If the polymer ratio and amount were decreased, the viscosity decreased as well, which could also be observed at high shear rates. For example, a gel containing 30% nanoparticles possessed a viscosity of $\sim 500 \text{ Pa}\cdot\text{s}$ and a gel with 20% nanoparticles possessed a viscosity of $\sim 175 \text{ Pa}\cdot\text{s}$ at a low shear rate, and both viscosities decreased significantly when a high shear rate was applied. Bünsow et al.³⁴⁷ developed mechanoresponsive polyelectrolyte brushes consisting of cationic poly[2-(methacryloyloxy)ethyl]trimethylammonium chl-

ide (PMETAC) brushes with a covalently attached fluorescent dye, 5(6)carboxyfluorescein. They investigated the pressure-dependent fluorescence quenching via atomic force microscopy, and upon application of force, the brushes were subsequently compressed due to the noncovalent electrostatic interaction. This might be an interesting approach for hydrogels functionalized with such groups to make them mechanoresponsive. The viscoelasticity and toughness of hydrogels could be controlled via the concentration of copolymers possessing cationic and anionic groups and the concentration of sodium chloride in the solution as shown by Gong and co-workers.^{348,349} They investigated different ionic pairs with the monomers sodium *p*-styrenesulfonate, 2-acrylamido-2-methylpropanesulfonic acid, [3-[(methacryloylamino)propyl]trimethylammonium chloride, [(acryloyloxy)ethyl]trimethylammonium chloride, and (*N,N'*-dimethylamino)ethyl acrylate and determined the swelling volume ratio, Young's modulus, the tensile/fracture stress, and the tearing energy of the materials. For example, a copolymer based on sodium *p*-styrenesulfonate and [3-(methacryloylamino)propyl]trimethylammonium chloride showed weak interactions at low concentrations of $< 1.6 \text{ M}$ with swelling ratios up to ~ 10 -fold which afterward decreased with higher concentrations, and the Young's modulus increased at the same time, leading to a tougher hydrogel.

Gels can also be cross-linked via coordination chemistry, e.g., with palladium- and amine-based ligands, which was investigated by Xu et al.³⁵⁰ to determine the effect on the gel's shear thinning/thickening properties³⁵⁰ and on the zero shear viscosity.³⁵¹ They used poly(4-vinylpyridine) cross-linked with bis-Pd(II) compounds called [2,3,5,6-tetrakis{((dimethylamino)methyl)phenylene}-1,4-bis(palladium trifluoromethanesulfonate) or [2,3,5,6-tetrakis{((diethylamino)methyl)phenylene}-1,4-bis(palladium trifluoromethanesulfonate)] in dimethyl sulfoxide or *N,N'*-dimethylformamide (DMF). The shear viscosity could be tuned via the temperature, polymer/cross-linker concentration, and kind of cross-linker that might be attractive for functional hydrogels with tunable properties. Jackson et al.^{352,353} prepared

metallopolymer films based on poly(butyl acrylate) containing 2,6-bis(1'-methylbenzimidazolyl)pyridine ligands for complexation of Cu²⁺, Zn²⁺, and Co²⁺ ions and tuning the material's mechanical stability. This approach might be used for stabilizing hydrogels via metal complexes.

5.2.5. Hydrogen Bonds. Polymers containing hydrogen bond side groups could be interesting for printing as these materials possess shear thinning properties. Lewis et al.³⁵⁴ prepared poly(*n*-butyl acrylate) containing acrylamidopyridine, acrylic acid, carboxyethyl acrylate, or ureidopyrimidinone acrylate in different ratios which lead to higher glass transition temperatures, higher storage modulus G' , and higher zero shear viscosities upon increased amount in the polymer. For example, a polymer with acrylic acid with a mole fraction of 6% possessed a zero shear viscosity of $\sim 2 \times 10^3$ Pa·s, and a polymer with acrylic acid with a mole fraction of 10% possessed a zero shear viscosity 10 times higher, $\sim 2 \times 10^4$ Pa·s. Vatankhah-Varnoosfaderani et al.³⁵⁵ synthesized copolymers containing *N*-isopropylacrylamide and dopamine methacrylate, which formed a gel in dimethyl sulfoxide (DMSO) solution when sodium hydroxide was added. This led to deprotonation of the dopamine units, which could interact with each other and subsequently formed a gel within seconds, whereas the same process in alkaline water took several hours. The gel showed shear thinning properties whereby at room temperature at low shear rate $G' \approx 250$ Pa and $G'' \approx 19$ Pa and at 900% strain G'' became higher than G' .

Further poly(*N*-isopropylacrylamide) was used with hydrogen bond moieties for cross-linking by Hackelbusch et al.³⁵⁶ They used diaminotriazine or cyanuric acid groups at the side chain and added the complementary bismaleimide or Hamilton wedge for gel formation in a methanol/chloroform (1/1) mixture. For example, a gel with the Hamilton wedge receptor with a polymer concentration of 200 mg mL⁻¹ possessed a viscosity of ~ 5.4 Pa·s at low shear rate and a yield stress of ~ 0.9 s⁻¹. Hydrogen bond segments can also be used in the polymer backbone and thus form gels via α -helix and β -sheet formation such as the polypeptide-based organolator methoxypoly(ethylene glycol)-block-poly(γ -benzyl-L-glutamate-*co*-glycine) in DMF described by Fan et al.³⁵⁷ The critical gelation concentration could be tuned via the monomer composition and the gel's properties via the α -helix/ β -sheet ratio, which increases with higher amounts of glycine *N*-carboxyanhydride. Additionally, the gel was injectable and showed self-healing properties. Ji et al.³⁵⁸ prepared a polymer possessing hydrogen bond and host–guest functionalities for gel formation. The polystyrene-based polymer contained 2,7-diamido-1,8-naphthyridine/dialkylammonium groups, and the poly(butyl methacrylate)-based polymer contained deazaguanosine/benzo-21-crown-7 groups, and both were separately dissolved in chloroform and formed a double-cross-linked gel by combination of the solutions.

5.3. Colloidal Systems

The scope of this section is systems containing solid particles as additives whose surface interacts in different ways with polymers or small organic molecules, thus yielding supramolecular hydrogels via self-assembly. Such strategies have so far been pursued using silica nanoparticles, laponite, carbon nanotubes, graphene sheets, titania sheets, and gold and silver nanoparticles as will be presented and discussed in detail. A most recent approach also demonstrated that interactions between latex particles or block copolymer micelles and polymers can lead to the formation of self-assembled hydrogels exhibiting shear thinning and self-healing properties.³⁵⁹ All the systems

containing solid particles described in this section show properties such as shear thinning, temperature/pH-induced reversible sol–gel transitions, or self-healing properties potentially exploitable for the design of printable hydrogels.

5.3.1. Silica Nanoparticles and Laponite-Based Hydrogels.

The hydroxide-rich surface of silica nanoparticles allows covalent immobilization, e.g., of trimethoxysilyl compounds, via condensation reaction. Guo et al.¹³⁹ modified the silica's surface with β -cyclodextrin, which formed host–guest complexes with mono-end-functionalized PEG in aqueous solution. The addition of α -cyclodextrin led to inclusion complexes with the free PEG chain ends forming a viscoelastic hybrid hydrogel. Its storage modulus G' was around 4 times higher than that of the formed hydrogel without β -cyclodextrin-functionalized silica nanoparticles (native hydrogel). The hydrogel's viscosity, at low shear rates, was $\sim 1.3 \times 10^3$ Pa·s and was about 8 times higher than that of the native hydrogel, 157 Pa·s. The hybrid hydrogel showed pronounced shear thinning properties and reached the same viscosity (10 Pa·s) as the native hydrogel at a shear rate of 1 s⁻¹.

The silicium-rich compound laponite ($\text{Na}_{0.66}[\text{Mg}_{8.34}\text{Li}_{0.66}\text{Si}_8\text{O}_{20}(\text{OH})_4]$) (clay nanosheet, CNS) was also investigated as an additive in hydrogels. Haraguchi et al.³⁶⁰ copolymerized laponite with *N,N'*-dimethylacrylamide and *N,N'*-methylenebis(acrylamide) in different ratios and thus obtained hydrogels with tensile moduli ranging from 1.16 to 15.55 kPa, tensile strengths from 7 to 255.6 kPa, and water contents from 55.2% to 90.9%. Further insights into the shear thinning properties of those hydrogels were given by Aida and co-workers, who investigated the interaction between the clay nanosheets and polymers and dendrimers. Laponite contains oxyanions at the surface which can interact with cationic compounds, leading to a hydrogel formation via self-assembly. Additionally, sodium polyacrylate is necessary for disentanglement of the CNS in solution. For example, dendrimers of first, second, and third generation abbreviated as G1, G2, and G3 binders were synthesized.³⁶¹ They possessed a linear PEG core with esterified 2,2'-(ethylenedioxy)-bis(ethylamine) branches terminated with positively charged guanidinium functionalities. It could be shown that the hydrogel's storage modulus G' and loss modulus G'' increased with higher amounts of CNS and higher generation of the dendrimers and thus with increasing guanidinium content. Additionally, the formed hydrogels showed shear thinning properties; e.g., a hydrogel containing 5% CNS, 0.38% G3 binder, and 0.15% sodium polyacrylate possessed a critical strain region at 9% where the loss modulus G'' became higher than the storage modulus G' and thus the solid hydrogel transformed into a quasi-liquid state. The shear thinning behavior was also confirmed via continuous step strain measurements where the quasi-liquid and quasi-solid states could be obtained in change. The storage modulus decreased from 0.5 MPa to 5 kPa and tan δ increased from 0.4–0.5 to 3.0–4.0 when 100% oscillatory force was applied with a frequency of 1 Hz. By decreasing the amplitude to 0.1% at the same frequency, the hydrogel recovered and G' and tan δ reached their initial values. In a follow-up study, Aida and co-workers also compared the influence of linear molecular binders with different chain lengths and amounts of guanidinium functionalities with a dendritic molecular binder in CNS-hydrogels.³⁶² The linear molecular binders consisted of ABA triblock polymers with guanidinium-functionalized poly-glycidol via thiol–ene click chemistry as A and polyethylene glycol as B. Dendritic molecular binder was a G3 binder as mentioned in the section before. Frequency sweep tests showed

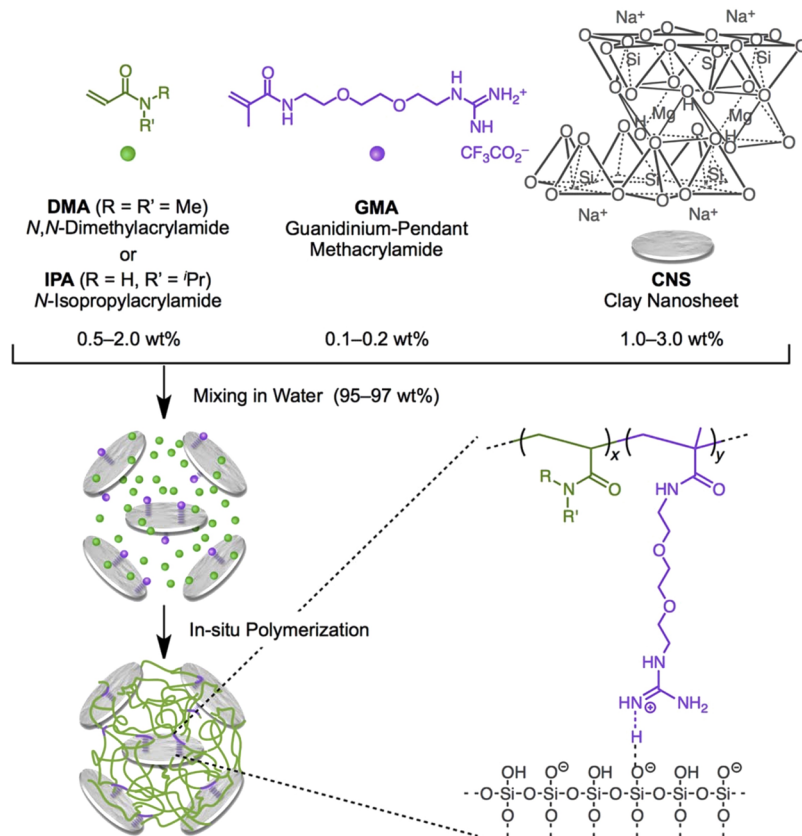


Figure 13. Schematic representation of CNS–polymer composite hydrogels reinforced by the incorporation of guanidinium pendant methacrylamide (GMA) in the polymer chains. Reprinted with permission from ref 363. Copyright 2013 John Wiley and Sons.

that with a higher amount of CNS and higher amount of guanidinium functionalities the storage modulus G' increased, which could also be observed for the loss modulus G'' but only up to a frequency of $\sim 10 \text{ rad s}^{-1}$. Shear thinning behavior of hydrogels was also shown via strain sweep tests at 0.05% and 100%, where the loss modulus G'' became higher than the storage modulus G' at a strain of 4%. Additionally, continuous step strain tests at 0.1% and 100% showed the reversibility between the quasi-solid and quasi-liquid states. The necessity of such cationic binders for the stabilization of CNS–hydrogels was further shown by the same research group in a follow-up study.³⁶³ *N,N*'-Dimethylacrylamide (DMA)/*N*-isopropylacrylamide (NIPAAm) was copolymerized with guanidinium-pendant methacrylamide (GMA) monomer and clay nanosheets in water (Figure 13). The resultant hydrogels showed shear thinning properties; e.g., with 2% CNS, 0.5% DMA, and 0.1% GMA, the loss modulus G'' was larger than the storage modulus G' at 10% strain at 6.0 rad s^{-1} and the hydrogel changed from a quasi-solid state to a quasi-liquid one. Stress–strain experiments with different cationic amine side chain functionalities showed that the guanidinium side groups lead to the most stable hydrogels. In the case of no cationic compound in the hydrogel, it will lose its form, and therefore, the stabilization of CNS via charge interaction is necessary.

Gels were also prepared with a solid content between 3 and 10 wt % and CNS/gelatin ratio from 1/0 to 0/1.³⁶⁴ Generally, the higher the CNS content, the larger the storage modulus, with a maximum of $\sim 1.4 \times 10^3 \text{ Pa}$. Alternating high and low strains show the hydrogel's shear thinning properties and its ability to recover after strain.

5.3.2. Carbon-Nanotube- and Graphene-Sheet-Rich Compounds.

Tan et al. synthesized an injectable supramolecular hydrogel based on single-walled carbon nanotubes (SWCNTs) with the bile salt sodium deoxycholate (NaDC).³⁶⁵ The amphiphilic bile salt interacted through its hydrophobic steroid group with the carbon nanotube's surface, leading to self-assembly in aqueous solution due to the additional interaction of the carboxyl group with water. Shear thinning experiments revealed that, with a higher content of SWCNTs, the hydrogel had a greater shearing modulus and a higher shear stress. The content of NaDC was kept constant at 30%, and the amount of SWCNTs was varied from 1% to 3%. For example, with 1% SWCNTs, a shear modulus of 100 Pa (at a shear stress of 1 Pa) could be achieved, and with 2% SWCNTs, a shear modulus of even 10^4 Pa (shear stress of 80 Pa) could be achieved. An injectable supramolecular hydrogel based on multiwalled carbon nanotubes (MWCNTs) was investigated by Du et al. which is responsive to pH, temperature, and near-infrared (NIR) light showing self-healing properties.³⁶⁶ MWCNTs were oxidized by treatment with a mixture of concentrated sulfuric and nitric acids, leading to a carboxylic acid-functionalized surface. The *N*-ethylamine-functionalized poly(ethylene imine) formed a hydrogel with the oxidized MWCNTs via hydrogen bonds ($\text{COO}^- \cdots \text{HN}$ and $\text{NH} \cdots \text{N}$), where the concentration of the polymer was varied from 25 to 75 wt % and that of the oxidized MWCNTS was varied from 0.015% to 0.5%. This system was sensitive to a variety of stimuli exploitable for printing. For example, the addition of HCl led to a protonation of the amine functionalities, which decreased the amount of hydrogen bonds, and therefore, a liquid was formed. After treatment with NaOH, the hydrogel retransformed by deprotonation of those amine groups. Gel–sol

transition could also be controlled via exposure to NIR light or via a temperature change. The temperature sensitivity could be tuned linearly with the oxidized MWCNT content. For example, a hydrogel containing 0.1 wt % oxidized MWCNTs heated to 55 °C for 30 s transformed into a liquid and retransformed into a hydrogel after being cooled to 20 °C for 3 min. The self-healing behavior was confirmed after treatment of the hydrogel containing 0.5 wt % oxidized MWCNTs with a deformation stress of 200 or 800 Pa, and the storage modulus returned to 90% or 80% after recovery. Furthermore, interesting studies on the stability of hybrid hydrogels of amine-functionalized polymers and oxidized carbon nanotubes (CNTs) were performed by Hashmi et al.³⁶⁷ They investigated poly(*N*-isopropylacrylamide) (PNIPAAm) and polymers with zwitterionic sulfobetaine functionalities with different ratios, CNT, and cross-linker in the hydrogel. SWCNTs were also used for supramolecular hydrogel formation via host–guest interactions. Wang and Chen³⁶⁸ and Hui et al.³⁶⁹ used Pluronic, whose hydrophobic poly(propylene oxide) (PPO) units interact with the SWCNTs' surface and whose hydrophilic poly(ethylene oxide) (PEO) units face into the hydrophilic solution after dispersion in water. Addition of α-CD led to a host–guest interaction with the PEO units and subsequently to hydrogel formation. For rheological measurements and comparison, a native hydrogel containing only Pluronic and α-CD was synthesized. In Wang's and Chen's work, surprisingly, the SWCNTs did not have a huge positive contribution to the storage modulus because all values were at least 1 order of magnitude smaller than those of the native hydrogel, and only the gel formation was accelerated by the addition of SWCNTs. The thermal reversibility and shear thinning properties of the hybrid hydrogel were retained. For example, at a shear rate of 0.01 s⁻¹, the native hydrogel possessed a viscosity of ~4.4 × 10⁴ Pa·s, whereas the hybrid hydrogel's viscosity was only ~4 × 10³ Pa·s. In Hui's work, the amount of α-CD was increased, yielding more stable hydrogels.

The following hydrogels could be interesting for printing as their sol–gel transition can be controlled. The interaction of pyrene-based compounds with the SWCNTs' surface via π–π interaction was exploited for supramolecular hydrogel formation by Ogoshi et al.³⁷⁰ They synthesized β-CD with a pyrene group which could be attached to the surface of the SWCNTs. After addition of poly(acrylic acid) containing 2 mol % dodecyl groups, host–guest complexes were formed by β-CD with the aliphatic side chains, and finally, a hydrogel was formed. The hydrogel could be transformed back to a solution either via addition of a competitive guest (sodium adamantine carboxylate) or by addition of a competitive host (α-CD). Yang et al.³⁷¹ used a one-pot hexacomponent system with π–π stacking, Ugi reaction, and reversible addition fragmentation chain transfer (RAFT) polymerization for a polymer conjugation on carbon nanotubes. The polymer PNIPAAm interacted with its pyrene end group on the CNTs' surface and was functionalized with an MPEG at its other chain end. This formed host–guest complexes with α-CD and subsequently led to a transformation from a CNT dispersion to a supramolecular hydrogel. A further hydrogel formation via host–guest complexes of CNTs was investigated by Tamesue et al.³⁷² The polysaccharide curdlan was functionalized with β-CD at the side chains and could helically wrap around SWCNTs in water, exposing β-CD functionalities to the liquid surroundings. By adding poly(acrylic acid) containing pendant azobenzene groups, a photochemically reversible hydrogel was formed via host–guest interaction with β-CD under visible light (430 nm). This could be turned back into a solution by irradiation with UV

light (365 nm) as the azobenzene group isomerized into the *trans*-conformation. A sol state could also be reached by adding a competitive host (α-CD) or a competitive guest (1,12-dodecanedicarboxylate sodium salt). Modified amino acid sequences possessing a long alkyl chain gelated in aqueous solution above the minimum gelation concentration (MGC). If they additionally possessed an aromatic group, they could interact with CNTs and were stabilized due to the π–π interactions. Such supramolecular hydrogels were investigated by Mandal et al.³⁷³ They varied the aromatic groups (imidazole, benzyl) and reached MGCs from 0.7% to 5.0% (w/v), enabling tunable gel-to-sol transition temperatures, e.g., with a fixed concentration of SWCNTs at 1.0% (w/v). In all cases, the hybrid hydrogel possessed a higher gel–sol transition temperature than the native hydrogel, and rheological measurements showed that in most cases the storage modulus G' increased with higher amounts of CNTs, which confirmed the stabilization via π–π interactions.

First, supramolecular hydrogels based on a mixture of graphene and Pluronics did not show any improvement in mechanical features through addition of the graphene sheets compared to native Pluronic hydrogels.³⁷⁴ A beneficial effect was observed by adding reduced graphene oxide (RGO) sheets into hydrogels based on short peptides as low molecular weight gelators.³⁷⁵ They possessed [(fluorenylemethyl)oxy]carbonyl (Fmoc) and Tyr (1)/Phe (2) as functional aromatic groups which interacted with the graphene sheets via π–π stacking and showed minimum gelation concentrations of 0.50% and 0.55% (w/v) for gelator peptides 1 and 2. Furthermore, the storage modulus G' of the hydrogels increased with higher amounts of graphene sheets. As the hybrid hydrogels also showed thermoresponsiveness, the gel–sol transition could be used for the 3D printing process by transferring the gel to a solution via temperature change. Oxidized graphene sheets (graphene oxide, GO) with carboxyl and hydroxyl groups on the surface enabled the electrostatic interaction with compounds possessing protonated amine or other positively charged functionalities. On the basis of these interactions, a variety of stable supramolecular hydrogels with a very low minimum gelation concentration were prepared and could be useful tools for the 3D printing process by changing the gelator's concentration, transferring solutions into the gel state. For example, Adhikari et al.³⁷⁶ used amino acids (L-arginine, L-tryptophan, L-histidine) with a minimum gelation concentration of 1.45% (w/v) and nucleosides (adenosine, guanosine, cytidine) with MGC = 2.0% (w/v) as gelators with GO. A nanofibrous robust 3D network structure was formed via self-assembly by heating the reaction solution above 100 °C and cooling it to room temperature afterward. Only a small amount of amino acids and nucleosides with respect to GO was needed (~2.21%, w/w), which confirmed their very good cross-linking ability between GO sheets. A hydrogel containing L-arginine possessed a very high storage modulus, $G' \approx 6 \times 10^4$ Pa, during the tested frequency range from 0.1 to 628 rad s⁻¹, displaying a positive effect on the hydrogel's stability. Similar experiments with polyamines (spermine, spermidine, tris(aminoethyl)amine) as incorporated cross-linkers in GO hydrogels were conducted by the same group.³⁷⁷ Tao et al. used (dimethylguanyl)guanidine hydrochloride (metformin hydrochloride, MFH) as an amine-functional cross-linker for GO sheets which formed a hydrogel via electrostatic interactions and hydrogen bonds.³⁷⁸ They investigated the hydrogel formation with respect to different cross-linkers: GO ratios need to be in the range of 1/13 to 1/10

with 1 wt % GO content. Therefore, the necessary concentration of the cross-linker was very low with respect to GO at <10% (w/w). The pH value of the solution and thus the degree of protonation of MFH and the carboxylic acid groups on the GO surface played an important role as well in the hydrogel stability. For example, the strongest interaction was displayed at pH 3, where six kinds of hydrogen bonds were formed between GO's $-\text{OH}/-\text{COOH}$ groups and MFH's $=\text{NH}/-\text{NH}/-\text{NH}_2$ groups along with electrostatic interaction of $-\text{COOH}$ and $=\text{NH}_2^+$. In contrast, at pH 1, only four hydrogen bonds were available and caused the weakest interaction between GO and MFH. These results make materials interesting for 3D printing as the hydrogel's properties can be tuned via the concentration and the pH value, having an influence on the strength of cross-linking. Another pH-responsive graphene oxide-based hydrogel was investigated by Cong et al., who used poly(acryloyl-6-amino-caproic acid) and Ca^{2+} for cross-linking.³⁷⁹ Ca^{2+} interacted with the carboxylic acid group of the polymer and with the graphene sheets' carboxylic acid groups on the surface, forming a highly porous hydrogel. Both components were varied from 1.0% to 9.5%, showing—with higher amounts—an increasing tensile stress of the hydrogel. In addition, it was stretchable, and in the case of ruptures, it showed self-healing properties at pH < 3. This pH range led to protonation of the carboxylic acid groups and therefore to a more flexible system which solidified at pH ≥ 7 reversibly. Yan and Han used chitosan as a cross-linker for GO, forming a hydrogel via electrostatic interactions.³⁸⁰ It showed self-healing properties, and the gelation could be tuned via the temperature and concentration of GO as it possessed a very low sol–gel concentration. For example, a solution containing 8.0 wt % chitosan remained a solution at room temperature with 0.2 wt % GO and became a gel at room temperature with 0.3 wt % GO. With a higher amount of chitosan and GO, the storage modulus G' increased; e.g., at 20 °C, $G' \approx 70$ Pa for 0 wt % GO and $G' \approx 670$ Pa for 0.3 wt % GO. G' and G'' additionally showed a strong temperature dependency and decreased with higher temperature, weakening the electrostatic interactions within the hydrogel. The incorporation of thermoresponsive polymers as cross-linkers for GO is an ideal approach to tune the gelation via temperature and was performed by Jiang and co-workers.³⁸¹ They modified the GO surface with β -CD moieties and added the block copolymer azo-PDMA-*b*-PNIPAAm (PDMA = poly(*N,N'*-dimethylacrylamide)), which led to cross-linking due to the host–guest interaction of β -CD with the azophenyl group. Hydrogelation started when the temperature was above PNIPAAm's lower critical solution temperature (LCST) (29.3–39.9 °C), which varied with the degree of polymerization and composition within the block copolymer. The sol–gel transition was confirmed via measurement of the viscosity and storage/loss modulus over time with a temperature decrease of 1 °C min⁻¹. The hydrogel with host–guest-bound polymers on GO had significantly higher storage/loss moduli than the one with loosely bound GO without β -CD moieties and polymers which showed the strong effect of supramolecular interactions in the hydrogel. Another interesting method to increase the stability of hydrogel-containing graphene sheets is to control their orientation in a magnetic field. Wu et al. polymerized *N,N'*-dimethylacrylamide containing *N,N'*-methylenebis(acrylamide) as a cross-linker with GO and confirmed the anisotropic behavior via rheological measurements.³⁸² The storage modulus increased when the sheer force was orthogonal to the graphene sheets in the hydrogel due to higher resistance to an external influence compared to the parallel case. Such an external magnetic field

during the 3D printing process could be used to control the hydrogels' properties.

5.3.3. Metal-Based Gels. *5.3.3.1. Titania Nanosheets.* Aida and co-workers controlled the orientation of titania nanosheets via an external magnetic field.^{383,384} They used *N,N'*-dimethylacrylamide as a monomer and *N,N'*-methylenebis(acrylamide) as a cross-linker for the UV-light induced polymerization. Thereby, titanium was used as the initiator which transfers an electron from the valence band to the conduction band upon exposure to UV light, which set free hydroxyl radicals in aqueous solution and afterward initiated the polymerization. This experiment could be an interesting approach for *in situ* hydrogelation during 3D printing and for controlling the hydrogel's strength.

5.3.3.2. Gold and Silver Nanoparticles. Chen and co-workers³⁸⁵ modified the gold's surface with monothiolated β -CD and used Pluronic as a cross-linker forming host–guest complexes between PEO moieties and β -CD, leading to a supramolecular hydrogel. The reversible transition to a solution could be conducted by adding 1-adamantanamine hydrochloride, which is a competitive guest for β -CD and destroyed the supramolecular network. Further insights into the mechanical properties of such host–guest formed hydrogels were given by Shi and co-workers.³⁸⁶ They modified the gold nanoparticles' (AuNPs) and nanorods' (AuNRs) surfaces with monothiolated mPEG. Addition of α -CD yielded a supramolecular hydrogel that showed thermo- and mechanoresponsivity. AuNP hydrogels possessed a gel–sol transition at 60 °C, and AuNR hydrogels possessed a gel–sol transition at 70 °C. Both could be transformed into a gel upon cooling of the solutions reversibly. The storage modulus G' was higher than the loss modulus G'' over the whole frequency range, displaying a stable hydrogel doped with gold moieties. This gel also showed shear thinning properties. Das and co-workers used low molecular weight gelators (LMWGs) for the incorporation of gold salts and subsequently *in situ* reduction to gold nanoparticles.³⁸⁷ The LMWGs consisted of dipeptides with a long aliphatic chain, different aromatic groups, and either a carboxylic acid or a sodium carboxylic group. The minimum gelation concentration of LMWGs was varied in water from 0.58% to 3% (w/v) and in aromatic solvents from 0.45% to 1.6% (w/v), which are very low contents. The *in situ* reduction and formation of AuNPs in the hydrogels increased their storage modulus G' and loss modulus G'' by around 1–2 orders of magnitude at low shear rates. Additionally, the supramolecular hydrogels showed shear thinning properties displayed by a change from the quasi-solid state to the quasi-liquid state with increasing oscillatory stress. Zhang and co-workers also synthesized supramolecular hydrogels based on low molecular weight gelators.³⁸⁸ They used different derivates of bile acids with low concentrations between 25 and 100 mM and incorporated silver and gold salts with concentrations between 5 and 50 mM, which were reduced *in situ* via irradiation of light. Here, the G' and G'' of supramolecular hydrogels containing nanoparticles were 1 order of magnitude higher than those of the native hydrogels. They possessed shear thinning properties, and their yield stress was even lower than that of the native one.

6. BIOTECHNOLOGICAL APPROACHES TOWARD BIOINKS

Section 5 focused on chemical approaches to implement molecular interaction mechanisms in artificial materials. Nature has used and optimized such mechanisms throughout evolution,

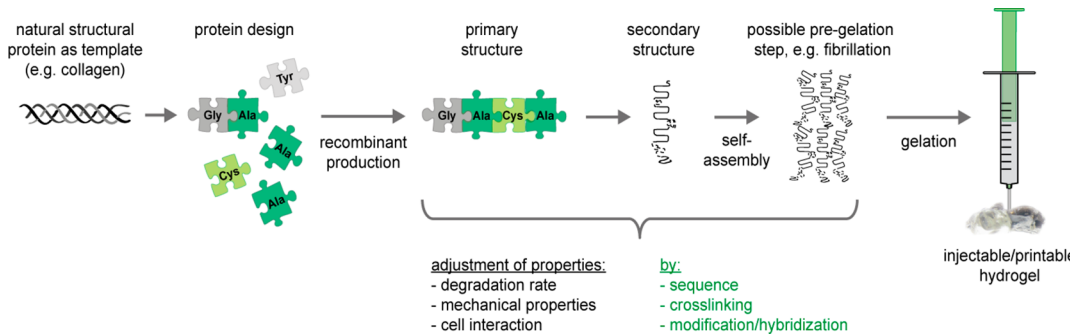


Figure 14. Schematic model of the steps along protein design to gain injectable/printable hydrogels.

together with a complex synthetic apparatus to synthesize the molecular building blocks with the highest precision. Nowadays, genetic engineering makes it possible to develop and design new biopolymers with a complexity and functionality not found in nature. Recombinant production of natural or artificial proteins allows tailoring of a material's properties such as mechanics, degradation, porosity, cell interaction, and cytocompatibility (Figure 14).³⁸⁹ Genetically engineered recombinant proteins are much more accessible in a defined molecular structure than synthetically produced materials.^{390–394} Specific design of functional groups along the constituent proteins (typically structural proteins such as collagen, elastin, or silk) allows biological activity similar to that of components of the natural ECM. One possibility is to combine different functional domains of natural proteins in one designed protein (e.g., a fusion protein), for example, merging cell interaction domains with structural ones. Alternatively, recombinant proteins can, by design, be easily modified with short peptide motifs such as RGD or IKVAV, which are unique ligands for cell receptors and mediate cell adhesion. In the context of this review, we will however primarily focus on (potential) printability.

Apart from the following exception, we will focus on recombinantly produced biopolymers as the main structural component of hydrogels, and not as a mediator or cross-linker for hydrogelation. Lu et al.³⁹⁵ modified hyaluronic acid with peptide sequences as an anchoring domain which forms an injectable, shear thinning, and self-healing physical gel via the dock-and-lock principle after addition of recombinantly produced dimerized docking polypeptide sequences. The hydrogel possessed at low strain $G' \approx 250 \text{ Pa}$ / $G'' \approx 6 \text{ Pa}$ and at high strain $G' \approx 20 \text{ Pa}$ / $G'' \approx 50 \text{ Pa}$, both of which were obtained in a repeatable way. Additionally, the hyaluronic acid was modified with methacrylate groups so that the hydrogel could be stabilized in a secondary step via photopolymerization. This approach is thus very promising as the initial step toward a printable hydrogel. For further details on the use of recombinant proteins as cross-linkers for hydrogelation, we refer to the review paper by Wang et al.³⁹⁶

It is important to mention that not all polypeptides and proteins can be recombinantly produced, nor can proteins be combined with nonpeptidic moieties, unless by chemical postproduction modification. In the case in which recombinant production is possible, receiving the proteins in sufficient yields is often challenging. This depends on the host organism selected for production, the fermentation process, and the protein itself. Especially the latter often creates certain unpredictability for the yield when a new process is initiated. Hence, so far there are not many recombinant protein materials available in sufficient amounts with properties such as shear thinning behavior and form stability, as well as cytocompatibility. However, biotechnol-

ogy holds the promise of overcoming this drawback and expanding the field of bioinks for biofabrication, and the so far only and very recently published report on the use of a recombinant protein (based on spider silk sequences) without any additive for 3D printing and biofabrication underlines the great potential.³⁰⁴

In this section, we will briefly introduce the different possibilities for production of recombinant proteins and then give an overview over the so far reported recombinantly produced proteins (elastin-like polypeptide, resilin-like polypeptide, recombinant collagen, recombinant silk) with properties potentially exploitable for 3D printing. Furthermore, examples for peptide–polymer and protein–polymer hybrid materials and polynucleotides will be reviewed which show promising properties and may in the future be tailored for the demands of printing processes.

6.1. Designable Biopolymers: Recombinantly Produced Proteins

6.1.1. Methods for Recombinant Protein Production.

Different host organisms can be used for recombinant protein production such as bacteria, yeast, plants, insect and mammalian cells, or transgenic animals.³⁰¹ *E. coli* is often used as a host organism for recombinant protein production, since this Gram-negative enterobacterium is suitable for a fast and inexpensive large-scale production due to its simplicity, its well-known genetics, and the capability of fast high-density cultivation, in addition to the availability of different plasmids, fusion protein partners, and mutated strains.³⁹⁷ Besides *E. coli*, other bacterial hosts have been employed for the recombinant production of proteins. In contrast to *E. coli*, the Gram-negative bacterium *Salmonella typhimurium*, for example, has the capability to secrete proteins, which simplifies the isolation of the target protein from the bacterial host proteins. Likewise, the Gram-positive bacterium *Bacillus subtilis* is able to secrete large quantities of recombinant proteins into the medium. The bacterial secretion systems are much simpler than those of yeasts and fungi, simplifying the efficient production.³⁹⁸ Nevertheless, yeasts, such as *Saccharomyces cerevisiae* and *Pichia pastoris*, can be attractive alternatives to bacterial hosts because they are able to correctly process high molecular weight proteins including more complex post-translational modifications such as glycosylations,³⁹⁹ and *P. pastoris* is even able to grow to high cell densities ($>100 \text{ g L}^{-1}$ dry cell mass).⁴⁰⁰ To obtain large amounts of recombinant proteins, transgenic plants such as *Arabidopsis thaliana* and *Nicotiana tabacum* (tobacco) have also been used. Plants are capable of producing foreign proteins on a large scale and at lower costs in comparison to most other organisms.⁴⁰¹ Disadvantages of plant hosts are a more complicated genetic manipulation than for

Table 6. Recombinantly Produced Proteins for Injectable/Printable Hydrogels

recombinant protein	3D printing technique	advantageous properties	applications	refs
collagen/collagen-like		biodegradability, biocompatibility	tissue repair (corneal substitutes), nerve regeneration, drug delivery	286, 407–410
silk-like	robotic dispensing	remarkable mechanical properties, biocompatibility, biodegradability	tissue repair, nerve regeneration, wound healing	304, 411
elastin-like		elastomeric properties, thermoresponsive behavior, biocompatibility, high solubility	tissue repair (cartilage), vascular grafts, soft-tissue replacement, drug delivery	412–419
resilin-like		low stiffness, high resilience, reversible extensibility	tissue repair (cartilage, vascular grafts)	420–422

microbes and longer generation intervals.⁴⁰² Additionally, the production of large proteins can cause problems, because the underlying genes are prone to genetic rearrangements.⁴⁰¹

Introducing foreign sequences and genes into animals can be achieved through different procedures, such as the integration of synthetic genes into the chromosomal DNA or by transporting a target DNA into cells, resulting in a transient expression.⁴⁰³ The transformation efficiency is low using both approaches; viruses as transporters are in some cases much more promising because they are extraordinarily efficient in transferring their own genome into foreign cells. For example, baculovirus has been widely used as a vector of target genes for their expression in insect cells.⁴⁰³ Using insect cells as expression hosts has advantages such as high-expression efficiencies, low feeding costs, the capability to secrete proteins, simplified purification, and possible post-translational modifications.^{402,404} Disadvantages are more complex cloning procedures and longer generation times of the insect cell lines compared to bacteria.⁴⁰⁵ Mammalian cells and even transgenic animals have also been used for recombinant protein production.⁴⁰⁶ Using transgenic animals to produce recombinant proteins allows, e.g., the secretion into body fluids such as milk or urine, enabling protein production for long time intervals, thus gaining a higher protein yield.^{301,402} Disadvantages of this system are that the creation of transgenic mammals is very time-consuming and complex. Additionally, as in the case of spider silk proteins that were secreted into the milk of goats and mice, the challenge is to separate the recombinant proteins from milk caseins, since several structural proteins and caseins show similar properties such as self-assembly, and especially mice only produce a small amount of milk.^{267,402} Table 6 gives an overview of recombinantly produced proteins that have been used for 3D printing or as injectable hydrogels, or exhibit properties potentially exploitable for printing purposes. The different approaches will be presented and discussed in more detail in the following sections.

6.1.2. Silk-like Proteins. Due to spiders' aggressive territorial behavior and their cannibalism, their large-scale farming is not feasible. Therefore, several prokaryotic and eukaryotic hosts have been tested concerning recombinant production of spider silk proteins, as recently summarized by Heidebrecht et al.³⁰¹ Different silk-like polymers (SLPs) have been produced with varying numbers (i.e., repeats) of single sequence motifs, different types of motifs, and different spacings between them.^{301,405,423,424} Spider silk offers a very high potential for biomedical applications due to the excellent mechanical properties of its fibers and the biocompatibility and biodegradation of materials processed from the underlying proteins.^{302,402,425–427} Recombinant spider silk proteins can self-assemble into nanofibrillar networks triggered by high protein concentrations, salts, and temperature, and they form hydrogels.^{428,429} Recently, it has been published that spider silk hydrogels can serve as a bioink for biofabrication.³⁰⁴ In contrast

to silk from *Bombyx mori*, the β -sheet-rich spider silk hydrogels showed moderate shear thinning behavior, with high viscosity at low angular frequencies and a decrease in viscosity at higher frequencies.²⁷¹ The elastic behavior dominated over the viscous behavior over the whole angular frequency range with a low-viscosity flow behavior and good form stability.^{304,429} No structural changes occurred during the printing process, and the hydrogels solidified immediately after printing by robotic dispensing. Due to the form stability, it was possible to directly print up to 16 layers on top of each other with a construct depth of approximately 3 mm without structural collapse. Strikingly, cell-loaded spider silk constructs were printed without the need for additional cross-linker or thickener for mechanical stabilization. The encapsulated cells showed good viability over at least 1 week in such spider silk hydrogels.³⁰⁴

6.1.3. Recombinant Collagen/Collagen-like Proteins. Almost every possible type of expression system, such as bacteria, yeast, transgenic tobacco, insect cells, mammalian cells, silk-worms, and transgenic mice, has been used for the recombinant expression of collagen, collagen-like proteins, and selected domains thereof.^{286,407,410,430} Compared to native collagen, recombinantly produced collagens have the benefit of being biologically safe (no infectious contaminations) with useful self-assembly features, and they can be functionalized with bioinstructive domains such as cell adhesion motifs.^{306,307,410} Recombinant expression of collagens is quite complex, since it can be necessary to introduce post-translational modifications important for cross-linking and helical stability. Therefore, biosynthesis of collagen might require specific enzymes, in particular prolyl 4-hydroxylase. In the absence of this enzyme, often non-triple-helical and nonfunctional collagen molecules are produced, which are unstable at physiological conditions and thus unsuitable for biomedical applications.⁴³¹ From the tested hosts, only mammalian cells produced collagen with an L-4-hydroxyproline content identical to that of natural collagen. However, this system yields only low levels of protein (0.6–20 mg L⁻¹). In *E. coli* and yeast, multigene expression is necessary to overcome the absence of the enzyme prolyl 4-hydroxylase.⁴⁰⁹ On the basis of the multigene expression technology, collagen types I, II, and III were produced with an L-4-hydroxyproline content identical to that of the native human proteins and titers of 0.2–0.6 g L⁻¹.⁴³² Alternatively, peptide-based supramolecules mimicking the collagen structure and function have been tested. However, two critical issues arise for the development of peptide-based collagen-like supramolecules. One is the difficulty to generate a higher order structure to mimic the assembly (or gelation) property of natural collagen. The second is the not so easy incorporation of biologically relevant motifs into the material. Kaplan and co-workers designed collagen triblock peptides with the sequences (Glu)₅-(Gly-X-Hyp-Gly-Pro-Hyp)₆-(Glu)₅, which self-assembled into highly organized supramolecular structures forming a triple helix.^{433,434} However,

Table 7. New Hybrid Materials for Hydrogel Formation

fusion protein	expression system	hybrid system	refs
resilin–elastin–collagen-like (REC)	<i>Escherichia coli</i>	protein–protein	444
silk–elastin-like (SELP)	<i>Escherichia coli</i>	protein–protein	446, 447
silk–collagen-like ($C_2S^{H_{48}}C_2$)	<i>Pichia pastoris</i>	protein–protein	448
elastin-like polypeptide + polyethylene glycol (ELP–PEG)		protein–synthetic polymer	449
resilin-like polypeptide + polyethylene glycol (RLP–PEG)		protein–synthetic polymer	422

the physical properties of the collagen-like peptide supramolecules were far from those of native collagen hydrogels. Fusion proteins made of recombinant collagen and silk have also been developed, showing significantly enhanced cell viability and cell proliferation; see section 6.1.6.⁴³⁵

6.1.4. Elastin-like Polypeptides. Elastin is an abundant component of the extracellular matrix found in elastic tissues in the human body and is responsible for keeping the tissue flexible. The elastomeric properties of elastin materials provided major motivation for the design of mimetic elastin-like polypeptides (ELPs).^{414,436} The study of ELPs was pioneered by Dan Urry, who synthesized a large number of polypeptides and studied their biophysical properties in solution and as cross-linked elastomeric materials.⁴¹⁴ The elastin-inspired sequence, derived from the hydrophobic domain of tropoelastin, is a pentapeptide repeat of VPGXG (where X is any residue except P), which is common in all ELPs.^{413,414} Elastin shows thermoresponsive behavior, allowing control over its thermal transition temperature by changing the hydrophobicity, molecular weight, and concentration of the polypeptide.^{414,437} The completely reversible phase transition can also be triggered by various environmental conditions such as temperature, ionic strength, redox state, and pH.^{413,415} ELPs are water-soluble below their characteristic thermal transition temperature. However, when the temperature is increased above the transition temperature, the ELPs undergo a phase transition into an aggregated state which reveals a physically cross-linked network favorable for printing.^{413,438} Materials made of elastin-like polypeptides show excellent mechanical properties (similar to those made of natural elastin), are biocompatible, and cause minimal cytotoxicity and immune response when implanted.^{419,439,440} Nagapudi and co-workers found that upon T_t-triggered physical cross-linking block copolymers with the most hydrophilic inner blocks formed hydrogels with complex shear moduli ranging from 4.5 to 10.5 kPa. Decreasing the hydrophilicity of the inner block resulted in the formation of hydrogels with significantly greater shear moduli of up to 280 kPa.⁴⁴¹ The critical temperature of the phase transition can be varied by changing the “X” amino acid.^{414,438} Therefore, depending on the guest residue, an ELP can be designed to be liquid at room temperature and to form a hydrogel *in situ* when the temperature is raised upon injection.

Using recombinant approaches allows incorporation of multiple physical or covalent cross-linking and reactive sites for specific mechanical properties and control.⁴⁴² For example, elastin-like polypeptides have been genetically designed, synthesized, and evaluated concerning enzyme-initiated covalent cross-links via tissue transglutaminase to form a network that sustains cartilage matrix synthesis and accumulation.^{412,415,443} Articular chondrocytes were successfully encapsulated in the *in situ* cross-linked hydrogels, which were then injected to fill an irregularly shaped cartilage defect and to integrate into the surrounding tissue. The ELP network supported cell viability and infiltration, as well as cartilage matrix synthesis and accumulation.

Whether the kinetics of enzymatic cross-linking can be adapted to be suitable for 3D printing remains an open question.

6.1.5. Resilin-like Polypeptides. Natural resilin is an elastomeric protein with remarkable mechanical properties. It is present in specialized regions of the insect cuticle and plays a key role in insect flight, the jumping mechanism of fleas, and vocalization of cicadas.⁴⁴⁴ Resilin possesses excellent mechanical properties such as low stiffness, high resilience, and effective energy storage. Recently, hydrogels made of recombinantly engineered resilin-like polypeptides (RLPs) have been produced with good mechanical (1–25 kPa) and cell-adhesive properties.⁴²⁰ The polypeptide contained 12 repeats of the resilin consensus sequence and a single, distinct biologically active domain.⁴⁴⁵ The approach allowed independent control over the concentration of cell-binding, MMP-sensitive, and polysaccharide-sequestration domains in hydrogels by mixing various RLPs. The RLP-based polypeptides exhibit a largely random coil conformation in solution and in the cross-linked hydrogels, on the basis of the repetitive motifs in the polypeptides. The randomly coiled, isotropic three-dimensional network has been shown to behave as an ideal rubber with near-perfect reversible long-range elasticity.⁴²² RLP hydrogels formed rapidly upon mixing with tris[(hydroxymethyl)phosphine], and they were able to maintain their mechanical integrity due to cross-linking as well as to allow the viability of encapsulated primary human mesenchymal stem cells (MSCs).⁴²¹

6.1.6. Hybrid Proteins. Hybrid materials are made by fusing different bioactive domains or protein motifs that are not otherwise found in nature (Table 7). Injectable hydrogels made therefrom can benefit from the advantages of both components. For the same reason, hybrid materials made of natural polymers and synthetic polymers have been developed as injectable hydrogels.²⁴²

One example of hybrid proteins is the combination of silk repeat sequences and ELP sequences (SELPs).^{447,450,451} By combining the silk-like and elastin-like blocks in various ratios and using different sequences, it is possible to produce a broad range of biomaterials with different material properties. The ELP blocks in the silk–elastin-like proteins influence the molecular chain properties of the protein.⁴⁵² The chimeric proteins were designed to retain the mechanical properties of silk, while incorporating the high solubility and environmental sensitivity of ELPs.^{453–455} SELPs irreversibly undergo a two-step self-assembly process under physiological conditions to form hydrogels depending on the number of silk-like blocks in the repeat unit.⁴⁵⁶ For example, increasing the number of silk-like blocks within a domain in a silk–elastin-like block copolymer increased the rate of gelation and decreased the rate of resorption of the polymer.^{442,456,457} The first step in the gelation process is consistent with the crystallization of the silk-like domains via hydrogen-bond-mediated physical cross-linking.^{456,457} The second assembly step is driven by the hydrophobic interaction between elastin blocks above a specific transition temperature, which leads to the ordered association of SELP molecules,

indicating that the temperature-sensitive behavior of ELPs is even retained in ELP hybrids.⁴⁵⁶ When hydrophobic residues were added to an otherwise hydrophilic SELP, the transition temperature was decreased.⁴⁵⁴ Some SELPs were injected via syringes and then formed insoluble hydrogels at the injection site without any additional cross-linker.⁴⁴⁶ It has been further demonstrated that genetically engineered SELPs (SELP-47 K) can be used to form injectable hydrogels for delivery of cell-based therapeutics.⁴⁴⁷

Hybrid materials made of silk and collagen blocks have also been designed, synthesized, and characterized.⁴⁴⁸ The polymer ($C_2S^{H_{48}}C_2$) consists of a middle block ($S^{H_{48}}$) composed of 48 identical silk-like octapeptides in tandem and two end blocks (C_2), each of which is composed of two identical 99 amino acid long collagen-like sequences in tandem.⁴⁵⁸ The hybrid protein formed nanofibrillar hydrogels exhibiting long-term stability, self-healing behavior, and tunable mechanical properties. Chimeric resilin-, elastin-, and collagen-like engineered polypeptides (RECs) have been designed and produced.⁴⁴⁴ The rubber-like proteins elastin and resilin exhibit a reversible deformation and very high resilience and elasticity. In combination with a collagen-like sequence, it has been shown that the material exhibits promising self-assembly properties potentially exploitable for printing.⁴⁴⁴ Parisi-Amon et al.⁴⁵⁹ reported on a mixing-induced two-component hydrogel for injection of stem cells which consists of two polymers called C7 and P9 possessing seven and nine repeating units of the CC43 WW domain (C) and the L-proline-rich peptide (P), respectively. Additionally, the C7 unit contains the cell-binding domain RGD. This system showed shear thinning and rehealing properties, cytocompatibility, and the ability to encapsulate cells at constant physiological conditions. Olsen et al.⁴⁰⁹ investigated the rheological behavior of coiled-coil telechelic association domains (APQMLRE, LQETNAA, LQDVREL, LRQQVKE, ITFLKNT, VMESDAS) possessing linker domains ([AGAGAGPEG]_n), with $n = 10$ and 30, which show shear thinning properties.

In general, several peptide–polymer hybrid hydrogels exist, but they are usually built upon a synthetic polymer and peptide sequences produced by solid-phase synthesis (and not biotechnologically), which is not the focus here. For more detailed information thereon, we refer the reader, e.g., to the paper by Altbandas et al.⁴⁶⁰ Recombinantly produced coiled-coil peptides have been combined with thermoresponsive polymers to yield thermoswitchable hydrogels. Therefore, a triblock copolymer⁴⁶¹ was prepared on the basis of the before mentioned peptides, such as APQMLRE, LQETNAA, LQDVREL, LRQQVKE, ITFLKNT, and VMESDAS, with $n = 10$, in the middle and two thiol–maleimide-conjugated PNIPAAm end blocks. Strain amplitude sweep measurements were performed at different temperatures and showed their influence on the storage modulus G' and loss modulus G'' . Thereby, PNIPAAm's free polymer chains collapsed upon their lower critical solution temperature behavior, leading to higher values of the moduli but still maintaining their shear thinning property. One further example is the elastin-like polypeptide–polyethylene glycol (ELP–PEG) hydrogel system combining the tenability of ELP hydrogels with the distinct advantages of PEG hydrogels. The hybrid hydrogel enabled flexible and tailored tuning of the material stiffness and the cell-adhesive RGD ligand density.⁴⁴⁹

6.2. Designable Biopolymers: Polynucleotides

Recent progress in DNA nanotechnology has also facilitated the design of a variety of DNA-based nanosized structures useful for

the generation of injectable hydrogels.^{462–466} DNA has specific secondary structures, and stimulus-sensitive features can be incorporated to modulate such a specific structure on the nanoscale. First reported by Um et al.,⁴⁶⁷ the connection of monomer (X-DNA) units resulted in the formation of DNA hydrogels. These hydrogels were biocompatible, biodegradable, inexpensive to fabricate, and easily molded into the desired shapes and sizes. In contrast to other bioinspired hydrogels (including alginate-based hydrogels), the gelation process of DNA hydrogels occurred under physiological conditions, and cell encapsulation was accomplished *in situ*. Drug molecules and even mammalian cells can be encapsulated in the liquid state, eliminating the cell loading step and also avoiding denaturing conditions.⁴⁶⁷ In another study, the DNA sequence was replaced with one containing immunostimulatory cytosine–phosphate–guanine (CpG) motifs.⁴⁶⁸ CpG-DNA induces the production of helper T-cell type 1 cytokines.^{469–471} Nishikawa et al. developed a novel method to produce ligase-free, injectable, self-gelling, biodegradable DNA hydrogels using oligodeoxynucleotides.⁴⁷² Therefore, the single-stranded 5'-ends of polypod-like structured DNA were extended to hybridize under physiological conditions. The gelation of the DNA hydrogels occurred instantaneously after injection using a syringe with a fine needle because of a dissociation/association process. When the hydrogel was stressed, a fraction of the bonds dissociated, and the resulting free ends changed their partner and quickly reassociated through hydrogen bonds. Guo et al.⁴⁷³ developed a pH-switchable DNA hydrogel which was stable at pH 5 and turned into a quasi-liquid at pH 8. This process is reversible and exhibited shape memory effects that would be interesting to assess regarding exploitability for 3D printing. In addition, it was shown that the DNA hydrogels can deliver tumor antigens (ovalbumin) for induction of antigen-specific immune responses.⁴⁷² Nevertheless, hydrogels formed by polynucleotides used for biomedical applications are still a challenge, since the carried genetic information might interfere with cellular function. Therefore, it remains to be seen whether they qualify as future bioinks.

7. CONCLUSIONS AND OUTLOOK

AM, often described as 3D printing in the popular media, has rapidly evolved into a very active field of research and is already used to produce medical implants. One strength of AM is the ability to fabricate hierarchical structures through the simultaneous printing of cells and supporting material in an approach termed biofabrication. In a holistic approach, materials for cell printing are predominantly limited to hydrogels, since the cells must be processed under cytocompatible conditions. We have presented and discussed the most prominent methods suitable for 3D hydrogel printing: (1) LIFT, (2) inkjet printing, and (3) robotic dispensing. While each method has its advantages and disadvantages, robotic dispensing is currently the only method that allows for the generation of clinically relevant constructs, albeit with lower resolutions than LIFT or inkjet printing. With our introduction into the rheological behavior of non-Newtonian liquids and other relevant flow phenomena, we developed general criteria that should be kept in mind for the development of a new bioink. The bioink formulation should have shear thinning properties (not being thixotropic) and should not show extrude swell. If cells are part of the formulation, the viscosity before printing must allow mixing and homogeneous 3D distribution of the cells throughout the printing process without affecting the viability, and shear forces cannot exceed limits tolerable for cell survival. Most importantly, the bioink must

rapidly gel after printing for good shape fidelity of the printing process.

These considerations underline the high demands that biofabrication imposes on the materials to be used for bioprinting. Hydrogels may generally be cross-linked either physically, through noncovalent molecular interactions, or chemically, through the formation of chemical bonds. Physical gels are dynamic due to the reversibility of the network-forming interaction, which is advantageous for the printing process, whereas their mechanical stability after printing is usually low. In contrast, chemically cross-linked gels are mechanically stronger but usually exhibit no reversibility once the network is formed. Dynamic chemical bonds are the exception to this rule and have in some most recent papers been successfully used for bioink development. However, the vast majority of studies which result in stable 3D printed cell loaded structures relies on a combination of both types of gel formation: a physical component for adjusting the rheological properties for printing and a postfabrication chemical cross-linking, often UV-mediated, for stabilizing the printed structure. This is also due to the fact that, since biofabrication originated from engineering and not from chemistry or materials science, most studies rely on established hydrogel systems for biomedical applications and rather optimize formulations than really develop new bioinks. Hence, we then summarized a number of strategies that have evolved in related fields of research, such as supramolecular chemistry and biotechnology, and selected studies that concern approaches potentially exploitable for 3D printing. This was intended to complete the toolbox for polymer chemists, materials researchers, and biotechnologists to be able to enter the field with a rational strategy for bioink development.

We believe that, for future bioink developments, a number of concepts from supramolecular chemistry can directly be transferred, for example, through multiple conjugation with polymers for multivalently interacting building blocks. Also, the concept of supramolecular polymers is a fascinating basis to assess the printability of such systems. Regarding chemical cross-linking of hydrogels in 3D printing, the concept of dynamic covalent bonds bears great potential for the development of novel bioinks. Also, stimulus-switchable chemical reactions, similar to the already used thermosensitive physically cross-linked hydrogels, may in the future be an option for printing hydrogels. Ideally, shear-stress-sensitive chemical bonds would be activated through the printing procedure and rapidly cross-link after the printing. Finally, biotechnology has evolved and is more and more able to produce bioinspired designer structures in yields that allow their use for materials science, and thus also for biofabrication. Further, this connection has just been initiated, and we are sure that this approach bears great potential for future bioink development, as the control over the primary sequence of recombinantly produced biomolecules exceeds the possibilities available in modern macromolecular chemistry, thus allowing for a far better control over structure–function relationships such as rheological properties. This outline for future developments shows the plethora of possibilities that arise for bioink development, especially through the convergence of strategies from related but different research fields.

AUTHOR INFORMATION

Corresponding Author

*E-mail juergen.groll@fmz.uni-wuerzburg.de.

Author Contributions

[§]T.J. and W.S. contributed equally to this work.

Notes

The authors declare no competing financial interest.

Biographies



Tomasz Jüngst was born in 1984 and studied nanostructural engineering in the Department of Physics at the University of Würzburg (Germany). After receiving his Dipl.-Ing. in 2011, he started working on his Ph.D. under the supervision of Jürgen Groll in the Department for Functional Materials in Medicine and Dentistry. During this time, he spent 3 months working at the Queensland University of Technology in Brisbane, Australia, with Dietmar W. Hutmacher and Paul D. Dalton, where he gained experience in the field of melt electrospinning writing granted by the DAAD (German Academic Exchange Service). His research is focused on three-dimensional structures for tissue engineering and biofabrication, where he is developing fabrication systems and processing materials.



Willi Smolan was born in 1989 and studied chemistry at the University of Göttingen (Germany) from 2008 to 2014, where he obtained his bachelor's and master's degrees. There he specialized in macromolecular chemistry and worked on several projects with functional polymers synthesized via RAFT polymerization. In 2011 and 2014, he worked with Martina Stenzel, Philipp Vana, and Peter Roth at the Centre for Advanced Macromolecular Design (Sydney, Australia) and in 2013 with David Fulton at the Chemical Nanoscience Laboratory (Newcastle upon Tyne, U.K.). During his studies, he also undertook industrial internships in the field of functional materials at ContiTECH AG (Northeim, Germany) in 2011 and at Merck KGaA (Darmstadt, Germany) in 2013/2014. Afterward, in 2014, he started his Ph.D. in the Department for Functional Materials in Medicine and Dentistry at the

University of Würzburg (Germany), supervised by Jürgen Groll, working on biocompatible polymers for 3D printing.



Kristin Schacht studied molecular biology and biochemistry at the Universität Bayreuth, where she received her M.Sc. in 2010. Afterward, she spent an 8^{1/2} month research internship in the Department of Biomedical Materials and Regenerative Medicine at CSIRO Materials Science and Engineering, Melbourne, Australia. There, she was involved in the Bioscaffold Project, which contained the expression, purification, and characterization of novel designed collagen-like proteins in bacteria for biomedical applications. She is currently working on her Ph.D. thesis under the supervision of Prof. Dr. Thomas Scheibel at the Universität Bayreuth. Her research focuses on the preparation and characterization of three-dimensional scaffolds (hydrogels and foams) made of recombinant spider silk proteins for biomedical applications.



Thomas Scheibel is Chair of Biomaterials at the Universität Bayreuth in Germany since 2007. He received both his diploma of biochemistry (1994) and a Dr. rer. nat. (1998) from the Universität Regensburg in Germany, and his habilitation (2007) from the Technische Universität München in Germany. He was a Kemper Foundation postdoctoral fellow and a DFG postdoctoral fellow at the University of Chicago. He received the Junior Scientist Award of the Center of Competence for New Materials in 2004. His and his colleagues' work on spider silk proteins won the second prize in the Science4life Venture Cup 2006. He also gained the Biomimetics Award of the German Bundesministerium für Bildung und Forschung (BMBF) in 2006, and the Innovation by Nature Award of the BMBF in 2007. He is 1 of 10 recipients of the 2006 innovation tribute of the Bavarian prime minister, and received the Heinz-Maier-Leibnitz Medal in 2007, the Karl-Heinz-Beckurts Award in 2008, and the Dechema Award of the Max-Buchner Foundation in 2013. Since 2015 he is member of the German National Academy of Science and Engineering (acatech).



Jürgen Groll was born in 1976 and studied chemistry at the University of Ulm (Germany) from 1995 to 2000. He received his Ph.D., during which he spent a 6 month research internship with Virgil Percec (Philadelphia, PA), in 2004 from the RWTH Aachen (Germany) with summa cum laude honors after working under the guidance of Martin Möller. From 2005 to 2009, he worked for 4 years in industry at SusTech GmbH & Co. KG (Darmstadt, Germany) in the field of functional coatings and nanotechnology. In parallel, he built up a research group on polymeric biomaterials at the DWI Interactive Materials Research Institute in Aachen, Germany. Since August 2010, he has held the Chair for Functional Materials in Medicine and Dentistry at the University of Würzburg (Germany). His research interest comprises applied polymer chemistry, nanobiotechnology, biomimetic scaffolds, immunomodulatory materials, and biofabrication. He is the coordinator of the large-scale integrated European project HydroZONES (Contract No. 309962; www.hydrozones.eu) and was awarded an ERC consolidator grant (Design2Heal, Contract No. 617989). For his work, he has received a number of awards, such as the Henkel Innovation Award (2007), the Bayer Early Excellence in Science Award (2009), the Reimund-Stadler Award of the German Chemical Society—Section Macromolecular Chemistry (2010), and the Unilever Prize of the Polymer Networks Group (2014). He currently serves as an editorial board member of the journal *Biofabrication* and as a board member of the International Society for Biofabrication.

ACKNOWLEDGMENTS

We thank Paul D. Dalton for proofreading the manuscript. This research has received funding (J.G., T.J., W.S.) from the European Union's Seventh Framework Programme (FP7/2007-2013) under Grant Agreement No. 309962 (HydroZONES project) and the European Research Council (ERC) under Grant Agreement No. 617989 (Design2Heal project).

REFERENCES

- (1) Gibson, I.; Rosen, D. W.; Stucker, B. *Additive Manufacturing Technologies. 3D Printing, Rapid Prototyping, and Direct Digital Manufacturing*; 2nd ed.; Springer: New York, 2010.
- (2) Kruth, J.-P.; Leu, M.-C.; Nakagawa, T. Progress in Additive Manufacturing and Rapid Prototyping. *CIRP Ann.* **1998**, *47*, 525–540.
- (3) Berman, B. 3-D Printing: The New Industrial Revolution. *Bus. Horizons* **2012**, *55*, 155–162.
- (4) Langer, R.; Vacanti, J. Tissue Engineering. *Science* **1993**, *260*, 920–926.
- (5) Leong, K. F.; Cheah, C. M.; Chua, C. K. Solid Freeform Fabrication of Three-Dimensional Scaffolds for Engineering Replacement Tissues and Organs. *Biomaterials* **2003**, *24*, 2363–2378.
- (6) Hutmacher, D. W.; Sittiger, M.; Risbud, M. V. Scaffold-Based Tissue Engineering: Rationale for Computer-Aided Design and Solid Free-Form Fabrication Systems. *Trends Biotechnol.* **2004**, *22*, 354–362.

- (7) Yang, S.; Leong, K.-F.; Du, Z.; Chua, C.-K. The Design of Scaffolds for Use in Tissue Engineering. Part II. Rapid Prototyping Techniques. *Tissue Eng.* **2002**, *8*, 1–11.
- (8) Yeong, W.-Y.; Chua, C.-K.; Leong, K.-F.; Chandrasekaran, M. Rapid Prototyping in Tissue Engineering: Challenges and Potential. *Trends Biotechnol.* **2004**, *22*, 643–652.
- (9) Mironov, V.; Boland, T.; Trusk, T.; Forgacs, G.; Markwald, R. R. Organ Printing: Computer-Aided Jet-Based 3D Tissue Engineering. *Trends Biotechnol.* **2003**, *21*, 157–161.
- (10) Guillemot, F.; Mironov, V.; Nakamura, M. Bioprinting is Coming of Age: Report from the International Conference on Bioprinting and Biofabrication in Bordeaux (3b'09). *Biofabrication* **2010**, *2*, 010201.
- (11) Derby, B. Printing and Prototyping of Tissues and Scaffolds. *Science* **2012**, *338*, 921–926.
- (12) Ferris, C. J.; Gilmore, K. G.; Wallace, G. G.; In het Panhuis, M. Biofabrication: An Overview of the Approaches used for Printing of Living Cells. *Appl. Microbiol. Biotechnol.* **2013**, *97*, 4243–4258.
- (13) Melchels, F. P.; Domingos, M. A.; Klein, T. J.; Malda, J.; Bartolo, P. J.; Hutmacher, D. W. Additive Manufacturing of Tissues and Organs. *Prog. Polym. Sci.* **2012**, *37*, 1079–1104.
- (14) Murphy, S. V.; Atala, A. 3D Bioprinting of Tissues and Organs. *Nat. Biotechnol.* **2014**, *32*, 773–785.
- (15) Buenger, D.; Topuz, F.; Groll, J. Hydrogels in Sensing Applications. *Prog. Polym. Sci.* **2012**, *37*, 1678–1719.
- (16) Tibbitt, M. W.; Anseth, K. S. Hydrogels as Extracellular Matrix Mimics for 3D Cell Culture. *Biotechnol. Bioeng.* **2009**, *103*, 655–663.
- (17) Hoffman, A. S. Hydrogels for Biomedical Applications. *Adv. Drug Delivery Rev.* **2012**, *64*, 18–23.
- (18) Seliktar, D. Designing Cell-Compatible Hydrogels for Biomedical Applications. *Science* **2012**, *336*, 1124–1128.
- (19) Peppas, N. A.; Hilt, J. Z.; Khademhosseini, A.; Langer, R. Hydrogels in Biology and Medicine: From Molecular Principles to Bionanotechnology. *Adv. Mater.* **2006**, *18*, 1345–1360.
- (20) Lee, K. Y.; Mooney, D. J. Hydrogels for Tissue Engineering. *Chem. Rev.* **2001**, *101*, 1869–1879.
- (21) Annabi, N.; Tamayol, A.; Uquillas, J. A.; Akbari, M.; Bertassoni, L. E.; Cha, C.; Camci-Unal, G.; Dokmeci, M. R.; Peppas, N. A.; Khademhosseini, A. 25th Anniversary Article: Rational Design and Applications of Hydrogels in Regenerative Medicine. *Adv. Mater.* **2014**, *26*, 85–124.
- (22) Patenaude, M.; Smeets, N. M.; Hoare, T. Designing Injectable, Covalently Cross-Linked Hydrogels for Biomedical Applications. *Macromol. Rapid Commun.* **2014**, *35*, 598–617.
- (23) Van Tomme, S. R.; Storm, G.; Hennink, W. E. In Situ Gelling Hydrogels for Pharmaceutical and Biomedical Applications. *Int. J. Pharm.* **2008**, *355*, 1–18.
- (24) Yu, L.; Ding, J. D. Injectable Hydrogels as Unique Biomedical Materials. *Chem. Soc. Rev.* **2008**, *37*, 1473–1481.
- (25) Guvendiren, M.; Lu, H. D.; Burdick, J. A. Shear-Thinning Hydrogels for Biomedical Applications. *Soft Matter* **2012**, *8*, 260–272.
- (26) Billiet, T.; Vandenhoute, M.; Schelfhout, J.; Van Vlierberghe, S.; Dubrule, P. A Review of Trends and Limitations in Hydrogel-Rapid Prototyping for Tissue Engineering. *Biomaterials* **2012**, *33*, 6020–6041.
- (27) Malda, J.; Visser, J.; Melchels, F. P.; Jüngst, T.; Hennink, W. E.; Dhert, W. J. A.; Groll, J.; Hutmacher, D. W. 25th Anniversary Article: Engineering Hydrogels for Biofabrication. *Adv. Mater.* **2013**, *25*, 5011–5028.
- (28) Skardal, A.; Atala, A. Biomaterials for Integration with 3-D Bioprinting. *Ann. Biomed. Eng.* **2015**, *43*, 730–746.
- (29) Vaezi, M.; Seitz, H.; Yang, S. A Review on 3D Micro-Additive Manufacturing Technologies. *Int. J. Adv. Manuf. Technol.* **2013**, *67*, 1721–1754.
- (30) Raimondi, M. T.; Eaton, S. M.; Nava, M. M.; Laganà, M.; Cerullo, G.; Osellame, R. Two-Photon Laser Polymerization: From Fundamentals to Biomedical Application in Tissue Engineering and Regenerative Medicine. *J. Appl. Biomater. Funct. Mater.* **2012**, *10*, 56–66.
- (31) Wust, S.; Müller, R.; Hofmann, S. Controlled Positioning of Cells in Biomaterials—Approaches Towards 3D Tissue Printing. *J. Funct. Biomater.* **2011**, *2*, 119–154.
- (32) Melchels, F. P.; Feijen, J.; Grijpma, D. W. A Review on Stereolithography and its Applications in Biomedical Engineering. *Biomaterials* **2010**, *31*, 6121–6130.
- (33) Tumbleston, J. R.; Shirvanyants, D.; Ermoshkin, N.; Janusziewicz, R.; Johnson, A. R.; Kelly, D.; Chen, K.; Pischmidt, R.; Rolland, J. P.; Ermoshkin, A.; et al. Continuous Liquid Interface Production of 3D Objects. *Science* **2015**, *347*, 1349–1352.
- (34) Chrisey, D. B.; Pique, A.; McGill, R.; Horwitz, J.; Ringeisen, B.; Bubb, D.; Wu, P. Laser Deposition of Polymer and Biomaterial Films. *Chem. Rev.* **2003**, *103*, 553–576.
- (35) Ringeisen, B. R.; Othon, C. M.; Barron, J. A.; Young, D.; Spargo, B. J. Jet-Based Methods to Print Living Cells. *Biotechnol. J.* **2006**, *1*, 930–948.
- (36) Schiele, N. R.; Corr, D. T.; Huang, Y.; Raof, N. A.; Xie, Y.; Chrisey, D. B. Laser-Based Direct-Write Techniques for Cell Printing. *Biofabrication* **2010**, *2*, 032001.
- (37) Gruene, M.; Pflaum, M.; Hess, C.; Diamantouros, S.; Schlie, S.; Deiwick, A.; Koch, L.; Wilhelmi, M.; Jockenhoevel, S.; Haverich, A.; et al. Laser Printing of Three-Dimensional Multicellular Arrays for Studies of Cell–Cell and Cell–Environment Interactions. *Tissue Eng., Part C* **2011**, *17*, 973–982.
- (38) Guillemot, F.; Souquet, A.; Catros, S.; Guillotin, B.; Lopez, J.; Faucon, M.; Pippenger, B.; Bareille, R.; Remy, M.; Bellance, S.; et al. High-Throughput Laser Printing of Cells and Biomaterials for Tissue Engineering. *Acta Biomater.* **2010**, *6*, 2494–2500.
- (39) Guillotin, B.; Souquet, A.; Catros, S.; Duocastella, M.; Pippenger, B.; Bellance, S.; Bareille, R.; Remy, M.; Bordenave, L.; Amedee, J.; et al. Laser Assisted Bioprinting of Engineered Tissue with High Cell Density and Microscale Organization. *Biomaterials* **2010**, *31*, 7250–7256.
- (40) Koch, L.; Deiwick, A.; Schlie, S.; Michael, S.; Gruene, M.; Coger, V.; Zychlinski, D.; Schambach, A.; Reimers, K.; Vogt, P. M.; et al. Skin Tissue Generation by Laser Cell Printing. *Biotechnol. Bioeng.* **2012**, *109*, 1855–1863.
- (41) Michael, S.; Sorg, H.; Peck, C. T.; Koch, L.; Deiwick, A.; Chichkov, B.; Vogt, P. M.; Reimers, K. Tissue Engineered Skin Substitutes Created by Laser-Assisted Bioprinting Form Skin-Like Structures in the Dorsal Skin Fold Chamber in Mice. *PLoS One* **2013**, *8*, e57741.
- (42) Nahmias, Y.; Schwartz, R. E.; Verfaillie, C. M.; Odde, D. J. Laser-Guided Direct Writing for Three-Dimensional Tissue Engineering. *Biotechnol. Bioeng.* **2005**, *92*, 129–136.
- (43) Koch, L.; Kuhn, S.; Sorg, H.; Gruene, M.; Schlie, S.; Gaebel, R.; Polchow, B.; Reimers, K.; Stoelting, S.; Ma, N.; et al. Laser Printing of Skin Cells and Human Stem Cells. *Tissue Eng., Part C* **2010**, *16*, 847–854.
- (44) Gruene, M.; Unger, C.; Koch, L.; Deiwick, A.; Chichkov, B. Dispensing Pico to Nanolitre of a Natural Hydrogel by Laser-Assisted Bioprinting. *Biomed. Eng. Online* **2011**, *10*, 19.
- (45) Barron, J. A.; Ringeisen, B. R.; Kim, H.; Spargo, B. J.; Chrisey, D. B. Application of Laser Printing to Mammalian Cells. *Thin Solid Films* **2004**, *453–454*, 383–387.
- (46) Lin, Y.; Huang, G.; Huang, Y.; Tzeng, T.-R. J.; Chrisey, D. Effect of Laser Fluence in Laser-Assisted Direct Writing of Human Colon Cancer Cell. *Rapid Prototyping J.* **2010**, *16*, 202–208.
- (47) Ringeisen, B. R.; Kim, H.; Barron, J. A.; Krizman, D. B.; Chrisey, D. B.; Jackman, S.; Auyeung, R.; Spargo, B. J. Laser Printing of Pluripotent Embryonal Carcinoma Cells. *Tissue Eng.* **2004**, *10*, 483–491.
- (48) Barron, J. A.; Wu, P.; Ladouceur, H. D.; Ringeisen, B. R. Biological Laser Printing: A Novel Technique for Creating Heterogeneous 3-Dimensional Cell Patterns. *Biomed. Microdevices* **2004**, *6*, 139–147.
- (49) Catros, S.; Guillotin, B.; Bačáková, M.; Fricain, J.-C.; Guillemot, F. Effect of Laser Energy, Substrate Film Thickness and Bioink Viscosity on Viability of Endothelial Cells Printed by Laser-Assisted Bioprinting. *Appl. Surf. Sci.* **2011**, *257*, 5142–5147.
- (50) Duocastella, M.; Fernández-Pradas, J. M.; Serra, P.; Morenza, J. L. Jet Formation in the Laser Forward Transfer of Liquids. *Appl. Phys. A: Mater. Sci. Process.* **2008**, *93*, 453–456.

- (51) Guillemot, F.; Souquet, A.; Catros, S.; Guillotin, B. Laser-Assisted Cell Printing: Principle, Physical Parameters Versus Cell Fate and Perspectives in Tissue Engineering. *Nanomedicine* **2010**, *5*, 507–515.
- (52) Lin, Y.; Huang, Y.; Chrisey, D. B. Droplet Formation in Matrix-Assisted Pulsed-Laser Evaporation Direct Writing of Glycerol-Water Solution. *J. Appl. Phys.* **2009**, *105*, 093111.
- (53) Mézel, C.; Hallo, L.; Souquet, A.; Breil, J.; Hébert, D.; Guillemot, F. Self-Consistent Modeling of Jet Formation Process in the Nanosecond Laser Pulse Regime. *Phys. Plasmas* **2009**, *16*, 123112.
- (54) Young, D.; Auyeung, R.; Pique, A.; Chrisey, D.; Dlott, D. Plume and Jetting Regimes in a Laser Based Forward Transfer Process as Observed by Time-Resolved Optical Microscopy. *Appl. Surf. Sci.* **2002**, *197*–198, 181–187.
- (55) Wilson, W. C., Jr.; Boland, T. Cell and Organ Printing 1: Protein and Cell Printers. *Anat. Rec.* **2003**, *272A*, 491–496.
- (56) Boland, T.; Xu, T.; Damon, B.; Cui, X. Application of Inkjet Printing to Tissue Engineering. *Biotechnol. J.* **2006**, *1*, 910–917.
- (57) Calvert, P. Inkjet Printing for Materials and Devices. *Chem. Mater.* **2001**, *13*, 3299–3305.
- (58) de Gans, B. J.; Duineveld, P. C.; Schubert, U. S. Inkjet Printing of Polymers: State of the Art and Future Developments. *Adv. Mater.* **2004**, *16*, 203–213.
- (59) Derby, B. Bioprinting: Inkjet Printing Proteins and Hybrid Cell-Containing Materials and Structures. *J. Mater. Chem.* **2008**, *18*, 5717–5721.
- (60) Derby, B. Inkjet Printing of Functional and Structural Materials: Fluid Property Requirements, Feature Stability, and Resolution. *Annu. Rev. Mater. Res.* **2010**, *40*, 395–414.
- (61) Martin, G. D.; Hoath, S. D.; Hutchings, I. M. Inkjet Printing - the Physics of Manipulating Liquid Jets and Drops. *J. Phys.: Conf. Ser.* **2008**, *105*, 012001.
- (62) Saunders, R. E.; Derby, B. Inkjet Printing Biomaterials for Tissue Engineering: Bioprinting. *Int. Mater. Rev.* **2014**, *59*, 430–448.
- (63) Singh, M.; Haverinen, H. M.; Dhagat, P.; Jabbari, G. E. Inkjet Printing-Process and its Applications. *Adv. Mater.* **2010**, *22*, 673–685.
- (64) Kim, J. D.; Choi, J. S.; Kim, B. S.; Choi, Y. C.; Cho, Y. W. Piezoelectric Inkjet Printing of Polymers: Stem Cell Patterning on Polymer Substrates. *Polymer* **2010**, *51*, 2147–2154.
- (65) Xu, T.; Jin, J.; Gregory, C.; Hickman, J. J.; Boland, T. Inkjet Printing of Viable Mammalian Cells. *Biomaterials* **2005**, *26*, 93–99.
- (66) Setti, L.; Fraleoni-Morgera, A.; Ballarin, B.; Filippini, A.; Frascaro, D.; Piana, C. An Amperometric Glucose Biosensor Prototype Fabricated by Thermal Inkjet Printing. *Biosens. Bioelectron.* **2005**, *20*, 2019–2026.
- (67) Fromm, J. E. Numerical Calculation of the Fluid Dynamics of Drop-on-Demand Jets. *IBM J. Res. Dev.* **1984**, *28*, 322–333.
- (68) Reis, N.; Derby, B. Ink Jet Deposition of Ceramic Suspensions: Modeling and Experiments of Droplet Formation. *MRS Online Proc. Libr.* **2000**, *625*, 117.
- (69) Jang, D.; Kim, D.; Moon, J. Influence of Fluid Physical Properties on Ink-Jet Printability. *Langmuir* **2009**, *25*, 2629–2635.
- (70) Xu, C.; Zhang, M.; Huang, Y.; Ogale, A.; Fu, J.; Markwald, R. R. Study of Droplet Formation Process During Drop-on-Demand Inkjetting of Living Cell-Laden Bioink. *Langmuir* **2014**, *30*, 9130–9138.
- (71) Campbell, P. G.; Miller, E. D.; Fisher, G. W.; Walker, L. M.; Weiss, L. E. Engineered Spatial Patterns of FGF-2 Immobilized on Fibrin Direct Cell Organization. *Biomaterials* **2005**, *26*, 6762–6770.
- (72) Sirringhaus, H.; Kawase, T.; Friend, R. H.; Shimoda, T.; Inbasekaran, M.; Wu, W.; Woo, E. P. High-Resolution Inkjet Printing of All-Polymer Transistor Circuits. *Science* **2000**, *290*, 2123–2126.
- (73) Cobas, R.; Muñoz-Pérez, S.; Cadogan, S.; Ridgway, M. C.; Obradors, X. Surface Charge Reversal Method for High-Resolution Inkjet Printing of Functional Water-Based Inks. *Adv. Funct. Mater.* **2015**, *25*, 768–775.
- (74) Soltman, D.; Subramanian, V. Inkjet-Printed Line Morphologies and Temperature Control of the Coffee Ring Effect. *Langmuir* **2008**, *24*, 2224–2231.
- (75) Stringer, J.; Derby, B. Formation and Stability of Lines Produced by Inkjet Printing. *Langmuir* **2010**, *26*, 10365–10372.
- (76) Chang, C. C.; Boland, E. D.; Williams, S. K.; Hoying, J. B. Direct-Write Bioprinting Three-Dimensional Biohybrid Systems for Future Regenerative Therapies. *J. Biomed. Mater. Res., Part B* **2011**, *98B*, 160–170.
- (77) Dababneh, A. B.; Ozbolat, I. T. Bioprinting Technology: A Current State-of-the-Art Review. *J. Manuf. Sci., Trans. ASME* **2014**, *136*, 061016.
- (78) Ozbolat, I. T.; Yu, Y. Bioprinting toward Organ Fabrication: Challenges and Future Trends. *IEEE Trans. Biomed. Eng.* **2013**, *60*, 691–699.
- (79) Yan, K. C.; Nair, K.; Sun, W. Three Dimensional Multi-Scale Modelling and Analysis of Cell Damage in Cell-Encapsulated Alginate Constructs. *J. Biomech.* **2010**, *43*, 1031–1038.
- (80) Schuurman, W.; Levett, P. A.; Pot, M. W.; van Weeren, P. R.; Dhert, W. J. A.; Hutmacher, D. W.; Melchels, F. P. W.; Klein, T. J.; Malda, J. Gelatin-Methacrylamide Hydrogels as Potential Biomaterials for Fabrication of Tissue-Engineered Cartilage Constructs. *Macromol. Biosci.* **2013**, *13*, 551–561.
- (81) Lewis, J. A. Direct Ink Writing of 3D Functional Materials. *Adv. Funct. Mater.* **2006**, *16*, 2193–2204.
- (82) Guillotin, B.; Guillemot, F. Cell Patterning Technologies for Organotypic Tissue Fabrication. *Trends Biotechnol.* **2011**, *29*, 183–190.
- (83) Khalil, S.; Nam, J.; Sun, W. Multi-Nozzle Deposition for Construction of 3D Biopolymer Tissue Scaffolds. *Rapid Prototyping J.* **2005**, *11*, 9–17.
- (84) Smith, C. M.; Stone, A. L.; Parkhill, R. L.; Stewart, R. L.; Simpkins, M. W.; Kachurin, A. M.; Warren, W. L.; Williams, S. K. Three-Dimensional Bioassembly Tool for Generating Viable Tissue-Engineered Constructs. *Tissue Eng.* **2004**, *10*, 1566–1576.
- (85) Madou, M. J. *Fundamentals of Microfabrication: The Science of Miniaturization*; CRC Press: Boca Raton, FL, 2002.
- (86) Sobral, J. M.; Caridade, S. G.; Sousa, R. A.; Mano, J. F.; Reis, R. L. Three-Dimensional Plotted Scaffolds with Controlled Pore Size Gradients: Effect of Scaffold Geometry on Mechanical Performance and Cell Seeding Efficiency. *Acta Biomater.* **2011**, *7*, 1009–1018.
- (87) Ovsianikov, A.; Gruene, M.; Pflaum, M.; Koch, L.; Maiorana, F.; Wilhelm, M.; Haverich, A.; Chichkov, B. Laser Printing of Cells into 3D Scaffolds. *Biofabrication* **2010**, *2*, 014104.
- (88) Strobl, G. R. *The Physics of Polymers*; Springer: Berlin, 2007.
- (89) Rubinstein, M.; Colby, R. H. *Polymer Physics*; Oxford University Press: Oxford, U.K., 2003.
- (90) Shenoy, A. V. *Rheology of Filled Polymer Systems*; Kluwer Academic Publishers: Dordrecht, The Netherlands, 1999.
- (91) Barnes, H. A.; Hutton, J. F.; Walters, K. *An Introduction to Rheology*; Elsevier: Amsterdam, 1989.
- (92) Bird, R. B.; Armstrong, R. C.; Hassager, O. *Dynamics of Polymeric Liquids*; John Wiley & Sons: New York, 1987.
- (93) Ferry, J. D. *Viscoelastic Properties of Polymers*; John Wiley & Sons: New York, 1980.
- (94) Möller, P. C. F.; Fall, A.; Bonn, D. Origin of Apparent Viscosity in Yield Stress Fluids Below Yielding. *Europhys. Lett.* **2009**, *87*, 38004.
- (95) Barnes, H.; Walters, K. The Yield Stress Myth? *Rheol. Acta* **1985**, *24*, 323–326.
- (96) Barnes, H. A. The Yield Stress—a Review or ‘Παντα Ρε’—Everything Flows? *J. Non-Newtonian Fluid Mech.* **1999**, *81*, 133–178.
- (97) Schurz, J. The Yield Stress—an Empirical Reality. *Rheol. Acta* **1990**, *29*, 170–171.
- (98) Coussot, P. Yield Stress Fluid Flows: A Review of Experimental Data. *J. Non-Newtonian Fluid Mech.* **2014**, *211*, 31–49.
- (99) Barnes, H. A. Thixotropy—a Review. *J. Non-Newtonian Fluid Mech.* **1997**, *70*, 1–33.
- (100) Mewis, J.; Wagner, N. J. Thixotropy. *Adv. Colloid Interface Sci.* **2009**, *147*–148, 214–227.
- (101) Larson, R. G.; Desai, P. S. Modeling the Rheology of Polymer Melts and Solutions. *Annu. Rev. Fluid Mech.* **2015**, *47*, 47–65.
- (102) Irgens, F. *Rheology and Non-Newtonian Fluids*; Springer: Heidelberg, Germany, 2014.
- (103) Aguado, B. A.; Mulyasasmita, W.; Su, J.; Lampe, K. J.; Heilshorn, S. C. Improving Viability of Stem Cells During Syringe Needle Flow

- through the Design of Hydrogel Cell Carriers. *Tissue Eng, Part A* **2012**, *18*, 806–815.
- (104) Pati, F.; Jang, J.; Ha, D. H.; Kim, S. W.; Rhie, J. W.; Shim, J. H.; Kim, D. H.; Cho, D. W. Printing Three-Dimensional Tissue Analogues with Decellularized Extracellular Matrix Bioink. *Nat. Commun.* **2014**, *5*, 1–11.
- (105) Schuurman, W.; Khristov, V.; Pot, M. W.; van Weeren, P. R.; Dhert, W. J. A.; Malda, J. Bioprinting of Hybrid Tissue Constructs with Tailorable Mechanical Properties. *Biofabrication* **2011**, *3*, 021001.
- (106) Lewis, J. A. Colloidal Processing of Ceramics. *J. Am. Ceram. Soc.* **2000**, *83*, 2341–2359.
- (107) Macosko, C. W. *Rheology: Principles, Measurements, and Applications*; Wiley-VCH: New York, 1994.
- (108) Mewis, J.; Wagner, N. J. *Colloidal Suspension Rheology*; Cambridge University Press: Cambridge, U.K., 2012.
- (109) Bergenholtz, J. Theory of Rheology of Colloidal Dispersions. *Curr. Opin. Colloid Interface Sci.* **2001**, *6*, 484–488.
- (110) Goodwin, J. W.; Hughes, R. W. *Rheology for Chemists: An Introduction*; Royal Society of Chemistry: Cambridge, U.K., 2000.
- (111) Krieger, I. M. Rheology of Monodisperse Latices. *Adv. Colloid Interface Sci.* **1972**, *3*, 111–136.
- (112) Lewis, J. A. Direct-Write Assembly of Ceramics from Colloidal Inks. *Curr. Opin. Solid State Mater. Sci.* **2002**, *6*, 245–250.
- (113) Ahn, B. Y.; Duoss, E. B.; Motala, M. J.; Guo, X.; Park, S.-I.; Xiong, Y.; Yoon, J.; Nuzzo, R. G.; Rogers, J. A.; Lewis, J. A. Omnidirectional Printing of Flexible, Stretchable, and Spanning Silver Microelectrodes. *Science* **2009**, *323*, 1590–1593.
- (114) Ahn, B. Y.; Shoji, D.; Hansen, C. J.; Hong, E.; Dunand, D. C.; Lewis, J. A. Printed Origami Structures. *Adv. Mater.* **2010**, *22*, 2251–2254.
- (115) Hanson Shepherd, J. N.; Parker, S. T.; Shepherd, R. F.; Gillette, M. U.; Lewis, J. A.; Nuzzo, R. G. 3D Microperiodic Hydrogel Scaffolds for Robust Neuronal Cultures. *Adv. Funct. Mater.* **2011**, *21*, 47–54.
- (116) Smay, J. E.; Gratson, G. M.; Shepherd, R. F.; Cesarano, J.; Lewis, J. A. Directed Colloidal Assembly of 3D Periodic Structures. *Adv. Mater.* **2002**, *14*, 1279–1283.
- (117) Schmid-Schönbein, H.; Wells, R.; Goldstone, J. Influence of Deformability of Human Red Cells Upon Blood Viscosity. *Circ. Res.* **1969**, *25*, 131–143.
- (118) Winkler, R. G.; Fedosov, D. A.; Gompper, G. Dynamical and Rheological Properties of Soft Colloid Suspensions. *Curr. Opin. Colloid Interface Sci.* **2014**, *19*, 594–610.
- (119) Vlassopoulos, D.; Cloitre, M. Tunable Rheology of Dense Soft Deformable Colloids. *Curr. Opin. Colloid Interface Sci.* **2014**, *19*, 561–574.
- (120) Singh, S. P.; Chatterji, A.; Gompper, G.; Winkler, R. G. Dynamical and Rheological Properties of Ultrasoft Colloids under Shear Flow. *Macromolecules* **2013**, *46*, 8026–8036.
- (121) Huang, C. C.; Sutmann, G.; Gompper, G.; Winkler, R. G. Tumbling of Polymers in Semidilute Solution under Shear Flow. *Europhys. Lett.* **2011**, *93*, 54004.
- (122) Huang, C.-C.; Winkler, R. G.; Sutmann, G.; Gompper, G. Semidilute Polymer Solutions at Equilibrium and under Shear Flow. *Macromolecules* **2010**, *43*, 10107–10116.
- (123) Huber, B.; Harasim, M.; Wunderlich, B.; Kröger, M.; Bausch, A. R. Microscopic Origin of the Non-Newtonian Viscosity of Semiflexible Polymer Solutions in the Semidilute Regime. *ACS Macro Lett.* **2014**, *3*, 136–140.
- (124) De Gennes, P.; Leger, L. Dynamics of Entangled Polymer Chains. *Annu. Rev. Phys. Chem.* **1982**, *33*, 49–61.
- (125) Watanabe, H. Viscoelasticity and Dynamics of Entangled Polymers. *Prog. Polym. Sci.* **1999**, *24*, 1253–1403.
- (126) Melchels, F. P. W.; Dhert, W. J. A.; Hutmacher, D. W.; Malda, J. Development and Characterisation of a New Bioink for Additive Tissue Manufacturing. *J. Mater. Chem. B* **2014**, *2*, 2282–2289.
- (127) Oyen, M. L. Mechanical Characterisation of Hydrogel Materials. *Int. Mater. Rev.* **2014**, *59*, 44–59.
- (128) Malkin, A. Y.; Isayev, A. I. *Rheology: Concepts, Methods, and Applications*; ChemTec Publishing: Toronto, Canada, 2012.
- (129) Picout, D. R.; Ross-Murphy, S. B. Rheology of Biopolymer Solutions and Gels. *Sci. World J.* **2003**, *3*, 105–121.
- (130) Yang, Y.; Urban, M. W. Self-Healing Polymeric Materials. *Chem. Soc. Rev.* **2013**, *42*, 7446–7467.
- (131) Pfister, A.; Landers, R.; Laib, A.; Hübner, U.; Schmelzeisen, R.; Mühlaupt, R. Biofunctional Rapid Prototyping for Tissue-Engineering Applications: 3D Bioplotting Versus 3D Printing. *J. Polym. Sci., Part A: Polym. Chem.* **2004**, *42*, 624–638.
- (132) Ko, D. Y.; Shinde, U. P.; Yeon, B.; Jeong, B. Recent Progress of in Situ Formed Gels for Biomedical Applications. *Prog. Polym. Sci.* **2013**, *38*, 672–701.
- (133) Yang, J.-A.; Yeom, J.; Hwang, B. W.; Hoffman, A. S.; Hahn, S. K. In Situ-Forming Injectable Hydrogels for Regenerative Medicine. *Prog. Polym. Sci.* **2014**, *39*, 1973–1986.
- (134) Bakaic, E.; Smeets, N. M. B.; Hoare, T. Injectable Hydrogels Based on Poly(Ethylene Glycol) and Derivatives as Functional Biomaterials. *RSC Adv.* **2015**, *5*, 35469–35486.
- (135) Nicodemus, G. D.; Bryant, S. J. Cell Encapsulation in Biodegradable Hydrogels for Tissue Engineering Applications. *Tissue Eng., Part B* **2008**, *14*, 149–165.
- (136) Lutolf, M. P.; Hubbell, J. A. Synthetic Biomaterials as Instructive Extracellular Microenvironments for Morphogenesis in Tissue Engineering. *Nat. Biotechnol.* **2005**, *23*, 47–55.
- (137) Cui, X.; Breitenkamp, K.; Finn, M. G.; Lotz, M.; D'Lima, D. D. Direct Human Cartilage Repair Using Three-Dimensional Bioprinting Technology. *Tissue Eng., Part A* **2012**, *18*, 1304–1312.
- (138) Maher, P. S.; Keatch, R. P.; Donnelly, K.; Mackay, R. E.; Paxton, J. Z. Construction of 3D Biological Matrices using Rapid Prototyping Technology. *Rapid Prototyping J.* **2009**, *15*, 204–210.
- (139) Guo, M.; Jiang, M.; Pispas, S.; Yu, W.; Zhou, C. Supramolecular Hydrogels Made of End-Functionalized Low-Molecular-Weight PEG and α -Cyclodextrin and their Hybridization with SiO₂ Nanoparticles through Host–Guest Interaction. *Macromolecules* **2008**, *41*, 9744–9749.
- (140) Rutz, A. L.; Hyland, K. E.; Jakus, A. E.; Burghardt, W. R.; Shah, R. N. A Multimaterial Bioink Method for 3D Printing Tunable, Cell-Compatible Hydrogels. *Adv. Mater.* **2015**, *27*, 1607–1614.
- (141) Pescosolido, L.; Schuurman, W.; Malda, J.; Matricardi, P.; Alhaique, F.; Coviello, T.; van Weeren, P. R.; Dhert, W. J. A.; Hennink, W. E.; Vermonden, T. Hyaluronic Acid and Dextran-Based Semi-IPN Hydrogels as Biomaterials for Bioprinting. *Biomacromolecules* **2011**, *12*, 1831–1838.
- (142) Billiet, T.; Gevaert, E.; De Schryver, T.; Cornelissen, M.; Dubrule, P. The 3D Printing of Gelatin Methacrylamide Cell-Laden Tissue-Engineered Constructs with High Cell Viability. *Biomaterials* **2014**, *35*, 49–62.
- (143) Gurkan, U. A.; El Assal, R.; Yildiz, S. E.; Sung, Y.; Trachtenberg, A. J.; Kuo, W. P.; Demirci, U. Engineering Anisotropic Biomimetic Fibrocartilage Microenvironment by Bioprinting Mesenchymal Stem Cells in Nanoliter Gel Droplets. *Mol. Pharmaceutics* **2014**, *11*, 2151–2159.
- (144) Hockaday, L.; Kang, K.; Colangelo, N.; Cheung, P.; Duan, B.; Malone, E.; Wu, J.; Girardi, L.; Bonassar, L.; Lipson, H.; et al. Rapid 3D Printing of Anatomically Accurate and Mechanically Heterogeneous Aortic Valve Hydrogel Scaffolds. *Biofabrication* **2012**, *4*, 035005.
- (145) Gao, G.; Yonezawa, T.; Hubbell, K.; Dai, G.; Cui, X. Inkjet-Bioprinted Acrylated Peptides and PEG Hydrogel with Human Mesenchymal Stem Cells Promote Robust Bone and Cartilage Formation with Minimal Printhead Clogging. *Biotechnol. J.* **2015**, DOI: [10.1002/biot.201400635](https://doi.org/10.1002/biot.201400635).
- (146) Skardal, A.; Zhang, J.; McCoard, L.; Xu, X.; Oottamasathien, S.; Prestwich, G. D. Photocrosslinkable Hyaluronan-Gelatin Hydrogels for Two-Step Bioprinting. *Tissue Eng., Part A* **2010**, *16*, 2675–2685.
- (147) Fedorovich, N. E.; Swennen, I.; Girones, J.; Moroni, L.; van Blitterswijk, C. A.; Schacht, E.; Alblas, J.; Dhert, W. J. A. Evaluation of Photocrosslinked Lutrol Hydrogel for Tissue Printing Applications. *Biomacromolecules* **2009**, *10*, 1689–1696.
- (148) Censi, R.; Schuurman, W.; Malda, J.; di Dato, G.; Burgisser, P. E.; Dhert, W. J. A.; van Nostrum, C. F.; di Martino, P.; Vermonden, T.;

- Hennink, W. E. A Printable Photopolymerizable Thermosensitive P(HPMAM-Lactate)-PEG Hydrogel for Tissue Engineering. *Adv. Funct. Mater.* **2011**, *21*, 1833–1842.
- (149) Zhang, W.; Lian, Q.; Li, D.; Wang, K.; Hao, D.; Bian, W.; Jin, Z. The Effect of Interface Microstructure on Interfacial Shear Strength for Osteochondral Scaffolds Based on Biomimetic Design and 3D Printing. *Mater. Sci. Eng., C* **2015**, *46*, 10–15.
- (150) Hoch, E.; Hirth, T.; Tovar, G. E. M.; Borchers, K. Chemical Tailoring of Gelatin to Adjust its Chemical and Physical Properties for Functional Bioprinting. *J. Mater. Chem. B* **2013**, *1*, 5675–5685.
- (151) Skardal, A.; Zhang, J.; Prestwich, G. D. Bioprinting Vessel-Like Constructs using Hyaluronan Hydrogels Crosslinked with Tetrahedral Polyethylene Glycol Tetracrylates. *Biomaterials* **2010**, *31*, 6173–6181.
- (152) Sasaki, J.-I.; Asoh, T.-A.; Matsumoto, T.; Egusa, H.; Sohmura, T.; Alsberg, E.; Akashi, M.; Yatani, H. Fabrication of Three-Dimensional Cell Constructs Using Temperature-Responsive Hydrogel. *Tissue Eng., Part A* **2010**, *16*, 2497–2504.
- (153) Wang, X.; Yan, Y.; Pan, Y.; Xiong, Z.; Liu, H.; Cheng, J.; Liu, F.; Lin, F.; Wu, R.; Zhang, R.; et al. Generation of Three-Dimensional Hepatocyte/Gelatin Structures with Rapid Prototyping System. *Tissue Eng.* **2006**, *12*, 83–90.
- (154) Zhang, T.; Yan, Y.; Wang, X.; Xiong, Z.; Lin, F.; Wu, R.; Zhang, R. Three-Dimensional Gelatin and Gelatin/Hyaluronan Hydrogel Structures for Traumatic Brain Injury. *J. Bioact. Compat. Polym.* **2007**, *22*, 19–29.
- (155) Xu, M.; Wang, X.; Yan, Y.; Yao, R.; Ge, Y. An Cell-Assembly Derived Physiological 3D Model of the Metabolic Syndrome, Based on Adipose-Derived Stromal Cells and a Gelatin/Alginate/Fibrinogen Matrix. *Biomaterials* **2010**, *31*, 3868–3877.
- (156) Li, S.; Xiong, Z.; Wang, X.; Yan, Y.; Liu, H.; Zhang, R. Direct Fabrication of a Hybrid Cell/Hydrogel Construct by a Double-Nozzle Assembling Technology. *J. Bioact. Compat. Polym.* **2009**, *24*, 249–265.
- (157) Yan, Y.; Wang, X.; Pan, Y.; Liu, H.; Cheng, J.; Xiong, Z.; Lin, F.; Wu, R.; Zhang, R.; Lu, Q. Fabrication of Viable Tissue-Engineered Constructs with 3D Cell-Assembly Technique. *Biomaterials* **2005**, *26*, 5864–5871.
- (158) Xu, T.; Binder, K. W.; Albanna, M. Z.; Dice, D.; Zhao, W.; Yoo, J. J.; Atala, A. Hybrid Printing of Mechanically and Biologically Improved Constructs for Cartilage Tissue Engineering Applications. *Biofabrication* **2013**, *5*, 015001.
- (159) Campos, D. F. D.; Blaeser, A.; Weber, M.; Jakel, J.; Neuss, S.; Jahnens-Decent, W.; Fischer, H. Three-Dimensional Printing of Stem Cell-Laden Hydrogels Submerged in a Hydrophobic High-Density Fluid. *Biofabrication* **2013**, *5*, 015003.
- (160) Visser, J.; Peters, B.; Burger, T. J.; Boomstra, J.; Dhert, W. J. A.; Melchels, F. P. W.; Malda, J. Biofabrication of Multi-Material Anatomically Shaped Tissue Constructs. *Biofabrication* **2013**, *5*, 035007.
- (161) Bakarich, S. E.; in het Panhuis, M.; Beirne, S.; Wallace, G. G.; Spinks, G. M. Extrusion Printing of Ionic–Covalent Entanglement Hydrogels with High Toughness. *J. Mater. Chem. B* **2013**, *1*, 4939–4946.
- (162) Hong, S.; Sycks, D.; Chan, H. F.; Lin, S.; Lopez, G. P.; Guilak, F.; Leong, K. W.; Zhao, X. 3D Printing of Highly Stretchable and Tough Hydrogels into Complex, Cellularized Structures. *Adv. Mater.* **2015**, *27*, 4035–4040.
- (163) Wilson, A.; Gasparini, G.; Matile, S. Functional Systems with Orthogonal Dynamic Covalent Bonds. *Chem. Soc. Rev.* **2014**, *43*, 1948–1962.
- (164) Rowan, S. J.; Cantrill, S. J.; Cousins, G. R.; Sanders, J. K.; Stoddart, J. F. Dynamic Covalent Chemistry. *Angew. Chem., Int. Ed.* **2002**, *41*, 898–952.
- (165) Belowich, M. E.; Stoddart, J. F. Dynamic Imine Chemistry. *Chem. Soc. Rev.* **2012**, *41*, 2003–2024.
- (166) Tan, H.; Chu, C. R.; Payne, K. A.; Marra, K. G. Injectable in Situ Forming Biodegradable Chitosan–Hyaluronic Acid Based Hydrogels for Cartilage Tissue Engineering. *Biomaterials* **2009**, *30*, 2499–2506.
- (167) Zehnder, T.; Sarker, B.; Boccaccini, A. R.; Detsch, R. Evaluation of an Alginate-Gelatine Crosslinked Hydrogel for Bioplotting. *Biofabrication* **2015**, *7*, 025001.
- (168) Meng, H.; Xiao, P.; Gu, J.; Wen, X.; Xu, J.; Zhao, C.; Zhang, J.; Chen, T. Self-Healable Macro-/Microscopic Shape Memory Hydrogels Based on Supramolecular Interactions. *Chem. Commun.* **2014**, *50*, 12277–12280.
- (169) Singh, S.; Zilkowski, I.; Ewald, A.; Maurell-Lopez, T.; Albrecht, K.; Möller, M.; Groll, J. Mild Oxidation of Thiofunctional Polymers to Cytocompatible and Stimuli-Sensitive Hydrogels and Nanogels. *Macromol. Biosci.* **2013**, *13*, 470–482.
- (170) Singh, S.; Topuz, F.; Hahn, K.; Albrecht, K.; Groll, J. Embedding of Active Proteins and Living Cells in Redox-Sensitive Hydrogels and Nanogels through Enzymatic Cross-Linking. *Angew. Chem., Int. Ed.* **2013**, *52*, 3000–3003.
- (171) Lehn, J.-M. From Supramolecular Chemistry Towards Constitutional Dynamic Chemistry and Adaptive Chemistry. *Chem. Soc. Rev.* **2007**, *36*, 151–160.
- (172) Seiffert, S.; Sprakler, J. Physical Chemistry of Supramolecular Polymer Networks. *Chem. Soc. Rev.* **2012**, *41*, 909–930.
- (173) Qi, Z.; Schalley, C. A. Exploring Macrocycles in Functional Supramolecular Gels: From Stimuli Responsiveness to Systems Chemistry. *Acc. Chem. Res.* **2014**, *47*, 2222–2233.
- (174) Tan, S.; Ladewig, K.; Fu, Q.; Blencowe, A.; Qiao, G. G. Cyclodextrin-Based Supramolecular Assemblies and Hydrogels: Recent Advances and Future Perspectives. *Macromol. Rapid Commun.* **2014**, *35*, 1166–1184.
- (175) Yu, G.; Jie, K.; Huang, F. Supramolecular Amphiphiles Based on Host–Guest Molecular Recognition Motifs. *Chem. Rev.* **2015**, *115*, 7240–7303.
- (176) Babu, S. S.; Praveen, V. K.; Ajayaghosh, A. Functional π -Gelators and their Applications. *Chem. Rev.* **2014**, *114*, 1973–2129.
- (177) Rosen, B. M.; Wilson, C. J.; Wilson, D. A.; Peterca, M.; Imam, M. R.; Percec, V. Dendron-Mediated Self-Assembly, Disassembly, and Self-Organization of Complex Systems. *Chem. Rev.* **2009**, *109*, 6275–6540.
- (178) Yang, L.; Tan, X.; Wang, Z.; Zhang, X. Supramolecular Polymers: Historical Development, Preparation, Characterization, and Functions. *Chem. Rev.* **2015**, *115*, 7196–7239.
- (179) Aida, T.; Meijer, E. W.; Stupp, S. I. Functional Supramolecular Polymers. *Science* **2012**, *335*, 813–817.
- (180) Noro, A.; Hayashi, M.; Matsushita, Y. Design and Properties of Supramolecular Polymer Gels. *Soft Matter* **2012**, *8*, 6416–6429.
- (181) Yan, X.; Wang, F.; Zheng, B.; Huang, F. Stimuli-Responsive Supramolecular Polymeric Materials. *Chem. Soc. Rev.* **2012**, *41*, 6042–6065.
- (182) Hart, L. R.; Harries, J. L.; Greenland, B. W.; Colquhoun, H. M.; Hayes, W. Healable Supramolecular Polymers. *Polym. Chem.* **2013**, *4*, 4860–4870.
- (183) Herbst, F.; Döhler, D.; Michael, P.; Binder, W. H. Self-Healing Polymers via Supramolecular Forces. *Macromol. Rapid Commun.* **2013**, *34*, 203–220.
- (184) Wei, Z.; Yang, J. H.; Zhou, J.; Xu, F.; Zrinyi, M.; Dussault, P. H.; Osada, Y.; Chen, Y. M. Self-Healing Gels Based on Constitutional Dynamic Chemistry and their Potential Applications. *Chem. Soc. Rev.* **2014**, *43*, 8114–8131.
- (185) Li, Y.; Rodrigues, J.; Tomas, H. Injectable and Biodegradable Hydrogels: Gelation, Biodegradation and Biomedical Applications. *Chem. Soc. Rev.* **2012**, *41*, 2193–2221.
- (186) Wang, H.; Heilshorn, S. C. Adaptable Hydrogel Networks with Reversible Linkages for Tissue Engineering. *Adv. Mater.* **2015**, *27*, 3717–3736.
- (187) Casuso, P.; Perez-San Vicente, A.; Iribar, H.; Gutierrez-Rivera, A.; Izeta, A.; Loinaz, I.; Cabanero, G.; Grande, H.-J.; Odriozola, I.; Dupin, D. Auophilically Cross-Linked “Dynamic” Hydrogels Mimicking Healthy Synovial Fluid Properties. *Chem. Commun.* **2014**, *50*, 15199–15201.
- (188) Odriozola, I.; Loinaz, I.; Pomposo, J. A.; Grande, H. J. Gold-Glutathione Supramolecular Hydrogels. *J. Mater. Chem.* **2007**, *17*, 4843–4845.
- (189) Aboudzadeh, M. A.; Muñoz, M. E.; Santamaría, A.; Marcilla, R.; Mecerreyres, D. Facile Synthesis of Supramolecular Ionic Polymers that

- Combine Unique Rheological, Ionic Conductivity, and Self-Healing Properties. *Macromol. Rapid Commun.* **2012**, *33*, 314–318.
- (190) Weng, W.; Beck, J. B.; Jamieson, A. M.; Rowan, S. J. Understanding the Mechanism of Gelation and Stimuli-Responsive Nature of a Class of Metallo-Supramolecular Gels. *J. Am. Chem. Soc.* **2006**, *128*, 11663–11672.
- (191) Dankers, P. Y. W.; Harmsen, M. C.; Brouwer, L. A.; Van Luyk, M. J. A.; Meijer, E. W. A Modular and Supramolecular Approach to Bioactive Scaffolds for Tissue Engineering. *Nat. Mater.* **2005**, *4*, 568–574.
- (192) Teunissen, A. J. P.; Nieuwenhuizen, M. M. L.; Rodríguez-Llansola, F.; Palmans, A. R. A.; Meijer, E. W. Mechanically Induced Gelation of a Kinetically Trapped Supramolecular Polymer. *Macromolecules* **2014**, *47*, 8429–8436.
- (193) Bastings, M. M. C.; Koudstaal, S.; Kieltyka, R. E.; Nakano, Y.; Pape, A. C. H.; Feyen, D. A. M.; van Slochteren, F. J.; Doevedans, P. A.; Sluijter, J. P. G.; Meijer, E. W.; et al. A Fast pH-Switchable and Self-Healing Supramolecular Hydrogel Carrier for Guided, Local Catheter Injection in the Infarcted Myocardium. *Adv. Healthcare Mater.* **2014**, *3*, 70–78.
- (194) Herbst, F.; Seiffert, S.; Binder, W. H. Dynamic Supramolecular Poly(Isobutylene)s for Self-Healing Materials. *Polym. Chem.* **2012**, *3*, 3084–3092.
- (195) Chen, J.; Yan, X.; Zhao, Q.; Li, L.; Huang, F. Adjustable Supramolecular Polymer Microstructures Fabricated by the Breath Figure Method. *Polym. Chem.* **2012**, *3*, 458–462.
- (196) Yan, X.; Xu, D.; Chen, J.; Zhang, M.; Hu, B.; Yu, Y.; Huang, F. A Self-Healing Supramolecular Polymer Gel with Stimuli-Responsiveness Constructed by Crown Ether Based Molecular Recognition. *Polym. Chem.* **2013**, *4*, 3312–3322.
- (197) Chen, J.; Yan, X.; Chi, X.; Wu, X.; Zhang, M.; Han, C.; Hu, B.; Yu, Y.; Huang, F. Dual-Responsive Crown Ether-Based Supramolecular Chain Extended Polymers. *Polym. Chem.* **2012**, *3*, 3175–3179.
- (198) Gao, L.; Xu, D.; Zheng, B. Construction of Supramolecular Organogels and Hydrogels from Crown Ether Based Unsymmetric Bolaamphiphiles. *Chem. Commun.* **2014**, *50*, 12142–12145.
- (199) Zhan, J.; Zhang, M.; Zhou, M.; Liu, B.; Chen, D.; Liu, Y.; Chen, Q.; Qiu, H.; Yin, S. A Multiple-Responsive Self-Healing Supramolecular Polymer Gel Network Based on Multiple Orthogonal Interactions. *Macromol. Rapid Commun.* **2014**, *35*, 1424–1429.
- (200) Zhang, Y.; Shi, B.; Li, H.; Qu, W.; Gao, G.; Lin, Q.; Yao, H.; Wei, T. Copillar[5]Arene-Based Supramolecular Polymer Gels. *Polym. Chem.* **2014**, *5*, 4722–4725.
- (201) Shi, B.; Xia, D.; Yao, Y. A Water-Soluble Supramolecular Polymer Constructed by Pillar[5]Arene-Based Molecular Recognition. *Chem. Commun.* **2014**, *50*, 13932–13935.
- (202) Song, S.; Wang, J.; Feng, H.-T.; Zhu, Z.-H.; Zheng, Y.-S. Supramolecular Hydrogel Based on Amphiphilic Calix[4]Arene and its Application in the Synthesis of Silica Nanotubes. *RSC Adv.* **2014**, *4*, 24909–24913.
- (203) Burattini, S.; Colquhoun, H. M.; Fox, J. D.; Friedmann, D.; Greenland, B. W.; Harris, P. J. F.; Hayes, W.; Mackay, M. E.; Rowan, S. J. A Self-Repairing, Supramolecular Polymer System: Healability as a Consequence of Donor-Acceptor π - π Stacking Interactions. *Chem. Commun.* **2009**, 6717–6719.
- (204) Harries, J.; Clifton, A.; Colquhoun, H.; Hayes, W.; Hart, L. WO Patent 2014111722 A1, 2014.
- (205) Lange, S. C.; Unsleber, J.; Drucker, P.; Galla, H.-J.; Waller, M. P.; Ravoo, B. J. pH Response and Molecular Recognition in a Low Molecular Weight Peptide Hydrogel. *Org. Biomol. Chem.* **2015**, *13*, 561–569.
- (206) Hirst, A. R.; Roy, S.; Arora, M.; Das, A. K.; Hodson, N.; Murray, P.; Marshall, S.; Javid, N.; Sefcik, J.; Boekhoven, J.; et al. Biocatalytic Induction of Supramolecular Order. *Nat. Chem.* **2010**, *2*, 1089–1094.
- (207) Smith, A. M.; Williams, R. J.; Tang, C.; Coppo, P.; Collins, R. F.; Turner, M. L.; Saiani, A.; Ulijn, R. V. Fmoc-Diphenylalanine Self Assembles to a Hydrogel via a Novel Architecture Based on π - π Interlocked β -Sheets. *Adv. Mater.* **2008**, *20*, 37–41.
- (208) Xie, Z.; Zhang, A.; Ye, L.; Wang, X.; Feng, Z.-g. Shear-Assisted Hydrogels Based on Self-Assembly of Cyclic Di peptide Derivatives. *J. Mater. Chem.* **2009**, *19*, 6100–6102.
- (209) Bernet, A.; Behr, M.; Schmidt, H.-W. Supramolecular Nanotube-Based Fiber Mats by Self-Assembly of a Tailored Amphiphilic Low Molecular Weight Hydrogelator. *Soft Matter* **2011**, *7*, 1058–1065.
- (210) Bernet, A.; Behr, M.; Schmidt, H.-W. Supramolecular Hydrogels Based on Antimycobacterial Amphiphiles. *Soft Matter* **2012**, *8*, 4873–4876.
- (211) Decoppet, J.-D.; Moehl, T.; Babkair, S. S.; Alzubaydi, R. A.; Ansari, A. A.; Habib, S. S.; Zakeeruddin, S. M.; Schmidt, H.-W.; Gratzel, M. Molecular Gelation of Ionic Liquid-Sulfolane Mixtures, a Solid Electrolyte for High Performance Dye-Sensitized Solar Cells. *J. Mater. Chem. A* **2014**, *2*, 15972–15977.
- (212) Lin, Q.; Yang, Q.-P.; Sun, B.; Fu, Y.-P.; Zhu, X.; Wei, T.-B.; Zhang, Y.-M. Competitive Coordination Control of the AIE and Micro States of Supramolecular Gel: An Efficient Approach for Reversible Dual-Channel Stimuli-Response Materials. *Soft Matter* **2014**, *10*, 8427–8432.
- (213) Stone, D. A.; Hsu, L.; Stupp, S. I. Self-Assembling Quinquethiophene-Oligopeptide Hydrogelators. *Soft Matter* **2009**, *5*, 1990–1993.
- (214) Awad, H. A.; Wickham, M. Q.; Leddy, H. A.; Gimble, J. M.; Guilak, F. Chondrogenic Differentiation of Adipose-Derived Adult Stem Cells in Agarose, Alginate, and Gelatin Scaffolds. *Biomaterials* **2004**, *25*, 3211–3222.
- (215) Tan, H. P.; Gong, Y. H.; Lao, L. H.; Mao, Z. W.; Gao, C. Y. Gelatin/Chitosan/Hyaluronan Ternary Complex Scaffold Containing Basic Fibroblast Growth Factor for Cartilage Tissue Engineering. *J. Mater. Sci.: Mater. Med.* **2007**, *18*, 1961–1968.
- (216) Kirchmajer, D.; Gorkin, R., III; in het Panhuis, M. An Overview of the Suitability of Hydrogel-Forming Polymers for Extrusion-Based 3D-Printing. *J. Mater. Chem. B* **2015**, *3*, 4105–4117.
- (217) Thiele, J.; Ma, Y. J.; Bruekers, S. M. C.; Ma, S. H.; Huck, W. T. S. 25th Anniversary Article: Designer Hydrogels for Cell Cultures: A Materials Selection Guide. *Adv. Mater.* **2014**, *26*, 125–148.
- (218) Draget, K. I.; Stokke, B. T.; Yuguchi, Y.; Urakawa, H.; Kajiwara, K. Small-Angle X-Ray Scattering and Rheological Characterization of Alginate Gels. 3. Alginic Acid Gels. *Biomacromolecules* **2003**, *4*, 1661–1668.
- (219) Jia, J.; Richards, D. J.; Pollard, S.; Tan, Y.; Rodriguez, J.; Visconti, R. P.; Trusk, T. C.; Yost, M. J.; Yao, H.; Markwald, R. R.; Mei, Y. Engineering Alginate as Bioink for Bioprinting. *Acta Biomater.* **2014**, *10*, 4323–4331.
- (220) Shoichet, M. S.; Li, R. H.; White, M. L.; Winn, S. R. Stability of Hydrogels used in Cell Encapsulation: An in Vitro Comparison of Alginate and Agarose. *Biotechnol. Bioeng.* **1996**, *50*, 374–381.
- (221) Fedorovich, N. E.; Schuurman, W.; Wijnberg, H. M.; Prins, H. J.; van Weeren, P. R.; Malda, J.; Alblas, J.; Dhert, W. J. A. Biofabrication of Osteochondral Tissue Equivalents by Printing Topologically Defined, Cell-Laden Hydrogel Scaffolds. *Tissue Eng., Part C* **2012**, *18*, 33–44.
- (222) Fedorovich, N. E.; De Wijn, J. R.; Verbout, A. J.; Alblas, J.; Dhert, W. J. A. Three-Dimensional Fiber Deposition of Cell-Laden, Viable, Patterned Constructs for Bone Tissue Printing. *Tissue Eng., Part A* **2008**, *14*, 127–133.
- (223) Catros, S.; Guillemot, F.; Nandakumar, A.; Ziane, S.; Moroni, L.; Habibovic, P.; van Blitterswijk, C.; Rousseau, B.; Chassande, O.; Amedee, J.; et al. Layer-by-Layer Tissue Microfabrication Supports Cell Proliferation in Vitro and in Vivo. *Tissue Eng., Part C* **2012**, *18*, 62–70.
- (224) Song, S.-J.; Choi, J.; Park, Y.-D.; Hong, S.; Lee, J. J.; Ahn, C. B.; Choi, H.; Sun, K. Sodium Alginate Hydrogel-Based Bioprinting using a Novel Multinozzle Bioprinting System. *Artif. Organs* **2011**, *35*, 1132–1136.
- (225) Arai, K.; Iwanaga, S.; Toda, H.; Genci, C.; Nishiyama, Y.; Nakamura, M. Three-Dimensional Inkjet Biofabrication Based on Designed Images. *Biofabrication* **2011**, *3*, 034113.
- (226) Cohen, D. L.; Malone, E.; Lipson, H.; Bonassar, L. J. Direct Freeform Fabrication of Seeded Hydrogels in Arbitrary Geometries. *Tissue Eng.* **2006**, *12*, 1325–1335.

- (227) Lee, H.; Ahn, S.; Bonassar, L. J.; Kim, G. Cell(MC3T3-E1)-Printed Poly(ϵ -Caprolactone)/Alginate Hybrid Scaffolds for Tissue Regeneration. *Macromol. Rapid Commun.* **2013**, *34*, 142–149.
- (228) Shim, J.-H.; Lee, J.-S.; Kim, J. Y.; Cho, D.-W. Bioprinting of a Mechanically Enhanced Three-Dimensional Dual Cell-Laden Construct for Osteochondral Tissue Engineering using a Multi-Head Tissue/Organ Building System. *J. Micromech. Microeng.* **2012**, *22*, 085014.
- (229) Cohen, D. L.; Lipton, J. I.; Bonassar, L. J.; Lipson, H. Additive Manufacturing for *In Situ* Repair of Osteochondral Defects. *Biofabrication* **2010**, *2*, 035004.
- (230) Zhang, Y.; Yu, Y.; Chen, H.; Ozbolat, I. T. Characterization of Printable Cellular Micro-Fluidic Channels for Tissue Engineering. *Biofabrication* **2013**, *5*, 025004.
- (231) Pataky, K.; Braschler, T.; Negro, A.; Renaud, P.; Lutolf, M. P.; Brugger, J. Microdrop Printing of Hydrogel Bioinks into 3D Tissue-Like Geometries. *Adv. Mater.* **2012**, *24*, 391–396.
- (232) Yan, J.; Huang, Y.; Chrisey, D. B. Laser-Assisted Printing of Alginate Long Tubes and Annular Constructs. *Biofabrication* **2013**, *5*, 015002.
- (233) Markstedt, K.; Mantas, A.; Tournier, I.; Martínez Ávila, H.; Hägg, D.; Gatenholm, P. 3D Bioprinting Human Chondrocytes with Nanocellulose–Alginate Bioink for Cartilage Tissue Engineering Applications. *Biomacromolecules* **2015**, *16*, 1489–1496.
- (234) Fedorovich, N. E.; Alblas, J.; de Wijn, J. R.; Hennink, W. E.; Verbout, A. J.; Dhert, W. J. A. Hydrogels as Extracellular Matrices for Skeletal Tissue Engineering: State-of-the-Art and Novel Application in Organ Printing. *Tissue Eng.* **2007**, *13*, 1905–1925.
- (235) Kim, B. S.; Mooney, D. J. Development of Biocompatible Synthetic Extracellular Matrices for Tissue Engineering. *Trends Biotechnol.* **1998**, *16*, 224–230.
- (236) Lee, K. Y.; Mooney, D. J. Alginate: Properties and Biomedical Applications. *Prog. Polym. Sci.* **2012**, *37*, 106–126.
- (237) Cohen, D. L.; Lo, W.; Tsavaris, A.; Peng, D.; Lipson, H.; Bonassar, L. J. Increased Mixing Improves Hydrogel Homogeneity and Quality of Three-Dimensional Printed Constructs. *Tissue Eng., Part C* **2011**, *17*, 239–248.
- (238) Xu, T.; Zhao, W.; Zhu, J.-M.; Albanna, M. Z.; Yoo, J. J.; Atala, A. Complex Heterogeneous Tissue Constructs Containing Multiple Cell Types Prepared by Inkjet Printing Technology. *Biomaterials* **2013**, *34*, 130–139.
- (239) Zhao, Y.; Yao, R.; Ouyang, L.; Ding, H.; Zhang, T.; Zhang, K.; Cheng, S.; Sun, W. Three-Dimensional Printing of HeLa Cells for Cervical Tumor Model *In Vitro*. *Biofabrication* **2014**, *6*, 035001.
- (240) Duan, B.; Hockaday, L. A.; Kang, K. H.; Butcher, J. T. 3D Bioprinting of Heterogeneous Aortic Valve Conduits with Alginate/Gelatin Hydrogels. *J. Biomed. Mater. Res., Part A* **2013**, *101A*, 1255–1264.
- (241) Wüst, S.; Godla, M. E.; Muller, R.; Hofmann, S. Tunable Hydrogel Composite with Two-Step Processing in Combination with Innovative Hardware Upgrade for Cell-Based Three-Dimensional Bioprinting. *Acta Biomater.* **2014**, *10*, 630–640.
- (242) Tan, H. P.; Marra, K. G. Injectable, Biodegradable Hydrogels for Tissue Engineering Applications. *Materials* **2010**, *3*, 1746–1767.
- (243) Cheng, J.; Lin, F.; Liu, H.; Yan, Y.; Wang, X.; Zhang, R.; Xiong, Z. Rheological Properties of Cell-Hydrogel Composites Extruding through Small-Diameter Tips. *J. Manuf. Sci., Trans. ASME* **2008**, *130*, 021014.
- (244) Landers, R.; Hübner, U.; Schmelzeisen, R.; Mühlaupt, R. Rapid Prototyping of Scaffolds Derived from Thermoreversible Hydrogels and Tailored for Applications in Tissue Engineering. *Biomaterials* **2002**, *23*, 4437–4447.
- (245) Mauck, R. L.; Soltz, M. A.; Wang, C. C. B.; Wong, D. D.; Chao, P. H. G.; Valhmu, W. B.; Hung, C. T.; Ateshian, G. A. Functional Tissue Engineering of Articular Cartilage through Dynamic Loading of Chondrocyte-Seeded Agarose Gels. *J. Biomech. Eng., Trans. ASME* **2000**, *122*, 252–260.
- (246) Landers, R.; Pfister, A.; Hübner, U.; John, H.; Schmelzeisen, R.; Mühlaupt, R. Fabrication of Soft Tissue Engineering Scaffolds by Means of Rapid Prototyping Techniques. *J. Mater. Sci.* **2002**, *37*, 3107–3116.
- (247) Norotte, C.; Marga, F. S.; Niklason, L. E.; Forgacs, G. Scaffold-Free Vascular Tissue Engineering using Bioprinting. *Biomaterials* **2009**, *30*, 5910–5917.
- (248) Duarte Campos, D. F.; Blaeser, A.; Korsten, A.; Neuss, S.; Jakel, J.; Vogt, M.; Fischer, H. The Stiffness and Structure of Three-Dimensional Printed Hydrogels Direct the Differentiation of Mesenchymal Stromal Cells toward Adipogenic and Osteogenic Lineages. *Tissue Eng., Part A* **2015**, *21*, 740–756.
- (249) Mano, J. F.; Silva, G. A.; Azevedo, H. S.; Malafaya, P. B.; Sousa, R. A.; Silva, S. S.; Boesel, L. F.; Oliveira, J. M.; Santos, T. C.; Marques, A. P.; Neves, N. M.; Reis, R. L. Natural Origin Biodegradable Systems in Tissue Engineering and Regenerative Medicine: Present Status and Some Moving Trends. *J. R. Soc., Interface* **2007**, *4*, 999–1030.
- (250) Czaja, W. K.; Young, D. J.; Kawecki, M.; Brown, R. M. The Future Prospects of Microbial Cellulose in Biomedical Applications. *Biomacromolecules* **2007**, *8*, 1–12.
- (251) Burdick, J. A.; Prestwich, G. D. Hyaluronic Acid Hydrogels for Biomedical Applications. *Adv. Mater.* **2011**, *23*, H41–H56.
- (252) Highley, C. B.; Rodell, C. B.; Burdick, J. A. Direct 3D Printing of Shear-Thinning Hydrogels into Self-Healing Hydrogels. *Adv. Mater.* **2015**, *27*, 5075–5079.
- (253) Ferris, C. J.; Gilmore, K. J.; Beirne, S.; McCallum, D.; Wallace, G. G.; in het Panhuys, M. Bio-Ink for on-Demand Printing of Living Cells. *Biomater. Sci.* **2013**, *1*, 224–230.
- (254) Du, H. W.; Hamilton, P.; Reilly, M.; Ravi, N. Injectable *In Situ* Physically and Chemically Crosslinkable Gellan Hydrogel. *Macromol. Biosci.* **2012**, *12*, 952–961.
- (255) Oliveira, J. T.; Martins, L.; Picciochi, R.; Malafaya, I. B.; Sousa, R. A.; Neves, N. M.; Mano, J. F.; Reis, R. L. Gellan Gum: A New Biomaterial for Cartilage Tissue Engineering Applications. *J. Biomed. Mater. Res., Part A* **2010**, *93A*, 852–863.
- (256) Matricardi, P.; Cencetti, C.; Ria, R.; Alhaique, F.; Covello, T. Preparation and Characterization of Novel Gellan Gum Hydrogels Suitable for Modified Drug Release. *Molecules* **2009**, *14*, 3376–3391.
- (257) Moon, S.; Hasan, S. K.; Song, Y. S.; Xu, F.; Keles, H. O.; Manzur, F.; Mikkilineni, S.; Hong, J. W.; Nagatomi, J.; Haeggstrom, E.; et al. Layer by Layer Three-Dimensional Tissue Epitaxy by Cell-Laden Hydrogel Droplets. *Tissue Eng., Part C* **2010**, *16*, 157–166.
- (258) Parenteau-Bareil, R.; Gauvin, R.; Berthod, F. Collagen-Based Biomaterials for Tissue Engineering Applications. *Materials* **2010**, *3*, 1863–1887.
- (259) Lee, W.; Lee, V.; Polio, S.; Keegan, P.; Lee, J.-H.; Fischer, K.; Park, J.-K.; Yoo, S.-S. On-Demand Three-Dimensional Freeform Fabrication of Multi-Layered Hydrogel Scaffold with Fluidic Channels. *Biotechnol. Bioeng.* **2010**, *105*, 1178–1186.
- (260) Shim, J.-H.; Kim, J. Y.; Park, M.; Park, J.; Cho, D.-W. Development of a Hybrid Scaffold with Synthetic Biomaterials and Hydrogel using Solid Freeform Fabrication Technology. *Biofabrication* **2011**, *3*, 034102.
- (261) Jakab, K.; Norotte, C.; Damon, B.; Marga, F.; Neagu, A.; Besch-Williford, C. L.; Kachurin, A.; Church, K. H.; Park, H.; Mironov, V.; et al. Tissue Engineering by Self-Assembly of Cells Printed into Topologically Defined Structures. *Tissue Eng., Part A* **2008**, *14*, 413–421.
- (262) Hersel, U.; Dahmen, C.; Kessler, H. RGD Modified Polymers: Biomaterials for Stimulated Cell Adhesion and Beyond. *Biomaterials* **2003**, *24*, 4385–4415.
- (263) Hori, K.; Sotozono, C.; Hamuro, J.; Yamasaki, K.; Kimura, Y.; Ozeki, M.; Tabata, Y.; Kinoshita, S. Controlled-Release of Epidermal Growth Factor from Cationized Gelatin Hydrogel Enhances Corneal Epithelial Wound Healing. *J. Controlled Release* **2007**, *118*, 169–176.
- (264) Xu, T.; Gregory, C. A.; Molnar, P.; Cui, X.; Jalota, S.; Bhaduri, S. B.; Boland, T. Viability and Electrophysiology of Neural Cell Structures Generated by the Inkjet Printing Method. *Biomaterials* **2006**, *27*, 3580–3588.
- (265) Schense, J. C.; Hubbell, J. A. Cross-Linking Exogenous Bifunctional Peptides into Fibrin Gels with Factor XIIIa. *Bioconjugate Chem.* **1999**, *10*, 75–81.
- (266) Cummings, C. L.; Gawlitta, D.; Nerem, R. M.; Stegemann, J. P. Properties of Engineered Vascular Constructs Made from Collagen,

- Fibrin, and Collagen-Fibrin Mixtures. *Biomaterials* **2004**, *25*, 3699–3706.
- (267) Xu, H. T.; Fan, B. L.; Yu, S. Y.; Huang, Y. H.; Zhao, Z. H.; Lian, Z. X.; Dai, Y. P.; Wang, L. L.; Liu, Z. L.; Fei, J.; et al. Construct Synthetic Gene Encoding Artificial Spider Dragline Silk Protein and its Expression in Milk of Transgenic Mice. *Anim. Biotechnol.* **2007**, *18*, 1–12.
- (268) Wang, X. H.; Yan, Y. N.; Zhang, R. J. Recent Trends and Challenges in Complex Organ Manufacturing. *Tissue Eng, Part B* **2010**, *16*, 189–197.
- (269) Janmey, P. A.; Winer, J. P.; Weisel, J. W. Fibrin Gels and their Clinical and Bioengineering Applications. *J. R. Soc., Interface* **2009**, *6*, 1–10.
- (270) Das, S.; Pati, F.; Chameettachal, S.; Pahwa, S.; Ray, A. R.; Dhara, S.; Ghosh, S. Enhanced Redifferentiation of Chondrocytes on Microperiodic Silk/Gelatin Scaffolds: Toward Tailor-Made Tissue Engineering. *Biomacromolecules* **2013**, *14*, 311–321.
- (271) Das, S.; Pati, F.; Choi, Y.-J.; Rijal, G.; Shim, J.-H.; Kim, S. W.; Ray, A. R.; Cho, D.-W.; Ghosh, S. Bioprintable, Cell-Laden Silk Fibroin-Gelatin Hydrogel Supporting Multilineage Differentiation of Stem Cells for Fabrication of 3D Tissue Constructs. *Acta Biomater.* **2015**, *11*, 233–246.
- (272) Kundu, B.; Rajkhowa, R.; Kundu, S. C.; Wang, X. G. Silk Fibroin Biomaterials for Tissue Regenerations. *Adv. Drug Delivery Rev.* **2013**, *65*, 457–470.
- (273) Suntivich, R.; Drachuk, I.; Calabrese, R.; Kaplan, D. L.; Tsukruk, V. V. Inkjet Printing of Silk Nest Arrays for Cell Hosting. *Biomacromolecules* **2014**, *15*, 1428–1435.
- (274) Wang, Y. Z.; Kim, H. J.; Vunjak-Novakovic, G.; Kaplan, D. L. Stem Cell-Based Tissue Engineering with Silk Biomaterials. *Biomaterials* **2006**, *27*, 6064–6082.
- (275) Snyder, J.; Hamid, Q.; Wang, C.; Chang, R.; Emami, K.; Wu, H.; Sun, W. Bioprinting Cell-Laden Matrigel for Radioprotection Study of Liver by Pro-Drug Conversion in a Dual-Tissue Microfluidic Chip. *Biofabrication* **2011**, *3*, 034112.
- (276) Arnott, S.; Fulmer, A.; Scott, W. E.; Dea, I. C. M.; Moorhouse, R.; Rees, D. A. Agarose Double Helix and its Function in Agarose-Gel Structure. *J. Mol. Biol.* **1974**, *90*, 269–284.
- (277) Velasco, D.; Tumarkin, E.; Kumacheva, E. Microfluidic Encapsulation of Cells in Polymer Microgels. *Small* **2012**, *8*, 1633–1642.
- (278) Normand, V.; Lootens, D. L.; Amici, E.; Plucknett, K. P.; Aymard, P. New Insight into Agarose Gel Mechanical Properties. *Biomacromolecules* **2000**, *1*, 730–738.
- (279) Chen, Q.; Zhu, L.; Chen, H.; Yan, H.; Huang, L.; Yang, J.; Zheng, J. A Novel Design Strategy for Fully Physically Linked Double Network Hydrogels with Tough, Fatigue Resistant, and Self-Healing Properties. *Adv. Funct. Mater.* **2015**, *25*, 1598–1607.
- (280) Fialho, A. M.; Moreira, L. M.; Granja, A. T.; Popescu, A. O.; Hoffmann, K.; Sa-Correia, I. Occurrence, Production, and Applications of Gellan: Current State and Perspectives. *Appl. Microbiol. Biotechnol.* **2008**, *79*, 889–900.
- (281) Freitas, F.; Alves, V. D.; Reis, M. A. M. Advances in Bacterial Exopolysaccharides: From Production to Biotechnological Applications. *Trends Biotechnol.* **2011**, *29*, 388–398.
- (282) Khan, T.; Park, J. K.; Kwon, J. H. Functional Biopolymers Produced by Biochemical Technology Considering Applications in Food Engineering. *Korean J. Chem. Eng.* **2007**, *24*, 816–826.
- (283) Miyoshi, E.; Takaya, T.; Nishinari, K. Gel-Sol Transition in Gellan Gum Solutions. I. Rheological Studies on the Effects of Salts. *Food Hydrocolloids* **1994**, *8*, 505–527.
- (284) Harkness, R. D. Biological Functions of Collagen. *Biol. Rev.* **1961**, *36*, 399–455.
- (285) Kadler, K. E.; Ballock, C.; Bella, J.; Boot-Handford, R. P. Collagens at a Glance. *J. Cell Sci.* **2007**, *120*, 1955–1958.
- (286) Gomes, S.; Leonor, I. B.; Mano, J. F.; Reis, R. L.; Kaplan, D. L. Natural and Genetically Engineered Proteins for Tissue Engineering. *Prog. Polym. Sci.* **2012**, *37*, 1–17.
- (287) Sheu, M. T.; Huang, J. C.; Yeh, G. C.; Ho, H. O. Characterization of Collagen Gel Solutions and Collagen Matrices for Cell Culture. *Biomaterials* **2001**, *22*, 1713–1719.
- (288) Kim, J. A.; Kim, H. N.; Im, S.-K.; Chung, S.; Kang, J. Y.; Choi, N. Collagen-Based Brain Microvasculature Model in Vitro using Three-Dimensional Printed Template. *Biomicrofluidics* **2015**, *9*, 024115.
- (289) Tan, H. P.; Huang, D. J.; Lao, L. H.; Gao, C. Y. RGD Modified PLGA/Gelatin Microspheres as Microcarriers for Chondrocyte Delivery. *J. Biomed. Mater. Res., Part B* **2009**, *91B*, 228–238.
- (290) Choi, Y. S.; Hong, S. R.; Lee, Y. M.; Song, K. W.; Park, M. H.; Nam, Y. S. Study on Gelatin-Containing Artificial Skin: I. Preparation and Characteristics of Novel Gelatin-Alginate Sponge. *Biomaterials* **1999**, *20*, 409–417.
- (291) Young, S.; Wong, M.; Tabata, Y.; Mikos, A. G. Gelatin as a Delivery Vehicle for the Controlled Release of Bioactive Molecules. *J. Controlled Release* **2005**, *109*, 256–274.
- (292) Sisson, K.; Zhang, C.; Farach-Carson, M. C.; Chase, D. B.; Rabolt, J. F. Evaluation of Cross-Linking Methods for Electrospun Gelatin on Cell Growth and Viability. *Biomacromolecules* **2009**, *10*, 1675–1680.
- (293) Kirchmajer, D. M.; Panhuis, M. i. h. Robust Biopolymer Based Ionic-Covalent Entanglement Hydrogels with Reversible Mechanical Behaviour. *J. Mater. Chem. B* **2014**, *2*, 4694–4702.
- (294) Smith, G. F. Fibrinogen-Fibrin Conversion - Mechanism of Fibrin-Polymer Formation in Solution. *Biochem. J.* **1980**, *185*, 1–11.
- (295) Zhao, W.; Jin, X.; Cong, Y.; Liu, Y. Y.; Fu, J. Degradable Natural Polymer Hydrogels for Articular Cartilage Tissue Engineering. *J. Chem. Technol. Biotechnol.* **2013**, *88*, 327–339.
- (296) Ho, W.; Tawil, B.; Dunn, J. C. Y.; Wu, B. M. The Behavior of Human Mesenchymal Stem Cells in 3D Fibrin Clots: Dependence on Fibrinogen Concentration and Clot Structure. *Tissue Eng.* **2006**, *12*, 1587–1595.
- (297) Drinnan, C. T.; Zhang, G.; Alexander, M. A.; Pulido, A. S.; Suggs, L. J. Multimodal Release of Transforming Growth Factor- β 1 and the BB Isoform of Platelet Derived Growth Factor from PEGylated Fibrin Gels. *J. Controlled Release* **2010**, *147*, 180–186.
- (298) Lee, Y. B.; Polio, S.; Lee, W.; Dai, G. H.; Menon, L.; Carroll, R. S.; Yoo, S. S. Bio-Printing of Collagen and VEGF-Releasing Fibrin Gel Scaffolds for Neural Stem Cell Culture. *Exp. Neurol.* **2010**, *223*, 645–652.
- (299) Eyrich, D.; Brandl, F.; Appel, B.; Wiese, H.; Maier, G.; Wenzel, M.; Staudenmaier, R.; Goepfertich, A.; Blunk, T. Long-Term Stable Fibrin Gels for Cartilage Engineering. *Biomaterials* **2007**, *28*, 55–65.
- (300) Gosline, J. M.; Demont, M. E.; Denny, M. W. The Structure and Properties of Spider Silk. *Endeavour* **1986**, *10*, 37–43.
- (301) Heidebrecht, A.; Scheibel, T. Recombinant Production of Spider Silk Proteins. *Adv. Appl. Microbiol.* **2013**, *82*, 115–153.
- (302) Altman, G. H.; Diaz, F.; Jakuba, C.; Calabro, T.; Horan, R. L.; Chen, J. S.; Lu, H.; Richmond, J.; Kaplan, D. L. Silk-Based Biomaterials. *Biomaterials* **2003**, *24*, 401–416.
- (303) Leal-Egana, A.; Scheibel, T. Silk-Based Materials for Biomedical Applications. *Biotechnol. Appl. Biochem.* **2010**, *55*, 155–167.
- (304) Schacht, K.; Jüngst, T.; Schweinlin, M.; Ewald, A.; Groll, J.; Scheibel, T. Biofabrication of Cell-Loaded 3D Recombinant Spider Silk Constructs. *Angew. Chem., Int. Ed.* **2015**, *54*, 2816–2820.
- (305) Schacht, K.; Scheibel, T. Processing of Recombinant Spider Silk Proteins into Tailor-Made Materials for Biomaterials Applications. *Curr. Opin. Biotechnol.* **2014**, *29*, 62–69.
- (306) Langer, R.; Tirrell, D. A. Designing Materials for Biology and Medicine. *Nature* **2004**, *428*, 487–492.
- (307) Romano, N. H.; Sengupta, D.; Chung, C.; Heilshorn, S. C. Protein-Engineered Biomaterials: Nanoscale Mimics of the Extracellular Matrix. *Biochim. Biophys. Acta, Gen. Subj.* **2011**, *1810*, 339–349.
- (308) Li, C.; Faulkner-Jones, A.; Dun, A. R.; Jin, J.; Chen, P.; Xing, Y.; Yang, Z.; Li, Z.; Shu, W.; Liu, D.; et al. Rapid Formation of a Supramolecular Polypeptide–DNA Hydrogel for in Situ Three-Dimensional Multilayer Bioprinting. *Angew. Chem., Int. Ed.* **2015**, *54*, 3957–3961.

- (309) Li, C.; Chen, P.; Shao, Y.; Zhou, X.; Wu, Y.; Yang, Z.; Li, Z.; Weil, T.; Liu, D. A Writable Polypeptide–DNA Hydrogel with Rationally Designed Multi-Modification Sites. *Small* **2015**, *11*, 1138–1143.
- (310) Hauser, C. A.; Loo, Y.; Lakshmanan, A.; Ni, M.; Toh, L. L.; Wang, S. Peptide Bioink: Self-Assembling Nanofibrous Scaffolds for 3D Organotypic Cultures. *Nano Lett.* **2015**, DOI: 10.1021/acs.nanolett.5b02859.
- (311) Dasgupta, A.; Mondal, J. H.; Das, D. Peptide Hydrogels. *RSC Adv.* **2013**, *3*, 9117–9149.
- (312) Apostolovic, B.; Danial, M.; Klok, H.-A. Coiled Coils: Attractive Protein Folding Motifs for the Fabrication of Self-Assembled, Responsive and Bioactive Materials. *Chem. Soc. Rev.* **2010**, *39*, 3541–3575.
- (313) Sathaye, S.; Mbi, A.; Sonmez, C.; Chen, Y.; Blair, D. L.; Schneider, J. P.; Pochan, D. J. Rheology of Peptide- and Protein-Based Physical Hydrogels: Are Everyday Measurements Just Scratching the Surface? *Wiley Interdiscip. Rev.: Nanomed. Nanobiotechnol.* **2015**, *7*, 34–68.
- (314) Chen, C.; Gu, Y.; Deng, L.; Han, S.; Sun, X.; Chen, Y.; Lu, J. R.; Xu, H. Tuning Gelation Kinetics and Mechanical Rigidity of β -Hairpin Peptide Hydrogels via Hydrophobic Amino Acid Substitutions. *ACS Appl. Mater. Interfaces* **2014**, *6*, 14360–14368.
- (315) Haines-Butterick, L.; Rajagopal, K.; Branco, M.; Salick, D.; Rughani, R.; Pilarz, M.; Lamm, M. S.; Pochan, D. J.; Schneider, J. P. Controlling Hydrogelation Kinetics by Peptide Design for Three-Dimensional Encapsulation and Injectable Delivery of Cells. *Proc. Natl. Acad. Sci. U. S. A.* **2007**, *104*, 7791–7796.
- (316) Schneider, J. P.; Pochan, D. J.; Ozbas, B.; Rajagopal, K.; Pakstis, L.; Kretzinger, J. Responsive Hydrogels from the Intramolecular Folding and Self-Assembly of a Designed Peptide. *J. Am. Chem. Soc.* **2002**, *124*, 15030–15037.
- (317) Yan, C.; Altunbas, A.; Yucel, T.; Nagarkar, R. P.; Schneider, J. P.; Pochan, D. J. Injectable Solid Hydrogel: Mechanism of Shear-Thinning and Immediate Recovery of Injectable β -Hairpin Peptide Hydrogels. *Soft Matter* **2010**, *6*, 5143–5156.
- (318) Rughani, R. V.; Branco, M. C.; Pochan, D. J.; Schneider, J. P. De Novo Design of a Shear-Thin Recoverable Peptide-Based Hydrogel Capable of Intrafibrillar Photopolymerization. *Macromolecules* **2010**, *43*, 7924–7930.
- (319) Bakota, E. L.; Wang, Y.; Danesh, F. R.; Hartgerink, J. D. Injectable Multidomain Peptide Nanofiber Hydrogel as a Delivery Agent for Stem Cell Secretome. *Biomacromolecules* **2011**, *12*, 1651–1657.
- (320) Huang, H. Z.; Shi, J. S.; Laskin, J.; Liu, Z. Y.; McVey, D. S.; Sun, X. Z. S. Design of a Shear-Thinning Recoverable Peptide Hydrogel from Native Sequences and Application for Influenza H1N1 Vaccine Adjuvant. *Soft Matter* **2011**, *7*, 8905–8912.
- (321) Huang, H.; Herrera, A. I.; Luo, Z.; Prakash, O.; Sun, X. S. Structural Transformation and Physical Properties of a Hydrogel-Forming Peptide Studied by NMR, Transmission Electron Microscopy, and Dynamic Rheometer. *Biophys. J.* **2012**, *103*, 979–988.
- (322) Tsurkan, M. V.; Chwalek, K.; Prokoph, S.; Zieris, A.; Levental, K. R.; Freudenberg, U.; Werner, C. Defined Polymer–Peptide Conjugates to Form Cell-Instructive starPEG–Heparin Matrices in Situ. *Adv. Mater.* **2013**, *25*, 2606–2610.
- (323) Wieduwild, R.; Tsurkan, M.; Chwalek, K.; Murawala, P.; Nowak, M.; Freudenberg, U.; Neinhuis, C.; Werner, C.; Zhang, Y. Minimal Peptide Motif for Non-Covalent Peptide–Heparin Hydrogels. *J. Am. Chem. Soc.* **2013**, *135*, 2919–2922.
- (324) Thompson, M. S.; Tsurkan, M. V.; Chwalek, K.; Bornhauser, M.; Schlierf, M.; Werner, C.; Zhang, Y. Self-Assembling Hydrogels Crosslinked Solely by Receptor–Ligand Interactions: Tunability, Rationalization of Physical Properties, and 3D Cell Culture. *Chem. - Eur. J.* **2015**, *21*, 3178–3182.
- (325) Iwami, K.; Noda, T.; Ishida, K.; Morishima, K.; Nakamura, M.; Umeda, N. Bio Rapid Prototyping by Extruding/Aspirating/Refilling Thermoreversible Hydrogel. *Biofabrication* **2010**, *2*, 014108.
- (326) Li, S.; Lu, H.-Y.; Shen, Y.; Chen, C.-F. A Stimulus-Response and Self-Healing Supramolecular Polymer Gel Based on Host–Guest Interactions. *Macromol. Chem. Phys.* **2013**, *214*, 1596–1601.
- (327) Zhang, M.; Xu, D.; Yan, X.; Chen, J.; Dong, S.; Zheng, B.; Huang, F. Self-Healing Supramolecular Gels Formed by Crown Ether Based Host–Guest Interactions. *Angew. Chem., Int. Ed.* **2012**, *51*, 7011–7015.
- (328) Rodell, C. B.; Kaminski, A. L.; Burdick, J. A. Rational Design of Network Properties in Guest-Host Assembled and Shear-Thinning Hyaluronic Acid Hydrogels. *Biomacromolecules* **2013**, *14*, 4125–4134.
- (329) Rodell, C. B.; MacArthur, J. W.; Dorsey, S. M.; Wade, R. J.; Wang, L. L.; Woo, Y. J.; Burdick, J. A. Shear-Thinning Supramolecular Hydrogels with Secondary Autonomous Covalent Crosslinking to Modulate Viscoelastic Properties in Vivo. *Adv. Funct. Mater.* **2015**, *25*, 636–644.
- (330) Himmelein, S.; Lewe, V.; Stuart, M. C. A.; Ravoo, B. J. A Carbohydrate-Based Hydrogel Containing Vesicles as Responsive Non-Covalent Cross-Linkers. *Chem. Sci.* **2014**, *5*, 1054–1058.
- (331) Kato, K.; Yasuda, T.; Ito, K. Viscoelastic Properties of Slide-Ring Gels Reflecting Sliding Dynamics of Partial Chains and Entropy of Ring Components. *Macromolecules* **2013**, *46*, 310–316.
- (332) Katsuno, C.; Konda, A.; Urayama, K.; Takigawa, T.; Kidowaki, M.; Ito, K. Pressure-Responsive Polymer Membranes of Slide-Ring Gels with Movable Cross-Links. *Adv. Mater.* **2013**, *25*, 4636–4640.
- (333) Okumura, Y.; Ito, K. The Polyrotaxane Gel: A Topological Gel by Figure-of-Eight Cross-Links. *Adv. Mater.* **2001**, *13*, 485–487.
- (334) Yu, J.; Fan, H.; Huang, J.; Chen, J. Fabrication and Evaluation of Reduction-Sensitive Supramolecular Hydrogel Based on Cyclodextrin/Polymer Inclusion for Injectable Drug-Carrier Application. *Soft Matter* **2011**, *7*, 7386–7394.
- (335) Ma, D.; Zhang, L.-M. Supramolecular Gelation of a Polymeric Prodrug for its Encapsulation and Sustained Release. *Biomacromolecules* **2011**, *12*, 3124–3130.
- (336) Liu, K. L.; Zhu, J.-l.; Li, J. Elucidating Rheological Property Enhancements in Supramolecular Hydrogels of Short Poly[(R,S)-3-Hydroxybutyrate]-Based Amphiphilic Triblock Copolymer and α -Cyclodextrin for Injectable Hydrogel Applications. *Soft Matter* **2010**, *6*, 2300–2311.
- (337) Tian, Z.; Chen, C.; Allcock, H. R. Injectable and Biodegradable Supramolecular Hydrogels by Inclusion Complexation between Poly-(Organophosphazenes) and α -Cyclodextrin. *Macromolecules* **2013**, *46*, 2715–2724.
- (338) Wu, Y.; Guo, B.; Ma, P. X. Injectable Electroactive Hydrogels Formed via Host–Guest Interactions. *ACS Macro Lett.* **2014**, *3*, 1145–1150.
- (339) Nakama, T.; Ooya, T.; Yui, N. Temperature-and pH-Controlled Hydrogelation of Poly (Ethylene Glycol)-Grafted Hyaluronic Acid by Inclusion Complexation with α -Cyclodextrin. *Polym. J.* **2004**, *36*, 338–344.
- (340) Tomatsu, I.; Hashidzume, A.; Harada, A. Redox-Responsive Hydrogel System Using the Molecular Recognition of β -Cyclodextrin. *Macromol. Rapid Commun.* **2006**, *27*, 238–241.
- (341) Loh, X. J. Supramolecular Host-Guest Polymeric Materials for Biomedical Applications. *Mater. Horiz.* **2014**, *1*, 185–195.
- (342) Park, K. M.; Yang, J.-A.; Jung, H.; Yeom, J.; Park, J. S.; Park, K.-H.; Hoffman, A. S.; Hahn, S. K.; Kim, K. In Situ Supramolecular Assembly and Modular Modification of Hyaluronic Acid Hydrogels for 3D Cellular Engineering. *ACS Nano* **2012**, *6*, 2960–2968.
- (343) Appel, E. A.; Loh, X. J.; Jones, S. T.; Biedermann, F.; Dreiss, C. A.; Scherman, O. A. Ultrahigh-Water-Content Supramolecular Hydrogels Exhibiting Multistimuli Responsiveness. *J. Am. Chem. Soc.* **2012**, *134*, 11767–11773.
- (344) Cross, D.; Jiang, X.; Ji, W.; Han, W.; Wang, C. Injectable Hybrid Hydrogels of Hyaluronic Acid Crosslinked by Well-Defined Synthetic Polycations: Preparation and Characterization in Vitro and in Vivo. *Macromol. Biosci.* **2015**, *15*, 668–681.
- (345) Hunt, J. N.; Feldman, K. E.; Lynd, N. A.; Deek, J.; Campos, L. M.; Spruell, J. M.; Hernandez, B. M.; Kramer, E. J.; Hawker, C. J. Tunable, High Modulus Hydrogels Driven by Ionic Coacervation. *Adv. Mater.* **2011**, *23*, 2327–2331.

- (346) Wang, Q.; Wang, L.; Detamore, M. S.; Berkland, C. Biodegradable Colloidal Gels as Moldable Tissue Engineering Scaffolds. *Adv. Mater.* **2008**, *20*, 236–239.
- (347) Bünsow, J.; Erath, J.; Biesheuvel, P. M.; Fery, A.; Huck, W. T. S. Direct Correlation between Local Pressure and Fluorescence Output in Mechanoresponsive Polyelectrolyte Brushes. *Angew. Chem., Int. Ed.* **2011**, *50*, 9629–9632.
- (348) Sun, T. L.; Kurokawa, T.; Kuroda, S.; Ihsan, A. B.; Akasaki, T.; Sato, K.; Haque, M. A.; Nakajima, T.; Gong, J. P. Physical Hydrogels Composed of Polyampholytes Demonstrate High Toughness and Viscoelasticity. *Nat. Mater.* **2013**, *12*, 932–937.
- (349) Luo, F.; Sun, T. L.; Nakajima, T.; Kurokawa, T.; Zhao, Y.; Sato, K.; Ihsan, A. B.; Li, X.; Guo, H.; Gong, J. P. Oppositely Charged Polyelectrolytes Form Tough, Self-Healing, and Rebuildable Hydrogels. *Adv. Mater.* **2015**, *27*, 2722–2727.
- (350) Xu, D.; Liu, C.-Y.; Craig, S. L. Divergent Shear Thinning and Shear Thickening Behavior of Supramolecular Polymer Networks in Semidilute Entangled Polymer Solutions. *Macromolecules* **2011**, *44*, 2343–2353.
- (351) Xu, D.; Craig, S. L. Scaling Laws in Supramolecular Polymer Networks. *Macromolecules* **2011**, *44*, 5465–5472.
- (352) Jackson, A. C.; Beyer, F. L.; Price, S. C.; Rinderspacher, B. C.; Lambeth, R. H. Role of Metal–Ligand Bond Strength and Phase Separation on the Mechanical Properties of Metallocopolymer Films. *Macromolecules* **2013**, *46*, 5416–5422.
- (353) Jackson, A. C.; Walck, S. D.; Strawhecker, K. E.; Butler, B. G.; Lambeth, R. H.; Beyer, F. L. Metallocopolymers Containing Excess Metal–Ligand Complex for Improved Mechanical Properties. *Macromolecules* **2014**, *47*, 4144–4150.
- (354) Lewis, C. L.; Stewart, K.; Anthamatten, M. The Influence of Hydrogen Bonding Side-Groups on Viscoelastic Behavior of Linear and Network Polymers. *Macromolecules* **2014**, *47*, 729–740.
- (355) Vatankhah-Varnoosfaderani, M.; GhavamiNejad, A.; Hashmi, S.; Stadler, F. J. Hydrogen Bonding in Aprotic Solvents, a New Strategy for Gelation of Bioinspired Catecholic Copolymers with N-Isopropylamide. *Macromol. Rapid Commun.* **2015**, *36*, 447–452.
- (356) Hackelbusch, S.; Rossow, T.; van Assenbergh, P.; Seiffert, S. Chain Dynamics in Supramolecular Polymer Networks. *Macromolecules* **2013**, *46*, 6273–6286.
- (357) Fan, J.; Zou, J.; He, X.; Zhang, F.; Zhang, S.; Raymond, J. E.; Wooley, K. L. Tunable Mechano-Responsive Organogels by Ring-Opening Copolymerizations of N-Carboxyanhydrides. *Chem. Sci.* **2014**, *5*, 141–150.
- (358) Ji, X.; Jie, K.; Zimmerman, S. C.; Huang, F. A Double Supramolecular Crosslinked Polymer Gel Exhibiting Macroscale Expansion and Contraction Behavior and Multistimuli Responsiveness. *Polym. Chem.* **2015**, *6*, 1912–1917.
- (359) Appel, E. A.; Tibbitt, M. W.; Webber, M. J.; Mattix, B. A.; Veiseh, O.; Langer, R. Self-Assembled Hydrogels Utilizing Polymer-Nanoparticle Interactions. *Nat. Commun.* **2015**, *6*, 6295.
- (360) Haraguchi, K.; Farnworth, R.; Ohbayashi, A.; Takehisa, T. Compositional Effects on Mechanical Properties of Nanocomposite Hydrogels Composed of Poly(N,N-Dimethylacrylamide) and Clay. *Macromolecules* **2003**, *36*, 5732–5741.
- (361) Wang, Q.; Mynar, J. L.; Yoshida, M.; Lee, E.; Lee, M.; Okuro, K.; Kinbara, K.; Aida, T. High-Water-Content Mouldable Hydrogels by Mixing Clay and a Dendritic Molecular Binder. *Nature* **2010**, *463*, 339–343.
- (362) Tamesue, S.; Ohtani, M.; Yamada, K.; Ishida, Y.; Spruell, J. M.; Lynd, N. A.; Hawker, C. J.; Aida, T. Linear Versus Dendritic Molecular Binders for Hydrogel Network Formation with Clay Nanosheets: Studies with ABA Triblock Copolyethers Carrying Guanidinium Ion Pendants. *J. Am. Chem. Soc.* **2013**, *135*, 15650–15655.
- (363) Wu, L.; Ohtani, M.; Tamesue, S.; Ishida, Y.; Aida, T. High Water Content Clay–Nanocomposite Hydrogels Incorporating Guanidinium-Pendant Methacrylamide: Tuning of Mechanical and Swelling Properties by Supramolecular Approach. *J. Polym. Sci., Part A: Polym. Chem.* **2014**, *52*, 839–847.
- (364) Gaharwar, A. K.; Avery, R. K.; Assmann, A.; Paul, A.; McKinley, G. H.; Khademhosseini, A.; Olsen, B. D. Shear-Thinning Nanocomposite Hydrogels for the Treatment of Hemorrhage. *ACS Nano* **2014**, *8*, 9833–9842.
- (365) Tan, Z.; Ohara, S.; Naito, M.; Abe, H. Supramolecular Hydrogel of Bile Salts Triggered by Single-Walled Carbon Nanotubes. *Adv. Mater.* **2011**, *23*, 4053–4057.
- (366) Du, R.; Wu, J.; Chen, L.; Huang, H.; Zhang, X.; Zhang, J. Hierarchical Hydrogen Bonds Directed Multi-Functional Carbon Nanotube-Based Supramolecular Hydrogels. *Small* **2014**, *10*, 1387–1393.
- (367) Hashmi, S.; GhavamiNejad, A.; Obiweluozor, F. O.; Vatankhah-Varnoosfaderani, M.; Stadler, F. J. Supramolecular Interaction Controlled Diffusion Mechanism and Improved Mechanical Behavior of Hybrid Hydrogel Systems of Zwitterions and CNT. *Macromolecules* **2012**, *45*, 9804–9815.
- (368) Wang, Z.; Chen, Y. Supramolecular Hydrogels Hybridized with Single-Walled Carbon Nanotubes. *Macromolecules* **2007**, *40*, 3402–3407.
- (369) Hui, Z.; Zhang, X.; Yu, J.; Huang, J.; Liang, Z.; Wang, D.; Huang, H.; Xu, P. Carbon Nanotube-Hybridized Supramolecular Hydrogel Based on PEO-b-PPO-b-PEO/α-Cyclodextrin as a Potential Biomaterial. *J. Appl. Polym. Sci.* **2010**, *116*, 1894–1901.
- (370) Ogoshi, T.; Takashima, Y.; Yamaguchi, H.; Harada, A. Chemically-Responsive Sol–Gel Transition of Supramolecular Single-Walled Carbon Nanotubes (SWNTs) Hydrogel Made by Hybrids of SWNTs and Cyclodextrins. *J. Am. Chem. Soc.* **2007**, *129*, 4878–4879.
- (371) Yang, B.; Zhao, Y.; Ren, X.; Zhang, X.; Fu, C.; Zhang, Y.; Wei, Y.; Tao, L. The Power of One-Pot: A Hexa-Component System Containing π–π Stacking, Ugi Reaction and Raft Polymerization for Simple Polymer Conjugation on Carbon Nanotubes. *Polym. Chem.* **2015**, *6*, 509–513.
- (372) Tamesue, S.; Takashima, Y.; Yamaguchi, H.; Shinkai, S.; Harada, A. Photochemically Controlled Supramolecular Curdlan/Single-Walled Carbon Nanotube Composite Gel: Preparation of Molecular Distaff by Cyclodextrin Modified Curdlan and Phase Transition Control. *Eur. J. Org. Chem.* **2011**, *2011*, 2801–2806.
- (373) Mandal, S. K.; Kar, T.; Das, P. K. Pristine Carbon-Nanotube-Included Supramolecular Hydrogels with Tunable Viscoelastic Properties. *Chem. - Eur. J.* **2013**, *19*, 12486–12496.
- (374) Zu, S.-Z.; Han, B.-H. Aqueous Dispersion of Graphene Sheets Stabilized by Pluronic Copolymers: Formation of Supramolecular Hydrogel. *J. Phys. Chem. C* **2009**, *113*, 13651–13657.
- (375) Adhikari, B.; Banerjee, A. Short Peptide Based Hydrogels: Incorporation of Graphene into the Hydrogel. *Soft Matter* **2011**, *7*, 9259–9266.
- (376) Adhikari, B.; Biswas, A.; Banerjee, A. Graphene Oxide-Based Supramolecular Hydrogels for Making Nanohybrid Systems with Au Nanoparticles. *Langmuir* **2012**, *28*, 1460–1469.
- (377) Adhikari, B.; Biswas, A.; Banerjee, A. Graphene Oxide-Based Hydrogels to Make Metal Nanoparticle-Containing Reduced Graphene Oxide-Based Functional Hybrid Hydrogels. *ACS Appl. Mater. Interfaces* **2012**, *4*, 5472–5482.
- (378) Tao, C.-a.; Wang, J.; Qin, S.; Lv, Y.; Long, Y.; Zhu, H.; Jiang, Z. Fabrication of pH-Sensitive Graphene Oxide-Drug Supramolecular Hydrogels as Controlled Release Systems. *J. Mater. Chem.* **2012**, *22*, 24856–24861.
- (379) Cong, H.-P.; Wang, P.; Yu, S.-H. Stretchable and Self-Healing Graphene Oxide–Polymer Composite Hydrogels: A Dual-Network Design. *Chem. Mater.* **2013**, *25*, 3357–3362.
- (380) Han, D.; Yan, L. Supramolecular Hydrogel of Chitosan in the Presence of Graphene Oxide Nanosheets as 2D Cross-Linkers. *ACS Sustainable Chem. Eng.* **2014**, *2*, 296–300.
- (381) Liu, J.; Chen, G.; Jiang, M. Supramolecular Hybrid Hydrogels from Noncovalently Functionalized Graphene with Block Copolymers. *Macromolecules* **2011**, *44*, 7682–7691.
- (382) Wu, L.; Ohtani, M.; Takata, M.; Saeki, A.; Seki, S.; Ishida, Y.; Aida, T. Magnetically Induced Anisotropic Orientation of Graphene Oxide Locked by In Situ Hydrogelation. *ACS Nano* **2014**, *8*, 4640–4649.

- (383) Liu, M.; Ishida, Y.; Ebina, Y.; Sasaki, T.; Aida, T. Photolatently Modular Hydrogels using Unilamellar Titania Nanosheets as Photocatalytic Crosslinkers. *Nat. Commun.* **2013**, *4*, 2029.
- (384) Liu, M.; Ishida, Y.; Ebina, Y.; Sasaki, T.; Hikima, T.; Takata, M.; Aida, T. An Anisotropic Hydrogel with Electrostatic Repulsion between Cofacially Aligned Nanosheets. *Nature* **2015**, *517*, 68–72.
- (385) Jing, B.; Chen, X.; Wang, X.; Zhao, Y.; Qiu, H. Sol-Gel-Sol Transition of Gold Nanoparticle-Based Supramolecular Hydrogels Induced by Cyclodextrin Inclusion. *ChemPhysChem* **2008**, *9*, 249–252.
- (386) Yu, J.; Ha, W.; Sun, J.-n.; Shi, Y.-p. Supramolecular Hybrid Hydrogel Based on Host–Guest Interaction and its Application in Drug Delivery. *ACS Appl. Mater. Interfaces* **2014**, *6*, 19544–19551.
- (387) Kar, T.; Dutta, S.; Das, P. K. pH-Triggered Conversion of Soft Nanocomposites: In Situ Synthesized AuNP-Hydrogel to AuNP-Organogel. *Soft Matter* **2010**, *6*, 4777–4787.
- (388) Shen, J.-S.; Chen, Y.-L.; Huang, J.-L.; Chen, J.-D.; Zhao, C.; Zheng, Y.-Q.; Yu, T.; Yang, Y.; Zhang, H.-W. Supramolecular Hydrogels for Creating Gold and Silver Nanoparticles in Situ. *Soft Matter* **2013**, *9*, 2017–2023.
- (389) Meyer, D. E.; Chilkoti, A. Genetically Encoded Synthesis of Protein-Based Polymers with Precisely Specified Molecular Weight and Sequence by Recursive Directional Ligation: Examples from the Elastin-Like Polypeptide System. *Biomacromolecules* **2002**, *3*, 357–367.
- (390) Arul, V.; Gopinath, D.; Gomathi, K.; Jayakumar, R. Biotinylated GHK Peptide Incorporated Collagenous Matrix: A Novel Biomaterial for Dermal Wound Healing in Rats. *J. Biomed. Mater. Res., Part B* **2005**, *73B*, 383–391.
- (391) Jun, H. W.; West, J. L. Modification of Polyurethaneurea with PEG and YIGSR Peptide to Enhance Endothelialization without Platelet Adhesion. *J. Biomed. Mater. Res.* **2005**, *72B*, 131–139.
- (392) Matsuda, A.; Kobayashi, H.; Itoh, S.; Kataoka, K.; Tanaka, J. Immobilization of Laminin Peptide in Molecularly Aligned Chitosan by Covalent Bonding. *Biomaterials* **2005**, *26*, 2273–2279.
- (393) Ranieri, J. P.; Bellamkonda, R.; Bekos, E. J.; Vargo, T. G.; Gardella, J. A.; Aebsicher, P. Neuronal Cell Attachment to Fluorinated Ethylene-Propylene Films with Covalently Immobilized Laminin Oligopeptides YIGSR and IKVAV. II. *J. Biomed. Mater. Res.* **1995**, *29*, 779–785.
- (394) Wong, J. Y.; Weng, Z. P.; Moll, S.; Kim, S.; Brown, C. T. Identification and Validation of a Novel Cell-Recognition Site (KNEED) on the 8th Type III Domain of Fibronectin. *Biomaterials* **2002**, *23*, 3865–3870.
- (395) Lu, H. D.; Soranno, D. E.; Rodell, C. B.; Kim, I. L.; Burdick, J. A. Secondary Photocrosslinking of Injectable Shear-Thinning Dock-and-Lock Hydrogels. *Adv. Healthcare Mater.* **2013**, *2*, 1028–1036.
- (396) Wang, H. M.; Shi, Y.; Wang, L.; Yang, Z. M. Recombinant Proteins as Cross-Linkers for Hydrogelations. *Chem. Soc. Rev.* **2013**, *42*, 891–901.
- (397) Sorensen, H. P.; Mortensen, K. K. Advanced Genetic Strategies for Recombinant Protein Expression in Escherichia Coli. *J. Biotechnol.* **2005**, *115*, 113–128.
- (398) Fahnestock, S. R.; Yao, Z.; Bedzyk, L. A. Microbial Production of Spider Silk Proteins. *Rev. Mol. Biotechnol.* **2000**, *74*, 105–119.
- (399) Cregg, J. M.; Cereghino, J. L.; Shi, J.; Higgins, D. R. Recombinant Protein Expression in Pichia Pastoris. *Mol. Biotechnol.* **2000**, *16*, 23–52.
- (400) Cereghino, G. P. L.; Cereghino, J. L.; Ilgen, C.; Cregg, J. M. Production of Recombinant Proteins in Fermenter Cultures of the Yeast Pichia Pastoris. *Curr. Opin. Biotechnol.* **2002**, *13*, 329–332.
- (401) Barr, L. A.; Fahnestock, S. R.; Yang, J. J. Production and Purification of Recombinant DP1B Silk-Like Protein in Plants. *Mol. Breed.* **2004**, *13*, 345–356.
- (402) Heim, M.; Keerl, D.; Scheibel, T. Spider Silk: From Soluble Protein to Extraordinary Fiber. *Angew. Chem., Int. Ed.* **2009**, *48*, 3584–3596.
- (403) Maeda, S. Expression of Foreign Genes in Insects Using Baculovirus Vectors. *Annu. Rev. Entomol.* **1989**, *34*, 351–372.
- (404) Miao, Y. G.; Zhang, Y. S.; Nakagaki, K.; Zhao, T. F.; Zhao, A. C.; Meng, Y.; Nakagaki, M.; Park, E. Y.; Maenaka, K. Expression of Spider Flagelliform Silk Protein in Bombyx Mori Cell Line by a Novel Bac-to-Bac/BmNPV Baculovirus Expression System. *Appl. Microbiol. Biotechnol.* **2006**, *71*, 192–199.
- (405) Heidebrecht, A.; Eisoldt, L.; Diehl, J.; Schmidt, A.; Geffers, M.; Lang, G.; Scheibel, T. Biomimetic Fibers Made of Recombinant Spidroins with the Same Toughness as Natural Spider Silk. *Adv. Mater.* **2015**, *27*, 2189–2194.
- (406) Lazaris, A.; Arcidiacono, S.; Huang, Y.; Zhou, J. F.; Duguay, F.; Chretien, N.; Welsh, E. A.; Soares, J. W.; Karatzas, C. N. Spider Silk Fibers Spun from Soluble Recombinant Silk Produced in Mammalian Cells. *Science* **2002**, *295*, 472–476.
- (407) Koide, T. Triple Helical Collagen-Like Peptides: Engineering and Applications in Matrix Biology. *Connect. Tissue Res.* **2005**, *46*, 131–141.
- (408) Liu, W.; Merrett, K.; Griffith, M.; Fagerholm, P.; Dravida, S.; Heyne, B.; Scaiano, J. C.; Watsky, M. A.; Shinozaki, N.; Lagali, N.; et al. Recombinant Human Collagen for Tissue Engineered Corneal Substitutes. *Biomaterials* **2008**, *29*, 1147–1158.
- (409) Olsen, D.; Yang, C. L.; Bodo, M.; Chang, R.; Leigh, S.; Baez, J.; Carmichael, D.; Perala, M.; Hamalainen, E. R.; Jarvinen, M.; et al. Recombinant Collagen and Gelatin for Drug Delivery. *Adv. Drug Delivery Rev.* **2003**, *55*, 1547–1567.
- (410) Werkmeister, J. A.; Ramshaw, J. A. M. Recombinant Protein Scaffolds for Tissue Engineering. *Biomed. Mater.* **2012**, *7*, 012002.
- (411) Kang, E.; Jeong, G. S.; Choi, Y. Y.; Lee, K. H.; Khademhosseini, A.; Lee, S. H. Digitally Tunable Physicochemical Coding of Material Composition and Topography in Continuous Microfibres. *Nat. Mater.* **2011**, *10*, 877–883.
- (412) Betre, H.; Ong, S. R.; Guilak, F.; Chilkoti, A.; Fermor, B.; Setton, L. A. Chondrocytic Differentiation of Human Adipose-Derived Adult Stem Cells in Elastin-Like Polypeptide. *Biomaterials* **2006**, *27*, 91–99.
- (413) Chilkoti, A.; Christensen, T.; MacKay, J. A. Stimulus Responsive Elastin Biopolymers: Applications in Medicine and Biotechnology. *Curr. Opin. Chem. Biol.* **2006**, *10*, 652–657.
- (414) Urry, D. W. Physical Chemistry of Biological Free Energy Transduction as Demonstrated by Elastic Protein-Based Polymers. *J. Phys. Chem. B* **1997**, *101*, 11007–11028.
- (415) McHale, M. K.; Setton, L. A.; Chilkoti, A. Synthesis and in Vitro Evaluation of Enzymatically Cross-Linked Elastin-Like Polypeptide Gels for Cartilaginous Tissue Repair. *Tissue Eng.* **2005**, *11*, 1768–1779.
- (416) Chang, D. T.; Chai, R. J.; DiMarco, R.; Heilshorn, S. C.; Cheng, A. G. Protein-Engineered Hydrogel Encapsulation for 3-D Culture of Murine Cochlea. *Otol. Neurotol.* **2015**, *36*, 531–538.
- (417) Liu, J. C.; Heilshorn, S. C.; Tirrell, D. A. Comparative Cell Response to Artificial Extracellular Matrix Proteins Containing the RGD and CS5 Cell-Binding Domains. *Biomacromolecules* **2004**, *5*, 497–504.
- (418) MacEwan, S. R.; Chilkoti, A. Elastin-Like Polypeptides: Biomedical Applications of Tunable Biopolymers. *Biopolymers* **2010**, *94*, 60–77.
- (419) Testera, A. M.; Girotti, A.; de Torre, I. G.; Quintanilla, L.; Santos, M.; Alonso, M.; Rodriguez-Cabello, J. C. Biocompatible Elastin-Like Click Gels: Design, Synthesis and Characterization. *J. Mater. Sci.: Mater. Med.* **2015**, *26*, 1–13.
- (420) Li, L.; Kiick, K. L. Resilin-Based Materials for Biomedical Applications. *ACS Macro Lett.* **2013**, *2*, 635–640.
- (421) Li, L. Q.; Tong, Z. X.; Jia, X. Q.; Kiick, K. L. Resilin-Like Polypeptide Hydrogels Engineered for Versatile Biological Function. *Soft Matter* **2013**, *9*, 665–673.
- (422) McGann, C. L.; Levenson, E. A.; Kiick, K. L. Resilin-Based Hybrid Hydrogels for Cardiovascular Tissue Engineering. *Macromol. Chem. Phys.* **2013**, *214*, 203–213.
- (423) Huemmerich, D.; Helsen, C. W.; Quedzuweit, S.; Oschmann, J.; Rudolph, R.; Scheibel, T. Primary Structure Elements of Spider Dragline Silks and their Contribution to Protein Solubility. *Biochemistry* **2004**, *43*, 13604–13612.
- (424) Vendrely, C.; Scheibel, T. Biotechnological Production of Spider-Silk Proteins Enables New Applications. *Macromol. Biosci.* **2007**, *7*, 401–409.

- (425) Gosline, J. M.; Guerette, P. A.; Ortlepp, C. S.; Savage, K. N. The Mechanical Design of Spider Silks: From Fibroin Sequence to Mechanical Function. *J. Exp. Biol.* **1999**, *202*, 3295–3303.
- (426) Leal-Egana, A.; Scheibel, T. Interactions of Cells with Silk Surfaces. *J. Mater. Chem.* **2012**, *22*, 14330–14336.
- (427) Müller-Herrmann, S.; Scheibel, T. Enzymatic Degradation of Films, Particles, and Nonwoven Meshes Made of a Recombinant Spider Silk Protein. *ACS Biomater. Sci. Eng.* **2015**, *1*, 247–259.
- (428) Rammensee, S.; Huemmerich, D.; Hermanson, K. D.; Scheibel, T.; Bausch, A. R. Rheological Characterization of Hydrogels Formed by Recombinantly Produced Spider Silk. *Appl. Phys. A: Mater. Sci. Process.* **2006**, *82*, 261–264.
- (429) Schacht, K.; Scheibel, T. Controlled Hydrogel Formation of a Recombinant Spider Silk Protein. *Biomacromolecules* **2011**, *12*, 2488–2495.
- (430) Ramshaw, J. A.; Werkmeister, J. A.; Dumsday, G. J. Bioengineered Collagens: Emerging Directions for Biomedical Materials. *Bioengineered* **2014**, *5*, 227–233.
- (431) Frank, S.; Kammerer, R. A.; Mechling, D.; Schultheiss, T.; Landwehr, R.; Bann, J.; Guo, Y.; Lustig, A.; Bachinger, H. P.; Engel, J. Stabilization of Short Collagen-Like Triple Helices by Protein Engineering. *J. Mol. Biol.* **2001**, *308*, 1081–1089.
- (432) Myllyharju, J.; Nokelainen, M.; Vuorela, A.; Kivirikko, K. I. Expression of Recombinant Human Type I–III Collagens in the Yeast *Pichia Pastoris*. *Biochem. Soc. Trans.* **2000**, *28*, 353–357.
- (433) Martin, R.; Waldmann, L.; Kaplan, D. L. Supramolecular Assembly of Collagen Triblock Peptides. *Biopolymers* **2003**, *70*, 435–444.
- (434) Valluzzi, R.; Kaplan, D. L. Sequence-Specific Liquid Crystallinity of Collagen Model Peptides. I. Transmission Electron Microscopy Studies of Interfacial Collagen Gels. *Biopolymers* **2000**, *53*, 350–362.
- (435) Hu, K.; Cui, F. Z.; Lv, Q.; Ma, J.; Feng, Q. L.; Xu, L.; Fan, D. D. Preparation of Fibroin/Recombinant Human-Like Collagen Scaffold to Promote Fibroblasts Compatibility. *J. Biomed. Mater. Res., Part A* **2008**, *84A*, 483–490.
- (436) Jia, X. Q.; Kiick, K. L. Hybrid Multicomponent Hydrogels for Tissue Engineering. *Macromol. Biosci.* **2009**, *9*, 140–156.
- (437) Li, B.; Alonso, D. O. V.; Daggett, V. The Molecular Basis for the Inverse Temperature Transition of Elastin. *J. Mol. Biol.* **2001**, *305*, 581–592.
- (438) Meyer, D. E.; Chilkoti, A. Quantification of the Effects of Chain Length and Concentration on the Thermal Behavior of Elastin-Like Polypeptides. *Biomacromolecules* **2004**, *5*, 846–851.
- (439) Urry, D. W. Elastic Molecular Machines in Metabolism and Soft-Tissue Restoration. *Trends Biotechnol.* **1999**, *17*, 249–257.
- (440) Urry, D. W.; Pattanaik, A.; Xu, J.; Woods, T. C.; McPherson, D. T.; Parker, T. M. Elastic Protein-Based Polymers in Soft Tissue Augmentation and Generation. *J. Biomater. Sci., Polym. Ed.* **1998**, *9*, 1015–1048.
- (441) Nagapudi, K.; Brinkman, W. T.; Thomas, B. S.; Park, J. O.; Srinivasarao, M.; Wright, E.; Conticello, V. P.; Chaikof, E. L. Viscoelastic and Mechanical Behavior of Recombinant Protein Elastomers. *Biomaterials* **2005**, *26*, 4695–4706.
- (442) Chow, D.; Nunalee, M. L.; Lim, D. W.; Simnick, A. J.; Chilkoti, A. Peptide-Based Biopolymers in Biomedicine and Biotechnology. *Mater. Sci. Eng., R* **2008**, *62*, 125–155.
- (443) Betre, H.; Setton, L. A.; Meyer, D. E.; Chilkoti, A. Characterization of a Genetically Engineered Elastin-Like Polypeptide for Cartilaginous Tissue Repair. *Biomacromolecules* **2002**, *3*, 910–916.
- (444) Bracalello, A.; Santopietro, V.; Vassalli, M.; Marletta, G.; Del Gaudio, R.; Bochicchio, B.; Pepe, A. Design and Production of a Chimeric Resilin-, Elastin-, and Collagen-Like Engineered Polypeptide. *Biomacromolecules* **2011**, *12*, 2957–2965.
- (445) Charati, M. B.; Ifkovits, J. L.; Burdick, J. A.; Linhardt, J. G.; Kiick, K. L. Hydrophilic Elastomeric Biomaterials Based on Resilin-Like Polypeptides. *Soft Matter* **2009**, *5*, 3412–3416.
- (446) Fernandez-Colino, A.; Arias, F. J.; Alonso, M.; Rodriguez-Cabello, J. C. Self-Organized ECM-Mimetic Model Based on an Amphiphilic Multiblock Silk-Elastin-Like Corecombinamer with a Concomitant Dual Physical Gelation Process. *Biomacromolecules* **2014**, *15*, 3781–3793.
- (447) Haider, M.; Cappello, J.; Ghandehari, H.; Leong, K. W. In Vitro Chondrogenesis of Mesenchymal Stem Cells in Recombinant Silk-Elastinlike Hydrogels. *Pharm. Res.* **2008**, *25*, 692–699.
- (448) Wlodarczyk-Biegum, M. K.; Werten, M. W.; de Wolf, F. A.; van den Beucken, J. J.; Leeuwenburgh, S. C.; Kamperman, M.; Cohen Stuart, M. A. Genetically Engineered Silk-Collagen-Like Copolymer for Biomedical Applications: Production, Characterization and Evaluation of Cellular Response. *Acta Biomater.* **2014**, *10*, 3620–3629.
- (449) Wang, H. Y.; Cai, L.; Paul, A.; Enejder, A.; Heilshorn, S. C. Hybrid Elastin-Like Polypeptide-Polyethylene Glycol (ELP-PEG) Hydrogels with Improved Transparency and Independent Control of Matrix Mechanics and Cell Ligand Density. *Biomacromolecules* **2014**, *15*, 3421–3428.
- (450) Dinerman, A. A.; Cappello, J.; Ghandehari, H.; Hoag, S. W. Swelling Behavior of a Genetically Engineered Silk-Elastinlike Protein Polymer Hydrogel. *Biomaterials* **2002**, *23*, 4203–4210.
- (451) Megeed, Z.; Cappello, J.; Ghandehari, H. Controlled Release of Plasmid DNA from a Genetically Engineered Silk-Elastinlike Hydrogel. *Pharm. Res.* **2002**, *19*, 954–959.
- (452) Cappello, J.; Crissman, J.; Dorman, M.; Mikolajczak, M.; Textor, G.; Marquet, M.; Ferrari, F. Genetic-Engineering of Structural Protein Polymers. *Biotechnol. Prog.* **1990**, *6*, 198–202.
- (453) Megeed, Z.; Cappello, J.; Ghandehari, H. Genetically Engineered Silk-Elastinlike Protein Polymers for Controlled Drug Delivery. *Adv. Drug Delivery Rev.* **2002**, *54*, 1075–1091.
- (454) Nagarsekar, A.; Crissman, J.; Crissman, M.; Ferrari, F.; Cappello, J.; Ghandehari, H. Genetic Synthesis and Characterization of pH- and Temperature-Sensitive Silk-Elastinlike Protein Block Copolymers. *J. Biomed. Mater. Res.* **2002**, *62*, 195–203.
- (455) Nagarsekar, A.; Crissman, J.; Crissman, M.; Ferrari, F.; Cappello, J.; Ghandehari, H. Genetic Engineering of Stimuli-Sensitive Silkelastin-Like Protein Block Copolymers. *Biomacromolecules* **2003**, *4*, 602–607.
- (456) Xia, X. X.; Xu, Q. B.; Hu, X.; Qin, G. K.; Kaplan, D. L. Tunable Self-Assembly of Genetically Engineered Silk-Elastin-Like Protein Polymers. *Biomacromolecules* **2011**, *12*, 3844–3850.
- (457) Cappello, J.; Crissman, J. W.; Crissman, M.; Ferrari, F. A.; Textor, G.; Wallis, O.; Whittle, J. R.; Zhou, X.; Burman, D.; Aukerman, L.; et al. R In-Situ Self-Assembling Protein Polymer Gel Systems for Administration, Delivery, and Release of Drugs. *J. Controlled Release* **1998**, *53*, 105–117.
- (458) Golinska, M. D.; Wlodarczyk-Biegum, M. K.; Werten, M. W. T.; Stuart, M. A. C.; de Wolf, F. A.; de Vries, R. Dilute Self-Healing Hydrogels of Silk-Collagen-Like Block Copolypeptides at Neutral pH. *Biomacromolecules* **2014**, *15*, 699–706.
- (459) Parisi-Amon, A.; Mulyasasmita, W.; Chung, C.; Heilshorn, S. C. Protein-Engineered Injectable Hydrogel to Improve Retention of Transplanted Adipose-Derived Stem Cells. *Adv. Healthcare Mater.* **2013**, *2*, 428–432.
- (460) Altunbas, A.; Pochan, D. J. Peptide-Based and Polypeptide-Based Hydrogels for Drug Delivery and Tissue Engineering. *Top. Curr. Chem.* **2012**, *310*, 135–167.
- (461) Glassman, M. J.; Chan, J.; Olsen, B. D. Reinforcement of Shear Thinning Protein Hydrogels by Responsive Block Copolymer Self-Assembly. *Adv. Funct. Mater.* **2013**, *23*, 1182–1193.
- (462) Chen, J. H.; Seeman, N. C. Synthesis from DNA of a Molecule with the Connectivity of a Cube. *Nature* **1991**, *350*, 631–633.
- (463) He, Y.; Ye, T.; Su, M.; Zhang, C.; Ribbe, A. E.; Jiang, W.; Mao, C. D. Hierarchical Self-Assembly of DNA into Symmetric Supramolecular Polyhedra. *Nature* **2008**, *452*, 198–202.
- (464) Li, Y. G.; Tseng, Y. D.; Kwon, S. Y.; d'Espaux, L.; Bunch, J. S.; Mceuen, P. L.; Luo, D. Controlled Assembly of Dendrimer-Like DNA. *Nat. Mater.* **2004**, *3*, 38–42.
- (465) Rothemund, P. W. K. Folding DNA to Create Nanoscale Shapes and Patterns. *Nature* **2006**, *440*, 297–302.
- (466) Um, S. H.; Lee, J. B.; Kwon, S. Y.; Li, Y.; Luo, D. Dendrimer-Like DNA-Based Fluorescence Nanobarcodes. *Nat. Protoc.* **2006**, *1*, 995–1000.

- (467) Um, S. H.; Lee, J. B.; Park, N.; Kwon, S. Y.; Umbach, C. C.; Luo, D. Enzyme-Catalysed Assembly of DNA Hydrogel. *Nat. Mater.* **2006**, *5*, 797–801.
- (468) Nishikawa, M.; Mizuno, Y.; Mohri, K.; Matsuoka, N.; Rattanakiat, S.; Takahashi, Y.; Funabashi, H.; Luo, D.; Takakura, Y. Biodegradable CpG DNA Hydrogels for Sustained Delivery of Doxorubicin and Immunostimulatory Signals in Tumor-Bearing Mice. *Biomaterials* **2011**, *32*, 488–494.
- (469) Klinman, D. M. Immunotherapeutic Uses of CpG Oligodeoxyribonucleotides. *Nat. Rev. Immunol.* **2004**, *4*, 249–259.
- (470) Krieg, A. M. Therapeutic Potential of Toll-Like Receptor 9 Activation. *Nat. Rev. Drug Discovery* **2006**, *5*, 471–484.
- (471) Roman, M.; Martin-Orozco, E.; Goodman, S.; Nguyen, M. D.; Sato, Y.; Ronagh, A.; Kornbluth, R. S.; Richman, D. D.; Carson, D. A.; Raz, E. Immunostimulatory DNA Sequences Function as T Helper-1-Promoting Adjuvants. *Nat. Med.* **1997**, *3*, 849–854.
- (472) Nishikawa, M.; Ogawa, K.; Umeki, Y.; Mohri, K.; Kawasaki, Y.; Watanabe, H.; Takahashi, N.; Kusuki, E.; Takahashi, R.; Takahashi, Y.; et al. Injectable, Self-Gelling, Biodegradable, and Immunomodulatory DNA Hydrogel for Antigen Delivery. *J. Controlled Release* **2014**, *180*, 25–32.
- (473) Guo, W.; Lu, C. H.; Orbach, R.; Wang, F.; Qi, X. J.; Cecconello, A.; Seliktar, D.; Willner, I. pH-Stimulated DNA Hydrogels Exhibiting Shape-Memory Properties. *Adv. Mater.* **2015**, *27*, 73–78.